

A SUSTAINABLE METHOD FOR THE RAPID ASSESSMENT OF THE EXTENT AND CAUSES OF METAPHYTON IN LAKE TAHOE



FINAL REPORT

SUBMITTED TO:
NEVADA DIVISION OF STATE LANDS

June 29, 2020



A Sustainable Method for the Rapid Assessment of the Extent and Causes of
Metaphyton in Lake Tahoe

Final Report

Submitted to:
Nevada Division of State Lands

Submitted by:
Tahoe Environmental Research Center
University of California, Davis

Scott Hackley, Brant Allen, Katie Senft, Brandon Berry and Geoffrey Schladow
(UC Davis TERC)
Andy Wong, Yi Chen, Qingyu Yu and Yufang Jin (UC Davis LAWR)
Mike Bruno (Hooked Wireless)

June 29, 2020

Table of Contents

Acknowledgments	5
Executive Summary.....	6
I. Introduction.....	12
II. Use of Aerial Imaging from a Helicopter to Assess the Distribution of Metaphyton in Lake Tahoe.....	13
II.A. Introduction.....	13
II.B. Methods.....	13
II.B.1. Helicopter, crew, flight paths, speed, heights.....	13
II.B.2. Configuration of cameras, camera types, mounting.....	14
II.B.3. Camera triggering, acquisition settings, reference markers placed in lake, resolution.....	16
II.B.4. Imaging locations.....	17
II.B.5. Evolving methods for inflight imaging.....	20
II.B.6. Image analysis.....	20
II.B.6.a. Image preprocessing.....	20
II.B.6.b. RGB and Multispectral Images Results and Utility.....	22
II.C. Results.....	23
II.C.1. Visual analysis of helicopter images and field ground-truthing.....	23
II.C.2. Helicopter imaging and water intakes.....	32
II.C.3.a. Development of method for distinguishing metaphyton, vegetation and other substrate from pure water, based on helicopter imaging....	32
II.C.3.b. Distinguishing metaphyton from vegetation and other substrate, and protocol for determination of percent cover.....	34
II.C.4. Results for estimates of metaphyton percent cover in 2018 and 2019 using helicopter imaging.....	36
II.D. Conclusions.....	42
III. Aerial Imaging by UAV.....	44
III.A. Introduction.....	44
III.B. Methods.....	44
III.C. Results.....	53
III.D. Periphyton Monitoring with UAV.....	57
III.E. Conclusions regarding UAV imaging of metaphyton.....	58
IV. In-lake work: Metaphyton Biomass, Percent Cover, Predominant Algal Types.....	58
IV.A. Introduction.....	58
IV.A.1. Description of the in-lake study sites.....	58
IV.B. Metaphyton Biomass Measurements.....	60
IV.B.1. Metaphyton Algae Biomass Collection and Ash Free Dry Weight Determination Methods.....	60
IV.B.2. Metaphyton AFDW Results.....	61
IV.C. Metaphyton percent cover.....	66
IV.C.1. Underwater Percent Cover Measurement Methods.....	66

IV.C.2. In-lake Estimates of Metaphyton Percent Cover Results.....	66
IV.C.3. Comparison of In-lake Measures of Percent Cover with Estimates from Helicopter and UAV.....	69
IV.D. Onshore Deposition of Metaphyton algae and Aquatic Plant Fragments.....	71
IV.E. Predominant Algal Types.....	73
IV.E.1. Predominant Algal Types Methods.....	73
IV.E.2. Predominant Algal Types in Metaphyton Results.....	73
V. Assessing Linkages between Metaphyton and Asian Clams: Sediment Pore Water and water column Nutrients, Asian Clam excretion, Asian Clam Abundance, Algae Stable Isotopes.....	77
V.A. Sediment Pore Water and Water Column Nutrients.....	77
V.A.1. Sediment Pore Water and Water Column Nutrients Methods.....	77
V.A.2. Sediment Pore Water and Water Column Nutrients Results.....	78
V.B. Nitrogen and Phosphorus in Asian Clam (<i>Corbicula fluminea</i>) Excretion.....	85
V.B.1. Nitrogen and Phosphorus in Asian Clam Excretion Methods.....	85
V.B.2. Nitrogen and Phosphorus in Asian Clam Excretion Results.....	85
V.B.3. Nutrient Accumulation under Bottom Barrier.....	88
V.C. Asian Clam Abundance.....	88
V.C.1. Asian Clam Abundance Methods.....	88
V.C.2. Asian Clam Abundance Results.....	89
V.C.3. Asian Clam Abundance Discussion.....	91
V.D. Stable Isotopes ¹³ C and ¹⁵ N in Metaphyton Algae.....	94
V.D.1. Methods.....	95
V.D.2. Results.....	96
VI. Conclusions and Recommendations for Regional Metaphyton Monitoring Program.....	100
VII. References.....	105
VIII. Appendices.....	107
Appendix 1. Summary of follow-up observations or ground-truthing of areas with possible metaphyton or other substrate of interest identified in aerial photos.....	107
Appendix 2. Additional Aerial and ground-truthing images.....	113
Appendix 3 – UAV Flight Parameters.....	116
Appendix 4. Accuracy tables, original UAV images and images after classification of pixels.....	121
Appendix 5. Predominant algal types and predominant genera present in samples.....	158

Acknowledgments

We are extremely grateful for the efforts of the many individuals and organizations who made this project possible. We are grateful for Raph Townsend's work in construction of different camera mounts for the helicopter. We wish to acknowledge TERC interns Madelyn Maffia, Hannah Kranz, Kian Bagheri, Jenna Chavez, and Audrey Dufresne for their help in the lab and in the field. We also thank volunteer Alex Daharsh for his assistance early in the project. We also wish to acknowledge TERC chemistry staff Steve Sesma, Anne Liston and Tina Hammell and their student assistants and interns for their work in the analytical labs. Lidia Tanaka provided assistance with some of the algae identifications. Dr. Shohei Watanabe contributed to the project through his management of data archiving. Carmen Woods provided administrative support throughout. We are grateful to the UC Davis Stable Isotope Facility for providing a Pilot Project Grant to support investigations of stable isotopes in algae and waters samples associated with this project. Dr. Scott Tyler (UNR) loaned us some camera equipment at the outset of the project, and provided valuable discussions.

Finally, we thank the Nevada Division of State Lands and in particular their Lake Tahoe License Plate Program for funding this project.

Executive Summary

Despite its massive size, the health of the lake is often judged by a narrow band of shallow water around its edge. The shore zone of Lake Tahoe is where the public interacts with the lake for the first time and where public opinion regarding the lake's aesthetic character is determined by these first impressions. In recent summers, metaphyton (drifting patches of green filamentous algae) have been observed over the sandy bottom in nearshore waters along the south shore of Lake Tahoe. This algae, which is not attached to substrate, is highly visible in the nearshore and occasionally washes onto the beaches and subsequently degrades the aesthetic conditions of the beaches through its visual impact and the odors produced through decomposition.

Indications are that concentrations and the areal distribution of metaphyton have increased in recent years based on anecdotal reports from long-time users of the south shore; however, little data have been collected on metaphyton. The Lake Tahoe Nearshore Evaluation and Monitoring Framework report (Heyvaert et al., 2013) recommended that metaphyton monitoring should be included as part of nearshore monitoring.

This project had the primary goal of developing and demonstrating a regional (lake-wide) monitoring approach for the status and trend monitoring of summer metaphyton growth and distribution using a combination of aerial surveillance via a helicopter and an unmanned aerial vehicle (UAV) or drone, and a ground-truthing program. Through the project we have tested both aerial platforms and have refined our ground-truthing methodology.

In addition, the project wished to test the association of metaphyton blooms with the occurrence of the invasive Asian clam (*Corbicula fluminea*), as these clams are known to excrete highly concentrated levels of nutrients and have been present in the lake for a similar amount of time for which metaphyton has anecdotally been of concern. Through funding obtained from UC Davis, we also experimented with the use of stable isotopes to quantitatively link metaphyton with Asian clam and other potential sources of nutrients.

The use of helicopter-based surveys was shown to have great potential for rapidly visualizing the entire shoreline of Lake Tahoe. Such a survey takes approximately one hour of flight time. A variety of cameras were used, with variable success for numerous technical reasons as described in the report. Currently the technical difficulties associated with vibration and accurately orthorectifying the imagery are the greatest drawbacks to using a helicopter-based approach. The speed and simplicity of the approach are its greatest attributes, making it in its current state ideal as a semi-quantitative, rapid surveillance tool. Most of the areas of metaphyton algae observed in helicopter images were found along the south and south east shores of the lake, extending from Tallac Point to Glenbrook Bay.

Spectral signatures of different types of algae and substrate had been collected by TERC as part of an earlier SNPLMA project. We experimented with using these spectral signatures as a way to

identify different algal and plant types. However, the similarities of the signatures, combined with the low reflection of shortwave signals from water, and the interference produced by dissolved and suspended material in the nearshore led us to conclude that this approach is still not feasible at the present time.

UAV, or drone-based surveys provided very high spatial resolution imagery (ground resolution < 3”). While limited in range compared to the helicopter, they were able to complete the quantitative surveillance of areas on the scale of 10 hectares (1 km x 100 m) in under 10 minutes. Using a combination of commercially available software and algorithms developed through this project, it was possible to identify different targets (metaphyton, periphyton, rooted plants, sand, rock, structures etc.) to a very high level of accuracy, repeatability and confidence. This post-processing can be accomplished in under 4 hours per site. This allowed for the very accurate calculation of the extent of cover by metaphyton. This was one of the primary goals of the project.

Ground-truthing techniques that had been developed through an earlier study were modified and refined. We now have the ability to rapidly collect metaphyton samples, and to process them to determine biomass. What became apparent was that the high degree of patchiness or spatial variability in metaphyton distribution led to large standard deviations in estimates of the measured biomass. The only way to reduce this would be to utilize many more ground-truthing sites, something that would greatly add to the cost of a monitoring program. However, by using UAV measurements to quantitatively determine the spatial variability and then using ground-truthing on specific patches of growth, it is possible to quantify the biomass within the very heterogeneous distribution.

The co-location of Asian clams and metaphyton was explored by taking nutrient measurements in the lake water and in the pore water, through quantifying the distribution of Asian clams (both live and dead) relative to the location of metaphyton patches, and measuring the nutrient flux produced by Asian clam excretion. The measurements of clam densities, nutrient excretion rates, and pore water nutrient concentrations were largely in agreement with earlier measurements. The clams were shown to excrete primarily $\text{NH}_4\text{-N}$ and SRP. In some cases, clam densities exceeded previous estimates, although these were highly variable. It was found that while there was a connection in the location of metaphyton patches and Asian clam populations, it was variable.

The reasons for this were:

- the inherent patchiness of Asian clam distribution makes it difficult to know where they are and what their areal concentration is;
- the movement of metaphyton patches by lake currents means that while they may have been initiated in concert with an area of Asian clams, the day on which they were observed their location may have been different;
- the effect of very localized bathymetric changes (e.g. depressions) in trapping metaphyton was an important factor in where they were found;

- the availability of other enriched sources of nutrients, such as the Upper Truckee River and stormwater outfalls made Asian clam excretion just one potential source of nutrient supply.

Specific measurements and sites were used during this study, allowing us to build up a picture of metaphyton and Asian clams at those sites. The sites were chosen as they were areas where metaphyton and Asian clams had been observed in the past or where metaphyton and Asian clams had not been observed (our control sites). The sites had the following characteristics:

At Lakeside there were large numbers of live clams and a large (approx. 75m X 200m) patch of metaphyton present. The presence of high levels of $\text{NH}_4\text{-N}$ in pore water concentrations inside and outside of the metaphyton patch and also high numbers of clams inside and outside the patch suggests a possible linkage between the clams and $\text{NH}_4\text{-N}$ concentrations. An experiment done during the study showed the clams to excrete $\text{NH}_4\text{-N}$ and SRP. Currents may naturally deposit the shells in this area which is a transition area from shallow to a slightly deeper shelf area offshore. It is possible the metaphyton similarly tends to accumulate or stay in place in this depression area. A combination of nutrient inputs from clams, topography, current effects as well as physical roughness provided by shells along the bottom (which may provide sites for algae to attach to), may contribute to the development of the metaphyton patch at Lakeside.

At Regan Beach there were very few live clams and shells in the nearshore. There were relatively large patches of metaphyton near the shore, a large amount of aquatic vegetation, much of it with algae and metaphyton filamentous green algae, as well as thick growth of attached periphyton *Cladophora* along the boulder breakwater lining the park. The productive aquatic plant and algae growth at Regan Beach may be due to nutrient inputs associated with surface runoff from the nearby Upper Truckee River, Trout Creek and urban drains, rather than nutrient inputs associated with Asian clams.

At Skyland, both the helicopter and UAV images show isolated dark patches of metaphyton over the sandy bottom in water 6-7m deep (up to 3m X 5m) with a much more extensive area (approx. 350m long X 100m wide) of uniform algal coverage on at least one date. Smaller (several inches long) patches of algae or a thin coating of algae over the bottom were also observed by divers, the algae was also observed to drift. The number of live clams inside and outside patches was more variable and the association with presence of metaphyton patches was not consistent. There were slightly more live clams outside metaphyton patches than inside patches for samplings done in Sept. 2018 and 2019. One patch did have substantial numbers of live clams and shells associated with it. Sediment pore water levels of $\text{NH}_4\text{-N}$ were low to moderate (5-158 $\mu\text{g/l}$) and SRP slightly elevated (3-12 $\mu\text{g/l}$) above background lake levels. The nutrients produced by the clams and observations of algae associated with shell patches near the edge of the shelf, suggest there is potential for a linkage between the algae growth and presence of clams, either due to nutrient inputs or physical impacts of the shells or both. Currents can impact movement of algae along the shelf at this site.

At Hidden Beach there were no Asian Clams or shells found. There was only a small amount of algae along the bottom which included detritus, cyanobacteria and some algae which appeared to be derived from the periphyton on nearby boulders. Asian Clams are not impacting this site.

Metaphyton algae types – Metaphyton was composed predominantly of filamentous green algae. The filaments of these algae are formed by long chains of cells. The filaments of one or more different types of algae can intertwine to form clouds or masses just above the bottom. The most predominant filamentous green algae genera observed were *Zygnema* and *Spirogyra*. Other filamentous green types were also predominant in samples from specific sites. For example, *Mougeotia* was prevalent in algae from deeper sites at Round Hill Pines and Skyland. *Oedogonium* was prevalent in many samples from Regan nearshore.

The stable isotope measurements were only partially concluded due to Covid-19 restrictions on lab operations at UC Davis. However, the results to date suggest that the data may be of limited use.

The data also showed that a range of factors are responsible for the observed metaphyton distribution year-to-year. The fact that we do not know how the distribution changes limits our ability to evaluate the importance of the various sources and the potential for management actions to control them or to mitigate them. Clearly the local bathymetry in conjunction with lake level plays an important role in trapping metaphyton. Likewise, the lake currents play an important role in moving patches and in breaking apart patches. It is currently within our ability to actually model the movement and growth of metaphyton, and through that provide guidance on future actions. What is lacking, however, is the data on the location of the metaphyton. That critical piece of information is what a lake wide (regional) monitoring program will provide.

The monitoring of metaphyton using a UAV and helicopter in this trial project proved to be both efficient and effective in quantifying the distribution of metaphyton over large areas of Lake Tahoe's nearshore, particularly when it could be combined with ongoing TERC field operations. The UAV monitoring process developed by TERC, coupled with in-lake biomass sampling, would allow future metaphyton monitoring to assess the timing, distribution, and abundance of nearshore nuisance algae on both a seasonal and interannual basis, information critical to an agency response to public and stakeholder concerns.

We would recommend that consideration be given to establishing a limited metaphyton monitoring project. Ideally this could be combined with the existing periphyton monitoring program, as significant economies could be realized.

We proposed that UAV flights be conducted on four occasions during favorable weather. These will be in July, August and September to capture peak metaphyton abundance and one flight during winter (February) to establish a baseline minimum.

The proposed sites are Hidden Beach (a control site, where no metaphyton has been observed to date), Sand Harbor, Skyland, and Lakeside. Skyland and Lakeside are areas with seasonally abundant metaphyton accumulation, near popular recreation beaches, where Asian clam populations are thriving. Sand Harbor represents a recreationally important area where Asian clam has recently become established but metaphyton has yet to reach nuisance levels. There is the possibility that in the near future Asian clam may contribute to a proliferation of metaphyton at Sand Harbor. As Sand Harbor is an extremely valuable public recreation site, we believe early monitoring is justified. UAV monitoring of Sand Harbor will provide management agencies annual information regarding any changes in the aesthetic value of the area in the presence, or absence, of continued Asian clam treatment and add further evidence of the linkage between Asian clams and localized metaphyton blooms.

All metaphyton monitoring sites will be ground sampled on the same day aerial surveys are conducted. Using SCUBA, divers will collect triplicate biomass samples for later analysis in the laboratory (wet weight and ash free dry weight (AFDW)). These collections will enable site wide determination of biomass accumulation (on the order of kg m^{-2}) adjacent to popular recreation resources.

Biomass sampling will be done based on experience of the researchers with typical distribution of filamentous algae metaphyton at the sites. Areas with representative levels of metaphyton will be selected for measurement. Patches with 100% cover with metaphyton will be sampled from a known area using the bucket/ pump method described in this document. If the distribution of biomass is very heterogeneous (for instance large patches visible from the air with other areas of thin growth also visible from the air), samples of biomass representative of the different zones of algae will be collected for biomass measurement. Samples will be returned to the lab, dried to damp consistency and a wet weight determined. A portion of this sample will be split off, weighed in a pre-tared, precombusted tin, dried overnight, then weighed again for determination of Ash Free Dry Weight (as described in this report). If chlorophyll *a* is to be analyzed, a sample will also be split off, weighed and frozen for later analysis.

Helicopter surveys are proposed to be taken twice each year in April (peak periphyton) and in August (peak metaphyton). While these surveys do not yet have the quantitative resolution of the UAV surveys, they have the ability to image the entire nearshore of the lake in only one hour. They have proven to be very effective in identifying areas of “concern”, where suddenly changed conditions can be identified and noted for follow up investigation. Photographic images will be collected on the flights to provide a record of conditions observed and archived.

The proposed work also leverages ongoing basin investments. The Nearshore network data will be used to complement the findings, especially if the breakdown products from metaphyton turn

out to be significant influencers of CDOM fluorescence. Similarly, planned 3-D lake modeling will be extremely useful in accounting for the distribution of metaphyton.

Proposed Schedule and Budget

The schedule below is for a two-year metaphyton monitoring program for the four sites recommended above. This presumes a July 1 start date.

		Jul	Aug	Sep	Oct	Nov	Dec	Jan	Feb	Mar	Apr	May	Jun	Jul	Aug	Sep	Oct	Nov	Dec	Jan	Feb	Mar	Apr	May	Jun
Task 1	Metaphyton Field and lab																								
Task 2	UAV data acqu. and image analysis																								
Task 3	Helicopter all-lake																								
Task 4	Reporting																								

The budget to support the monitoring described above for the **full two year period** is \$74,100 in direct costs (approximately \$37,000 per year). Note that indirect costs would need to be applied, which vary depending on the source of the funding or the limitations imposed by the funding agency.

I. Introduction

Lake Tahoe is the 11th deepest lake in the world (501m) with an average depth of 300m. Its 33 trillion gallons of water are surrounded by 116 km of shoreline. Despite its large volume of clear water, the health of the lake is often judged by a narrow band of shallow water around its edge. The shore zone of Lake Tahoe is where the public interacts with the lake and where public opinion regarding the lake's aesthetic character is often first formed. Beyond the aesthetics, the condition of the shore zone is an important indicator of the overall health of the entire ecosystem.

For decades, nearshore research and monitoring has focused on the growth of periphyton, algae attached to hard surfaces (boulders, piers, etc.) around the shoreline. The research was driven by concerns over increased eutrophication and the public's negative response to thick growth along portions of shore, typically in the spring. A recent report (Hackley et al., 2016) evaluated periphyton biomass on rock along shore over the past four decades and found no lake-wide trend of increased algae growth since the early 1980s. A separate peer review of that report and the underlying sampling methodology that was conducted by the Tahoe Science Advisory Council (https://246902d0-6125-43ca-8e73-f2d67ba3ff27.filesusr.com/ugd/c115bf_851ce391f97a4ea4a5c1bbd521c89f72.pdf) validated that conclusion. Despite this scientific conclusion, the perception that shorezone algae has increased remains real for many users of the lake.

This persistence in public perception raises the possibility that what is being measured and what is being perceived may not be one and the same. Specifically, the general public neither knows nor likely cares about the types of algae they are observing. They do, however, react when they see an over-abundance of algae. It was this concern, and the possibility that the public response may have been in part a reaction to metaphyton, an algal form that had not been routinely monitored, that motivated this study.

Following the discovery of a proliferation of invasive Asian clams (*Corbicula fluminea*) in 2008 along the south east shore, localized summer blooms of metaphyton algae (composed of filamentous green algae) were observed. Varied levels of metaphyton have been observed in the summers since. The distribution of metaphyton coincided with known populations of clams suggesting a possible linkage.

Though levels of metaphyton are thought to have increased in the 2000s based on anecdotal accounts, long-term monitoring data are not available for this form of algae. The Lake Tahoe Nearshore Evaluation and Monitoring Framework report (Heyvaert et al., 2013) recommended that metaphyton monitoring sites should be included as part of nearshore monitoring. Studies were done in 2015-2017 by TERC (Hackley et al., 2018) to assess methods to monitor metaphyton percent cover at localized sites. While these in-lake methods have potential for use on a local scale, it became evident that metaphyton is prone to drift and very localized transect studies may not characterize the levels of growth year to year on a regional scale.

The current study involved development of methods for assessing metaphyton distribution around the Tahoe shoreline on a regional scale. Based on the wide distribution of metaphyton and Tahoe's extensive shoreline, helicopter and Unmanned Aerial Vehicle (UAV) platforms were evaluated for their ability to image the metaphyton on a regional scale, while achieving

high resolution underwater detail. Methods of ground truthing aerial imagery and quantifying metaphyton biomass in-lake were developed. Estimates of metaphyton percent cover based on aerial images are used to assess regional biomass. In the present study we also sought to provide additional experimental evidence for linkages between Asian clam populations and filamentous algae growth. The following report summarizes the findings and makes recommendations for repeatable monitoring protocols that are cost efficient, accurate, and appropriate for assessing long term trends in the annual metaphyton accumulation in Tahoe's most publicly visited environment.

II. Use of Aerial Imaging from a Helicopter to Assess the Distribution of Metaphyton

II.A. Introduction

Aerial imaging from relatively low-flying aircraft such as a helicopter or UAV (drone) provides the potential to observe and photo-document features of interest, such as algae and plant growth on a regional scale. Use of a helicopter also creates potential to make observations around the lake shore in a short period of time (a little over an hour for Lake Tahoe). This section summarizes the work done in the summers of 2018 and 2019 to image the extent of metaphyton distribution on a regional and lake-wide scale, using a helicopter.

II.B. Methods

II.B.1. Helicopter, crew, flight paths, speed, heights

Helicopter aerial images were acquired from a Eurocopter EC120B (Airbus H120) helicopter. Flight crew consisted of a pilot, plus one researcher to manage and monitor the data acquisition from the externally-mounted cameras during the flight. On most occasions, this crew was augmented with a member of the surface research vessel crew acting as a spotter for metaphyton blooms and sites of particular interest. The spotter was equipped with a hand-held DSLR camera to document areas of interest.

For all data acquisition, the helicopter was flown at a speed of 70 knots (130 km/hr., 36 m/sec) at a height of 700 feet (213 m) above the lake surface. This corresponds to an altitude of approximately 7000 feet (2134 m) amsl. Flights originated from the South Lake Tahoe airport (KTVL). For data collection, the entire lake perimeter was flown in a clockwise direction, starting and finishing near Regan Beach in South Lake Tahoe (Figure 1). In areas of specific interest, multiple passes were usually flown to ensure that the metaphyton was fully imaged.

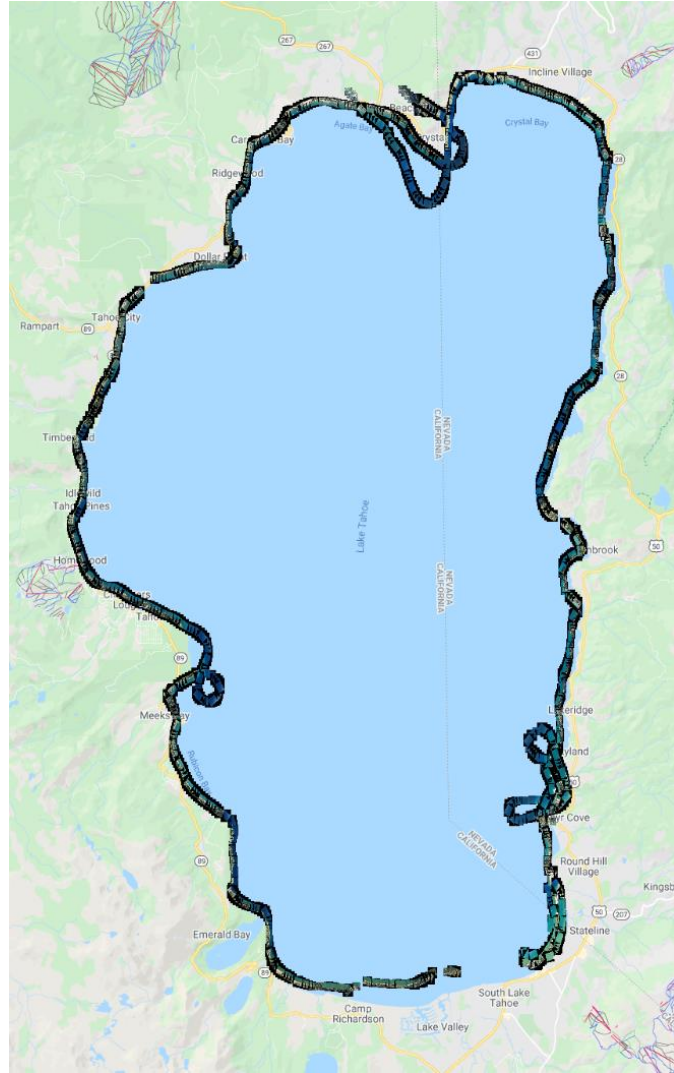


Figure 1. Flight path and visualization of one in every three RGB (red green blue hues to create different colors) images captured along the shore on September 6, 2018 using Sony HX400v.

II.B.2. Configuration of cameras, camera types, mounting

For each flight, a combination of drone and consumer still-picture cameras was used to acquire images. Each camera was mounted with the long edge of its image sensor parallel to the centerline of the helicopter, and in a position that kept its front lens plane approximately parallel to the lake surface during flight. To achieve this, the leading edge of the camera lens plane was tilted up slightly towards the tail of the helicopter to compensate for the slightly nose-down attitude of the helicopter in level forward flight at 70 knots

The drone cameras are lightweight, low power devices using a continuous/rolling shutter. For this study, they were mounted to the left (port)-side helicopter skid step (Figure 2). This was done so that during clockwise flight around the lake shore, the multispectral camera, which had the narrowest field of view (FOV), was in an inshore position.



Figure 2. Left image shows that two RGB cameras were mounted on the right skid step and the drone cameras are mounted on the left. Right images show engineering that was done on the drone mount and cameras to collect images on a helicopter.

Several consumer/prosumer digital still cameras were tested over the course of the project, representing a variety of designs and camera types. In all cases, these cameras were attached to the right-hand (starboard) skid step of the helicopter, using custom-fabricated aluminum fixtures that could accommodate one or two cameras. In some cases, two fixtures were mounted simultaneously so that three cameras could be flown (Figure 2). The cameras were attached to the fixtures with a clamping mechanism in combination with their quarter-inch tripod mounting screw. For the zoom lenses on several of the cameras, the focal length was set and locked to the shortest available value in order to obtain the widest FOV. FOV figures below are quoted for this setting. Table 1 summarizes the sensor, lens, HFOV, VFOV and information on mounting for the cameras tested in this study.

Table 1. Cameras used for image acquisition from the helicopter. * HFOV and VFOV is estimated based on altitude of 700 feet (213 m) above the lake surface.

Camera	Type	Position	Mount	Sensor	Lens	HFOV (m)	VFOV (m)
DJI Zenmuse X3	Drone RGB	Left	Drone body w/isolation mount & gimbal lock. 3D-printed nylon mounts to skid step	1/2.3” 12.4 Mp	Integrated 20 mm (35 mm equiv.) f 2.8	365.1	201.9 (16:9)
Micasense Rededge	Drone 5-channel multi-spectral	Left	Drone body or stainless rigid mount	4.8*3.6mm 1.2 Mp	Integrated 5.5mm	185.9	139.4
Canon Powershot XS260HS	Consumer screenview	Right	Aluminum rigid mount	1/2.3” 12.1 Mp	Integrated 25 – 500mm (35 mm equiv.) f 3.5- 6.8	292	215
Canon Rebel T6i	Consumer DSLR	Right	Aluminum rigid mount	1/1.14” 24.2 Mp	Detachable 27.2 – 136 mm (35 mm equiv.) F3.5 – 5.6	279.4	186.7
Sony HX400v	Consumer EVF	Right	Aluminum rigid mount	1/2.3” 20.4 Mp	Integrated 24.5-1225.5mm (35 mm equiv.) f2.8 – 6.3	305.6	225.4
Sony QX1	Consumer “smartlens”	Right	Aluminum rigid mount	1/1.1” 20 Mp	Detachable 30 mm (35 mm equiv.) f 1.8	247.1	164

II.B.3. Camera triggering, acquisition settings, reference markers placed in lake, resolution

Flying at 700 feet, the drone RGB, 5-channel multi-spectral, and Canon Powershot has a ground distance resolution of 9, 14.5, and 7.19 cm/ pixel respectively. In theory, the three other consumer grade cameras have much higher ground distance resolution, but their images were blurrier than the images from the drone cameras during 2018 flights. In an attempt to acquire sharper images, we tried many camera settings and reduced the vibration of the aluminum rigid mounts. We tested the Canon Powershot and Sony HX400v in 2018, and Canon Rebel and QX1 in 2019. The images acquired by QX1 and Rebel in 2019 were much sharper than those acquired 2018 and were better than the drone RGB image (less distortion, higher resolution, better color). These cameras were triggered at the fastest possible rate, generally between 1.5-2 seconds, within the constraints on battery life and image quality. The cameras have different trigger mechanics. The drone cameras and the Canon Powershot were pre-programmed using the camera’s software interface. The other consumer cameras were initially triggered with an

intervalometer; which was replaced by an open-sourced drone flight controller in 2019. Figure 3 shows configuration of equipment inside the helicopter.



Figure 3. The ipad and the white controller is wirelessly connected to the drone mount. The system captures drone DJI RGB images and powers the multispectral camera. The laptop is connected to the multispectral camera with an Ethernet cable. It is programmed to transfer images from camera to laptop and monitor the camera status and field of view. The system on the ground in the right center side of the image is a drone flight controller. It triggers the prosumer camera while recording the GPS coordinates.

II.B.4. Imaging Locations

Nearly the whole shoreline was imaged with one or more cameras on each flight. Due to curvature of the shorelines and difficulty of the helicopter in tracking the shoreline perfectly, occasionally sections of shoreline were missed. Technical difficulties also resulted in some areas not being imaged during flights. Tables 2,3,4 below summarize the drone RGB and multispectral data availability from each helicopter flight. We acquired significantly fewer images with the other RGB cameras. Note that the multispectral camera captures five images at different wavelengths in a single shot. Although images were collected over the entire lake shore, we selected five study sites to develop and evaluate the metaphyton identification approach. The sites (shown in Figure 4 a-e) are Hidden Beach (39.220810° , -119.929051°), Lakeside (38.960246° , -119.951522°), Regan Beach (38.944674° , -119.983436°), Skyland (39.015494° , -119.953546°), and Sugar Pine (39.056015° , -120.112875°). The boundaries of the study sites used for image analysis are also indicated.

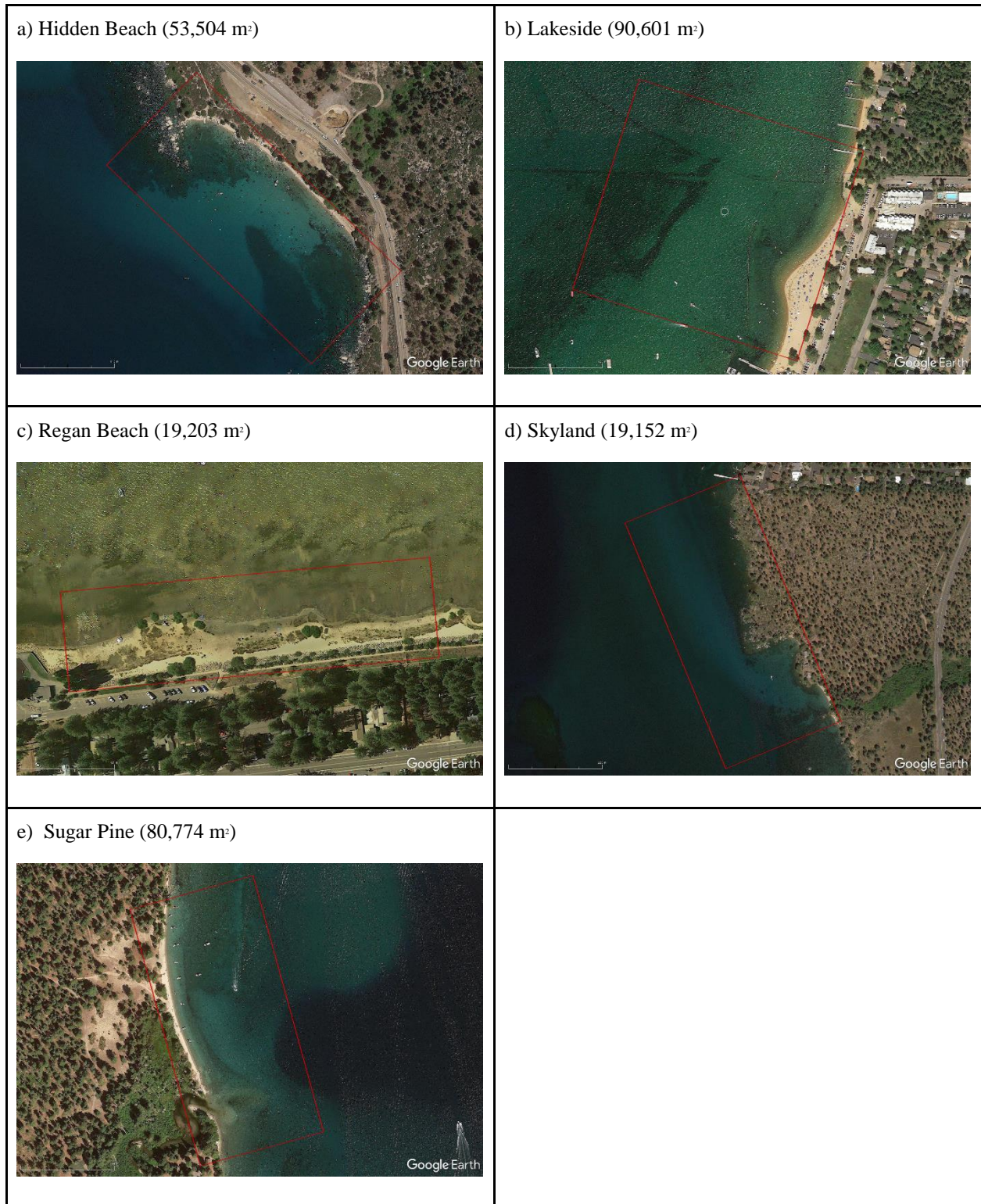


Figure 4.a-e. Five study sites selected to develop and evaluate the metaphyton identification approach. Red lines represent boundaries used for analysis of metaphyton percent cover analysis.

Table 2. Summary of data availability for images taken on helicopter flights in summers of 2018 and 2019.

Date	07/03/2018	08/01/2018	09/06/2018	08/01/2019	09/04/2019
# of DJI Images available	668	1743	1427	1387	1456
# of micasense Images available	573	6624	4690	11373	2892
Section	East shore From Marla Bay to Regan Beach + South shore from El Dorado to Camp Richardson	Full Shore + East Shore from Lakeside to Regan Beach	Full Shore	Full Shore	Full Shore + East shore from Skyland to Regan Beach

Table 3. Summary of DJI RGB image availability for helicopter flights in summers of 2018 and 2019.

Date/ Site	Regan Beach	Hidden	Skyland	Lakeside	Sugar Pine
20180703	✓	Missing	Missing	✓	Missing
20180801	✓	✓(partially covered)	✓(partially covered)	✓	✓
20180906	✓	✓(partially covered)	✓	✓	Missing
20190801	✓	✓	✓	✓	✓
20190904	✓	✓	✓	✓	Missing

Table 4. Summary of Micasense multispectral image availability for helicopter flights in summers of 2018 and 2019

Date/ Site	Regan Beach	Hidden	Skyland	Lakeside	Sugar Pine
20180703	✓	Missing	Missing	✓	Missing
20180801	✓	✓(partially covered)	Missing	✓	✓
20180906	Missing				
20190801	✓	✓	✓	✓	✓
20190904	✓	Missing	✓	✓	✓

II.B.5. Evolving methods for inflight imaging

Throughout the study some difficulties were encountered with imaging. The following briefly describes some of the improvements made to the inflight imaging equipment and methods to obtain better quality and consistent images and to make the imaging system more efficient and reliable. It also points out where additional work will be needed to solve certain issues.

- We stripped down a drone and mounted it on the helicopter to collect RGB images with a drone camera. This camera provided the most reliable imaging throughout the study at a resolution of 9 cm/pixel. In addition, we experimented with four other commercially available RGB cameras. We did many mount adjustments and test flights in an attempt to acquire sharper RGB images at higher spatial resolution. Initially, we triggered the four cameras using an intervalometer. It was difficult to use these images for spatial analysis because the collected images lacked GPS coordinates. Therefore, in 2019 we engineered and programmed a drone controller system to record GPS coordinates every time it triggered the cameras. The system worked well during the first flight in 2019 but malfunctioned during the second flight. We hired an undergraduate student with electrical engineering and drone building background to investigate the issue and improve the system for future flights.
- While the multispectral camera has an internal GPS and an automated triggering function, it had data storage and reliability issues. Storage issues were addressed by integrating the camera with an Ethernet port and programming a laptop to transfer data from and empty storage in the camera during flight. Reliability issues related to the multispectral camera sometimes malfunctioning and continuously rebooting during a flight. We suspect this issue was associated with a faulty power plug on the drone system. This issue will require additional testing to solve.
- As mentioned above, some areas of shoreline were missed in imaging due to frequent bends and the inability of the helicopter to exactly track right over the shoreline at constant speed. Additional evaluation of flight paths could be made to ensure collection of images in high interest areas. In some areas, missing portions of shoreline may not be considered critical based on monitoring needs.

II.B.6. Image analysis

II.B.6.a. Image preprocessing

Civilian compact GPS devices with a clear view of the sky have a horizontal error of 3-5m, and the error is much higher vertically. Since our GPS device was positioned on the side skid step, the GPS did not have a clear view of the sky and was subject to inconsistent error. Unlike cameras on a drone with a gimbal mount or on a plane, cameras on a helicopter rarely point exactly perpendicular to the earth surface. The location uncertainty and deformation of images due to pitch, yaw, roll orientation of the helicopter makes geo-registration and stitching of images challenging.

Initially, we used a commercially available drone image processing software, Pix4D, to geo-register, correct for distortion, and stitch images. Pix4D works very well on drone images, especially on images with heterogeneous surfaces. It could automatically identify common points between images and use that information to preprocess images. The full workflow generally

required little manual labor. Unfortunately, Pix4D performed poorly on helicopter images over the lake. We tried various settings and manually selected common points among images in Pix4D, but the quality of the output was inconsistent. There is a possibility of implementing advanced computer vision algorithms to automatically identify a large portion of common points to enhance the image preprocessing results, as well as automating the set up and execution of Pix4D process over the entire Lake Tahoe shore. For now, we chose a different preprocessing approach for images collected over our study sites. Although this approach requires manual execution, we have more control over the process, thus the results are more consistent.

For each study site, we overlaid the sharpest historical satellite images available on Google Earth with the boundary of the study area, and took a snapshot as seen on Figure 5. The snapshot was not geo-registered, therefore we extracted the latitude and longitude information of the four corners of the study area boundaries on Google Earth and used the four corners to geo-register the snapshot on ArcMap. Specifically, we opened the snapshot and set the data frame's coordinate system in ArcMap. By using ArcMap's Georeferencing Toolbar, we assigned real-world coordinates to reference points on the images. After geo-registering the Google basemaps, we used the Georeferencing Toolbar again to align all drone RGB images captured within each study site over the Google basemaps. We repeated this task for all images taken in both 2018 and 2019. It was challenging to pick reference points that are visible on both the high-resolution drone RGB images and the Google satellite base map, especially since the pairs are often captured from months to years apart. There was road construction at Hidden Beach, making projection of drone RGB images over the Google satellite basemap even more difficult. To ensure accuracy, we chose at least ten Ground Control Points (GCPs – which are features in images for which the ground coordinates are known) for each image. If multiple images were needed to cover a study area, we did additional alignment between each pair of adjacent drone RGB images by using reference points that are visible on the overlapping areas. To better detect changes occurring at the study site between two summer months in 2018 and in 2019, we further aligned images taken from one month over the images taken from a different month of the same year. Although the whole process is time-consuming, it is more rigorous than the Pix4D automated approach.

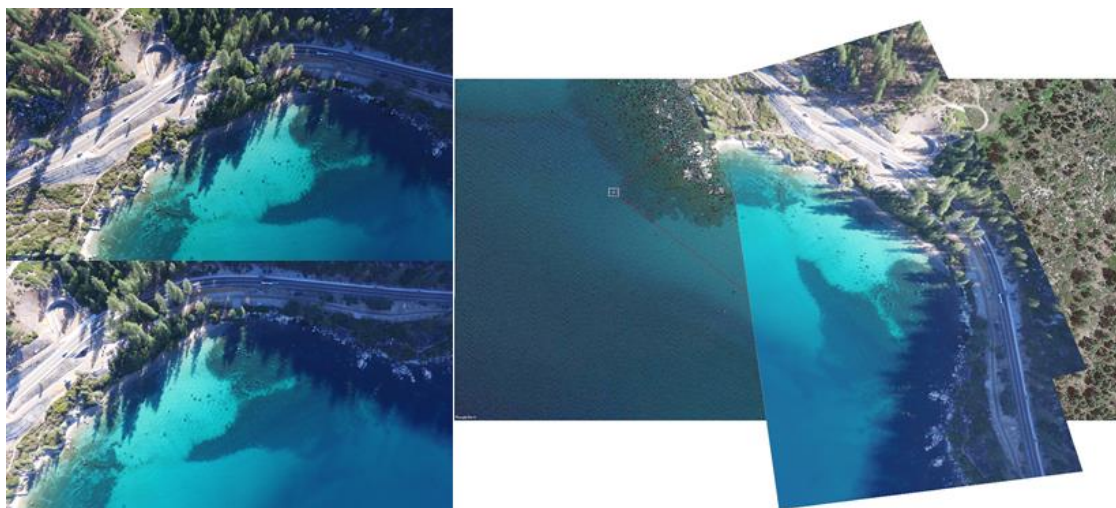


Figure 5. Demonstration of manually geo-registered RGB images (DJI-0825, 0826) over Google Earth basemap.

II.B.6.b. RGB and Multispectral Images Results and Utility

While RGB images can be visualized immediately after flight, multispectral images require additional pre-processing for image visualization and analysis. Unlike RGB cameras, the multispectral camera has five separate lenses, with each capturing images in a specific range of wavelength (Blue, Green, Red, Red Edge, and Near Infrared). We modified an open source tool (<https://github.com/micasense/imageprocessing>) to align and combine the five images from different wavelengths into a single RGB/False Color image for further analysis. We also developed an approach to identify shadow and above water objects with the multispectral images (Figure 6).

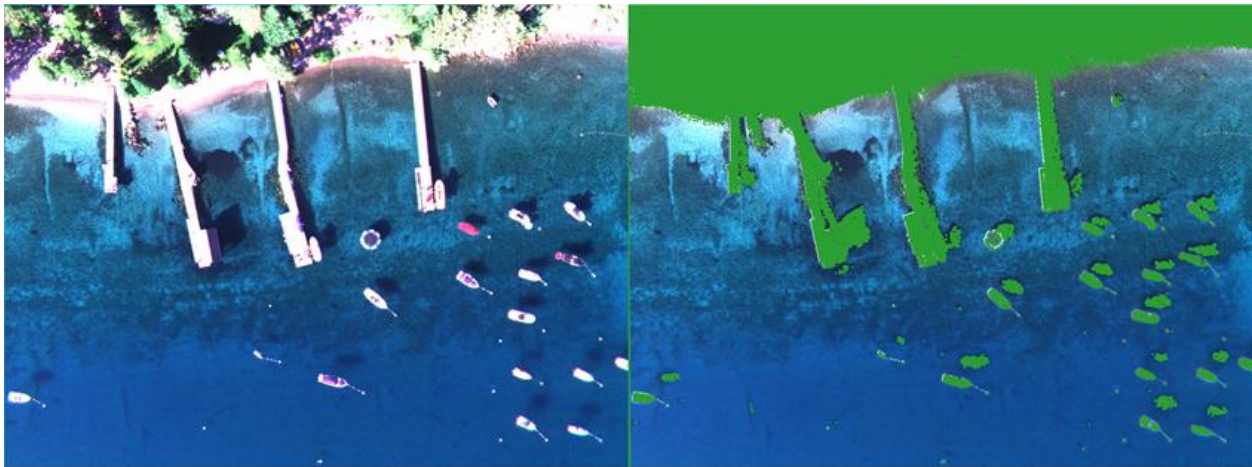


Figure 6. Demonstration of using multispectral images to remove above water objects and shadows.

The multispectral camera provides some advantages over RGB cameras. First, it has an internal GPS and orientation sensor. This information could potentially be extracted to geo-reference and project images. Second, cameras usually adjust the value of image pixels to provide a visually appealing image. The multispectral camera recorded the parameter for adjusting the image, allowing us to perform the correction. This would be useful if we were to utilize spectral signatures for classification. Third, the near infrared image is needed for our current method to automatically identify shadow and above water objects. However, the multispectral camera has some disadvantages when compared to RGB cameras. First, it has a smaller field of view. Although a smaller field of view reduces image distortion, it creates challenges in capturing images that include both shore and water. If there are too few shore pixels within an image, finding reference points for image geo-registration and stitching would be extremely difficult or even impossible. If there are too many land pixels captured within an image, we might miss out on capturing the offshore algae clusters. It is possible to address this issue by putting two multispectral cameras on both sides of the helicopter, but a single camera costs nearly \$5000 and we will need to develop a photogrammetric algorithm for this specialized use. Nonetheless, it may be possible to pursue research in this direction by borrowing two multispectral cameras from other labs at the University.

II.C. Results

II.C.1. Visual analysis of helicopter images and field ground-truthing

Images were provided by the UCD LAWR researchers to TERC field team members for review usually within several days of collection. RGB images were downloaded either to Google Earth Explorer (in 2018), or to Google Drive. Individual photos were examined and areas with possible metaphyton algae or other unknown substrate identified. Some of the characteristics looked for in the images included: patches of relatively uniform, dark green coloration relatively close to shore and patches or objects with green, tan or dark coloration. This process usually took about a day for one researcher to complete. The TERC field crew then visited a portion of the identified sites, either by boat or from the shoreline, to ground-truth and check what was observed in the image. Appendix 1 presents the sites selected for ground-truthing, together with ground-truthing results for 2018 and 2019. Figure 7 shows a map of ground-truthing locations around the lake as colored dots, where the color and shading in the dot represents: presence of metaphyton, aquatic vegetation, aquatic vegetation with associated algae, heavy periphyton (at one site); stretches of shoreline with known Asian Clam (*Corbicula fluminea*) are also shown.

Most of the areas of metaphyton algae (green dots or green triangles in Figure 7) were found along the south and south east shores of the lake, extending from Tallac Point to Glenbrook Bay. From Camp Richardson along the west, north and north east shore areas very few areas of metaphyton were observed. Very light algae were observed associated with patches of woody debris in Rubicon. Very small amounts of algae along the bottom were observed at Hidden Beach in 2019. These were generally isolated small clumps of detritus, with some algae associated and were below the minimum size (9cm or about 3 inches) that could be distinguished in helicopter images. One site near Tahoe City did have metaphyton, mixed in with a growth of low-growing aquatic grasses and associated green filamentous algae (*Zygnema*). The stretches of shoreline with known populations of Asian Clam include portions of Emerald Bay extending around the south shore and up the southeast shore over to Glenbrook Bay. There are also some populations present near Sand Harbor.

Looking at the results of ground-truthing in more detail, some additional patterns were present. Along the south shore there were several areas with lines of metaphyton just offshore of El Dorado Beach (see Figure 8), Regan Beach (see Figure 9), and the Timber Cove area. These appeared to occur in areas where the relatively flat bottom, transitioned to a steeper slope to the beach (metaphyton tended to accumulate at the base of the slope). Also patches developed in areas of shoreline near rocky breakwaters. At Regan Beach, El Dorado Beach, Timber Cove, offshore of Lakeside Beach and Marina, the metaphyton tended to accumulate in relatively uniform layers of loose metaphyton which was typically a mix of several different types of filamentous green algae (*Zygnema*, *Spirogyra*, *Mougeotia*, *Oedogonium* and others). The metaphyton layer offshore at Lakeside was quite expansive (approx. 75m X 200m) and relatively thick (4-6 inches) (see Figures 10,11).

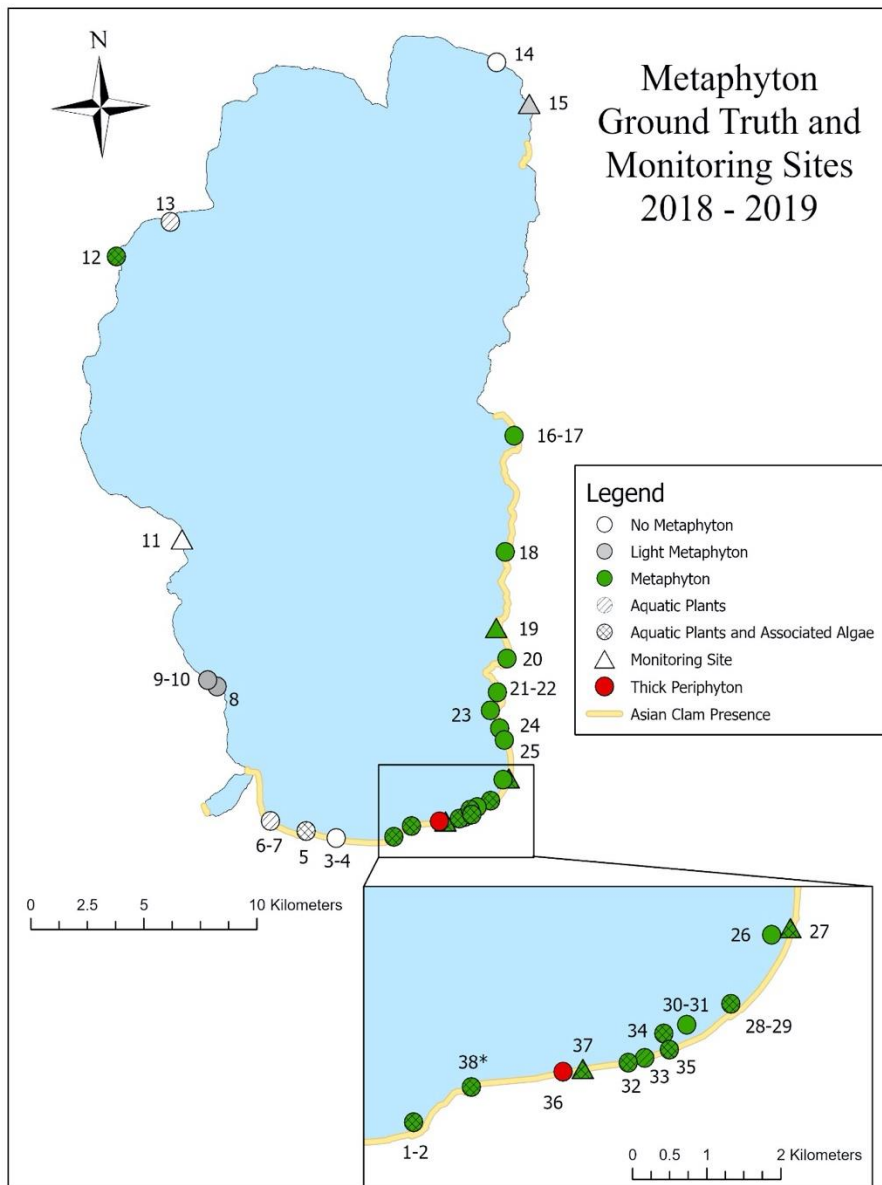


Figure 7. Locations of ground-truthing sites selected after reviewing images collected from the helicopter and results of ground-truthing. Presence of metaphyton (green), absence (no color), light metaphyton (gray), vegetation (///), vegetation with associated algae (cross-hatched), areas where Asian Clams are present, and an area of heavy summer periphyton growth (red) are shown. If metaphyton was observed on at least one sampling date it was indicated as present.

Aquatic plants also contributed to some of the green or dark shading observed in images along the south shore from Tallac Point (just east of Taylor Cr.) over to at least Lakeside at Stateline. Substantial amounts of both low-growing aquatic plants, as well as taller aquatic vegetation (such as the invasive plant Curly Leaf Pondweed, *Potamogeton crispus*) was present

at Regan Beach. Aquatic vegetation was also present along with metaphyton at El Dorado Beach and offshore east of El Dorado Beach, near Ski Run Marina, in the swim area at Lakeside and other areas.

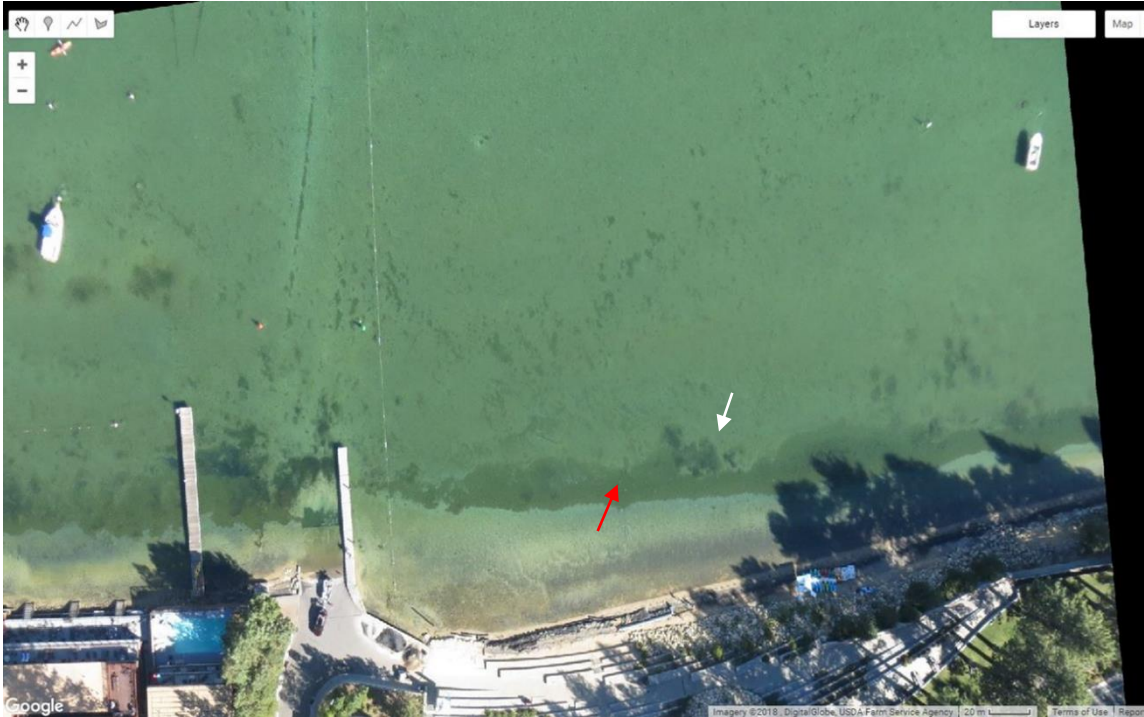


Figure 8. El Dorado Beach 9/6/18, green line of metaphyton offshore, from helicopter. The metaphyton appeared to accumulate where the relatively flat bottom changed to a steeper slope to the beach. Metaphyton is indicated by red arrow, aquatic plants were also present (white arrow).

At many of the sites, the aquatic vegetation had filamentous algae or other algae associated with it. This was true of Regan Beach, El Dorado Beach, near Ski Run and in the nearshore area at Lakeside. The offshore area east of El Dorado Beach had much bright green filamentous algae associated with low-growing vegetation. The aquatic vegetation and filamentous algae associated with aquatic vegetation made it challenging to discern the metaphyton in the aerial images. The association of algae with the aquatic plants in the south portion of the lake in the summer suggests it could contribute to the drifting metaphyton when it breaks free from the plants.

Along the southeast section of shore primarily metaphyton algae was present. In Zephyr cove, some lines of metaphyton were observed in between sand riffles nearshore. Near Nevada Beach, there appeared to be some metaphyton over Asian clam shell beds. Accumulations of green filamentous algae metaphyton were observed along a water pipe extending offshore near Kahle Drive.

A valuable result of the helicopter imaging was that it located metaphyton in areas we were previously unaware it was present at. One of these sites was in water about 7m deep off a section of shore just south of Skyland, NV. The patches appeared as small dark blotchy areas or green patches in images (see Figure 12) from that area in Aug. and Sept. 2018 and in Sept. 2019. Ground-truthing revealed these patches to be relatively large masses (some patches as big as 3X5 meters) of green filamentous algae metaphyton (identified as *Mougeotia*, *Zygnema* and *Spirogyra*) (see Figures 13,14). Areas of the bottom also had smaller clumps of metaphyton algae. The images also showed many white patches slightly further offshore, which were found to be large patches of Asian clam shells, with partial coverage with algae or metaphyton in some



Figure 9. Regan Beach Park and areas of metaphyton nearshore (red arrows show examples), with many patches of aquatic plants nearby (white arrows show some examples), 8/1/19 RGB image from helicopter.

cases. After confirmation of metaphyton at Skyland, we included this site as one of our five study sites.

One other area where such large green patches were observed in images was a buoy field north of Cave rock in Aug. 2018. The green patches appeared suspended in the water creating dark shadows underneath on the bottom. In ground-truthing of this site many days later however, no patches were found to be present. In the interim period between imaging and ground-truthing a period of winds had occurred. The patches had likely either moved or had been dispersed due to the lake currents.

The helicopter images also showed distinct green patches in Marla Bay in September 2019. Significant metaphyton has also been observed in the past in Marla Bay, (i.e. in 2008 when large amounts of bright green *Zygnema* were observed). In helicopter imaging for the present study, a

relatively large area of bright green patches of metaphyton were detected in the buoy field near the Round Hill Pines pier in Sept. 2019 (Figure 15). Ground-truthing revealed the bright green patches to be metaphyton, (predominantly a filamentous green algae *Mougeotia*), along the bottom. This metaphyton green filamentous algae was quite visible from the pier and also from boats in the buoy field (Figures 16,17).

Images collected for much of the west, north and northeast shoreline regions were free of material along the bottom which appeared to be metaphyton. Black patches were seen in images from a few areas (i.e. some nearshore sandy areas in Rubicon Bay (see Figure A2-1 in Appendix), at Sugar Pine Pt. and at the northeast corner of the lake near Incline Cr.). Ground-truthing showed these often to consist of woody debris. Similar black patches were seen along parts of the south shore (i.e. near Baldwin Beach and Camp Richardson) and along the south east shore in Zephyr Cove.

We were also previously unaware of the patches of aquatic grasses and associated filamentous algae and metaphyton detected near Tahoe City by the helicopter imaging in September 2019 (see Appendix figure A2-2). There, two large green patches were observed along the shorelines both south and north of the outlet to the Truckee River. Ground-truthing revealed these areas to have low-growing aquatic grass, with substantial filamentous green algae (*Zygnema*) associated with it. There were also bright green patches of metaphyton between many of the grass-algae patches and aggregations of filamentous green algae metaphyton in some bottom depressions. The predominant algae in this metaphyton was also *Zygnema*. A similar area of aquatic grasses was identified at Lake Forest, however there was no associated filamentous algae or metaphyton there.

There were also some incidences where no metaphyton patches were apparent in the images, yet when the site was visited for in-lake work, some algae was observed to be present. This was the case for Elk Pt. which was visited 7/24/19. There, isolated very small (~ a few inches long) clumps of green metaphyton along the bottom were observed - yet metaphyton was not apparent in the helicopter images taken about a week later on 8/1/19. It is likely the small clumps were less than the minimum size to image from the helicopter on this date. At Hidden Beach in 2019 sampling, isolated clumps of detritus and algae, several inches long were observed along the bottom while snorkeling. These also were less than the minimum size of detection for the UAV imaging. They also had neutral coloration which made them difficult to see from the surface.

Finally, there were other areas where quite heavy algae growth was observed in 2018 and 2019 imaging. One of these areas was an extremely heavy filamentous algae growth at the mouth of the Upper Truckee River, in August and Sept. 2019 images. The aerial images showed patchy green areas right on the surface and slight orange shading underwater (see Appendix Figure A2-3). Ground-truthing revealed there to be both surface and subsurface vegetation with extremely heavy growth of a filamentous Xanthophyte algae (*Tribonema*) among the vegetation (see Appendix figure A2-4). Due to poor clarity of the water and thick concentrations of algae in the

water column, it was difficult to know to what extent metaphyton was present on the bottom there.

The other area of note was a very heavy growth of periphyton (attached algae) consisting of a green filamentous algae called *Cladophora* which was growing on boulders along the wall bordering Regan Beach Park. This algae was observed during several site visits to the area and was found to be observable in some of the helicopter images (see Appendix Figure A2-5). The *Cladophora* had stringy filaments up to 6 inches long (see Appendix Figure A2-6). It is particularly notable since it is one of the few locations around the lake where heavy growth of summer periphyton attached to rocks was observed. *Cladophora* can be associated with more fertile water quality conditions (Wehr et al., 2015).



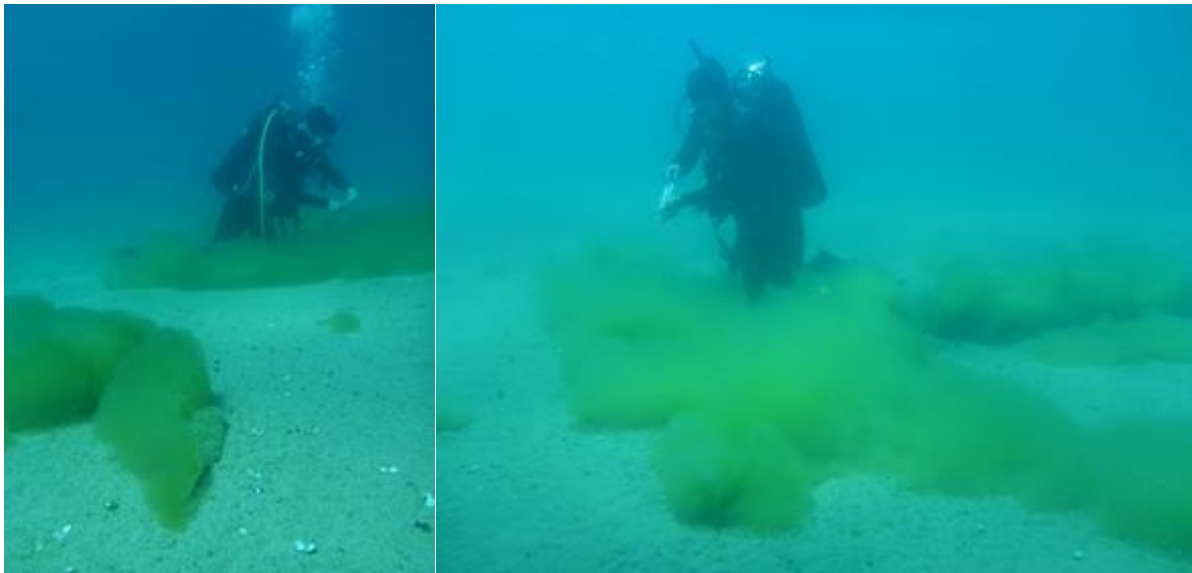
Figure 10. Large metaphyton algae patch offshore of Lakeside Marina, image from helicopter 9/4/19.



Figure 11. Diver collecting filamentous green algae from Lakeside metaphyton patch. The metaphyton formed a uniform layer above the sediments about 4-6 inches thick.



Figure12. Skyland south point, very small dark objects offshore are metaphyton (filamentous green algae) patches (red arrows), further offshore, white patches of clamshells can be seen (white arrows) image from helicopter, 9/4/19.



Figures 13,14. Large metaphyton patches (filamentous green algae primarily *Mougeotia*, some *Zygnema*) at Skyland, 9/3/19. Clams shells on the surface are evident in Fig. 13.



Figure 15. Metaphyton (red arrows show examples) in buoy field near Round Hill Pines pier, Marla Bay 9/4/19, zoom-in on section of RGB image from helicopter.



Figures 16,17. Above and below water views of filamentous green algae metaphyton, taken during ground-truthing at Round Hill Pines 9/11/19.

II.C.2. Helicopter imaging and water intakes

The helicopter images were also reviewed to see the extent to which water intake pipes were visible and whether metaphyton was also present in the same vicinity. Though water intake system pipes were visible, the terminal ends or actual water intakes in some instances were beyond the field of view, or too deep to see the bottom around the intake. Metaphyton algae was however, visible near some of the pipes extending away from shore. At those sites, accumulations of metaphyton were observable along one or both sides of the pipe. In a limited number of areas, the terminal end of the water pipe was visible in very clear water areas. The helicopter imaging can indicate presence of metaphyton in the nearshore region through which a pipe passes.

II.C.3.a. Development of method for distinguishing metaphyton, vegetation and other substrate from water, based on helicopter imaging

Metaphyton algae was difficult to distinguish from aquatic vegetation and aquatic vegetation with associated algae in images. To estimate the distribution of metaphyton it was necessary to discern aquatic vegetation from the metaphyton. The use of multispectral imaging cameras was tested to see if spectral characteristics could be used to separate algae from plants and other substrates. However, the trials done using the multispectral camera showed that the spectral signature differences between these submerged substrates was very small. This phenomenon was driven by two factors. First, pure water absorbs most of the sunlight and reflects only 5-7% of it back to the sky. Second, the varying depth of water causes spectral signatures of different submerged objects to be indistinguishable on an image. For example, a metaphyton patch in shallow water may have an identical RGB value of relatively deeper pure water. So it was not possible to use the multi-spectral characteristics to separate metaphyton from vegetation and other substrate types reliably.¹

¹ We also did follow-up work, investigating the capabilities of a spectral radiometer to distinguish underwater algae from above the surface. A SVC HR-1024i spectral radiometer was used to measure spectral characteristics of algae associated with underwater vegetation near Regan Beach. The results of that testing indicated it was difficult to discern the particular spectral signature of the algae underwater, from above water. There were substantial differences in the spectral reflectance values in multiple measurements of the same target from the boat (which was subject to movement), which made it difficult to conclude what was the expected spectral signature from above water. To determine if a better multispectral imaging system might be able to detect differences, testing in a more controlled environment (e.g. sample the algae and vegetation, and soil, submerge them at different depths under consistent lighting) would be needed. On top of paying premium to narrow and specify the sensor wavelengths, we were not sure if it would work in aerial imaging.

We used a “change detection method” for distinguishing metaphyton at sites from vegetation and other substrates. In simple terms, we first overlaid images captured on two different dates, then highlighted the water regions that have underwater substrates, and compared the extent of the location of substrates between the two dates. If a patch of substrates moved or grew or disappeared, it is very likely that patch was metaphyton. A more detailed discussion of the method development and current method is presented in the following. We tried dozens of image classification approaches, from executing out-of-the-box algorithms (e.g. spectral information divergence, spectral angle mapper, neural net) in ENVI, a professional remote sensing software, to developing multi-steps algorithms on Python (e.g. use of a moving window to obtain dominant color value, classification with k-mean, and Random Walker segmentation). The method described below is our most recent approach. It only uses the DJI RGB images, and is developed based on several insights we discovered from previous tests. It is simple in concept, easy to implement, and consistent among images. The manual point selection portion needs to be done locally, but the remaining process can operate both locally or over the cloud using Google Colab. To view the automated script, visit:

<https://drive.google.com/open?id=1ytixjznHj1OIUwFxU0CYYcp-IOKAQEah>.

Manual Point selection: We wrote a python script using the open CV module to assist the manual point selection process. For each RGB image at our study sites, we selected dozens of points of clear water pixels; those points are selected for covering the whole picture horizontally, vertically and diagonally. We also selected points associated with submerged objects (e.g. metaphyton, rocks, aquatic plants).²

Convex Hull: Upon selecting clear water pixels, the previous program automatically recorded the RGB, and the Hue Saturation Value (HSV) of the pixel on a table. HSV is an alternative to RGB in representing colors. In Figure 18, we plotted the HSV Hue and HSV Value of selected pixels (blue circle as pure water and orange square as submerged objects) on the x and y axis. With Hue and Value of pure water pixel, a convex hull is computed and visualized as a dash line in Figure 18. Using the lower boundary of the hull, and extending the HSV Value of points that have the smallest or largest hue value, we defined a HSV Value threshold to separate submerged object pixels from pure water. The approach works very well at Sugar Pine, Regan Beach, and Lakeside, but not as well at Hidden Beach in 2019 and at Skyland.

² Note, these points may potentially be useful for developing a more advanced and automated approach for metaphyton recognition.

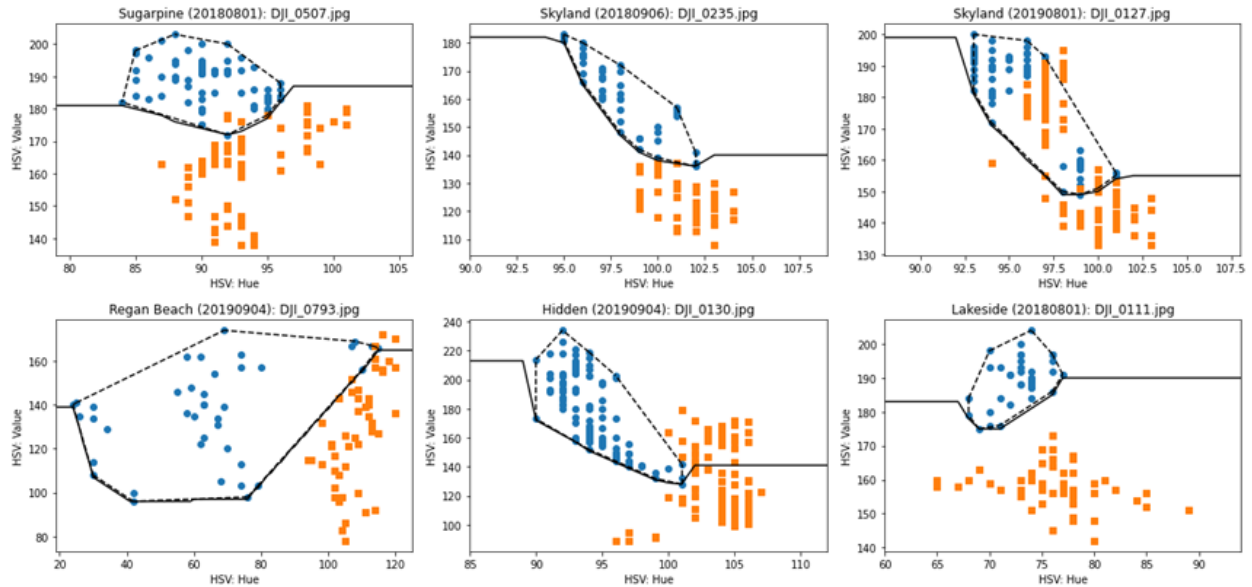


Figure 18. Demonstration of a Convex Hull.

II.C.3.b. Distinguishing metaphyton from vegetation and other substrate, and protocol for determination of percent cover

Once the threshold is derived for each image using Convex Hull, it is applied over the geo-registered RGB image to generate a mask, with 0, 1, 2 representing image border, pure water, and submerged objects respectively. If multiple images were needed to cover a study area at a given date, both the masks and geo-registered RGB images were mosaicked. (Table 5 presents a list of the images used for analysis.) Then, a pair of masks from two different dates was resampled into an identical spatial resolution on the same grid. The two masks were compared to identify: (a) a common area captured for the two set of images; (b) submerged objects that remained stationary between two dates; (c) submerged objects that remained stationary were visible on the earlier date but disappeared later; and (d) submerged object that were not visible on the earlier date but emerged on a later date. The stationary, disappeared, emerged submerged objects were encoded as 1, 2, 3 respectively.

Table 5. List of input images used in this study

Site	Date 1	List Pic Used	Date 2	List Pic Used
Sugar Pine	20180801	0507,0510	20190801	0298,0299
Skyland	20180801	0784,0788	20180906	0232,0235,0238
Skyland	20190801	0123,0127	20190904	0408,0411,0412
Hidden	20180801	0142,0143,0144,0145	20180906	0903
Hidden	20190801	0825,0826	20190904	0130
Lakeside	20180801	0111	20180906	0422
Lakeside	20190801	0619,0620	20190904	0682
Regan Beach	20180703	0209	20180906	0648
Regan Beach	20190801	0667	20190904	0793

Because convex hulls with only RGB images cannot distinguish water from above water objects, we manually modified the study area boundaries on ArcMap to exclude above water structures along the shore. The boundaries were then rasterized into the same resolution and grid of the masks. This enabled us to compute how many pixels in the image were water, and how many were stationary submerged objects, how many pixels disappeared, or emerged. With this information, we estimated the maximum percent cover of metaphyton using either stationary+disappeared or stationary+emerged submerged object pixels, whichever has the largest value. We also estimated the minimum percent cover using either disappeared or emerged submerged object pixels, whichever has the smallest value.

II.C.4. Results for estimates of metaphyton percent cover in 2018 and 2019 using helicopter imaging

The results for estimation of percent cover using helicopter images are presented in Table 6. Images graphically presenting determination of percent cover are shown in Figures 19 to 23. Relatively broad ranges for percent cover were obtained using the change detection method. In some areas such as Hidden Beach and Sugar Pine, higher values than expected were obtained for percent cover. We believe presence of woody debris at Sugar Pine Point may have contributed to the elevated values there, also difficulties associated with georegistration as described below. At Hidden Beach it's possible woody debris or detritus may have contributed. The high values for Regan were similar to percent cover estimates obtained using the AUV (Section III). At Lakeside, boundaries for the area used for calculation of percent cover were different and so the results were not directly comparable.

Table 6. Minimum and Maximum values for percent cover based on imaging from the helicopter. (Also shown are Site, Date 1, Date 2, Total Valid Px (pixels), % unmoved, % disappeared, % emerged)

Site	Date 1	Date 2	Total Px	Unmoved	Disappeared	Emerged	Min	Max
Sugar Pine	20180801	20190801	11987198	14.61%	7.75%	5.11%	5.11%	22.36%
Skyland	20180801	20180906	13486135	23.12%	4.72%	12.74%	4.72%	35.86%
Skyland	20190801	20190904	13392217	16.61%	12.58%	7.5%	7.5%	29.19%
Hidden	20180801	20180906	8776666	13.19%	3.17%	1.48%	1.48%	16.36%
Hidden	20190801	20190904	5840157	13.37%	15.13%	4.94%	4.94%	28.50%
Lakeside	20180801	20180906	6605827	15.73%	6.69%	4.8%	4.8%	22.42%
Lakeside	20190801	20190904	7902516	14.93%	9.8%	1.81%	1.81%	24.73%
Regan Beach	20180703	20180906	6605744	6.3 %	2.95%	5.3%	2.95%	11.6%
Regan Beach	20190801	20190904	7505227	8.96%	4.57%	1.63%	.63%	13.53%

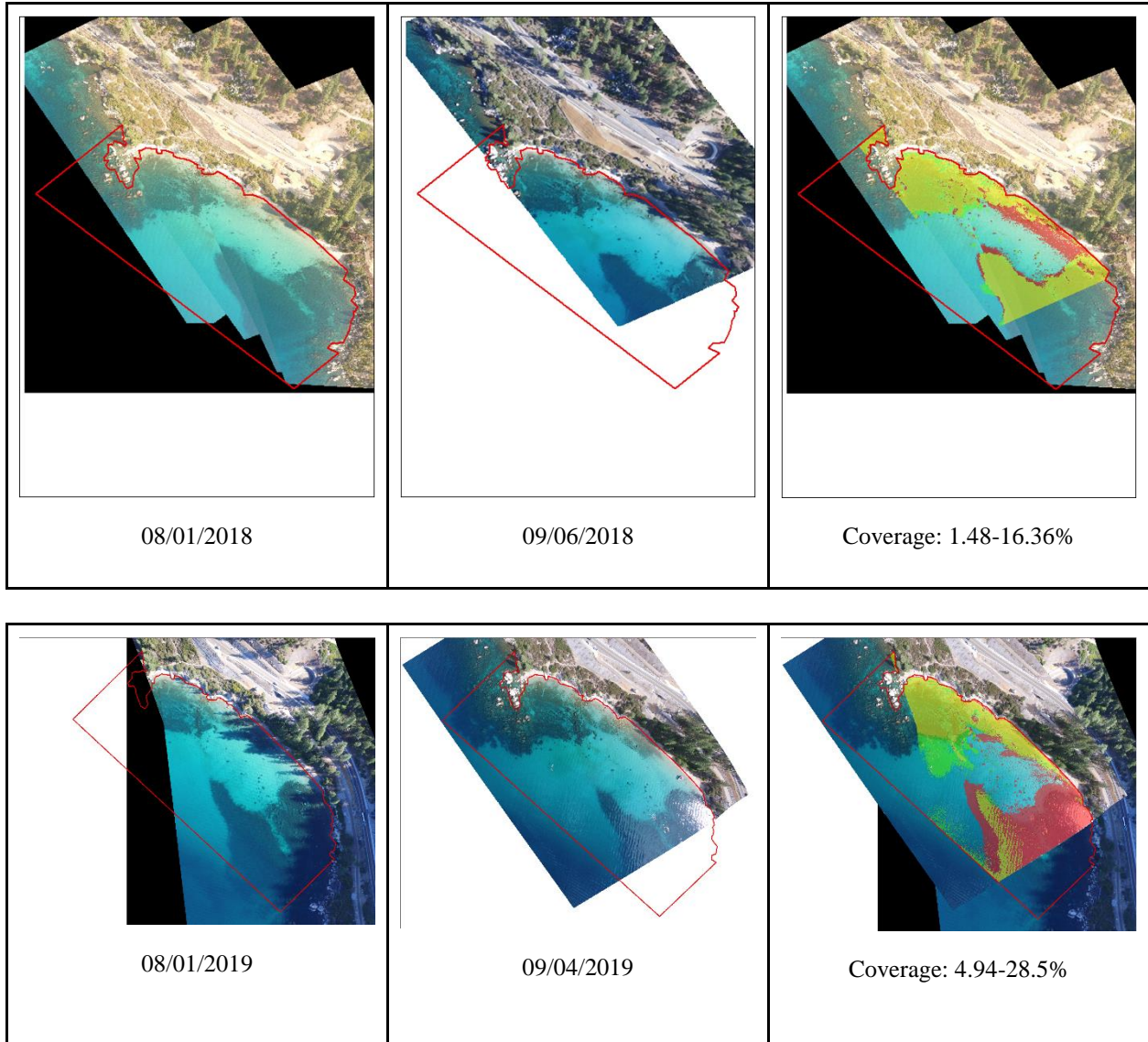


Figure 19. Hidden Beach images used for change detection method and graphic presentation of results for flights in 2018 and 2019. In right panel red shading indicates an 'object' that disappeared between two dates, yellow represents 'object' that appeared in both images, green represents newly emerged 'object'.

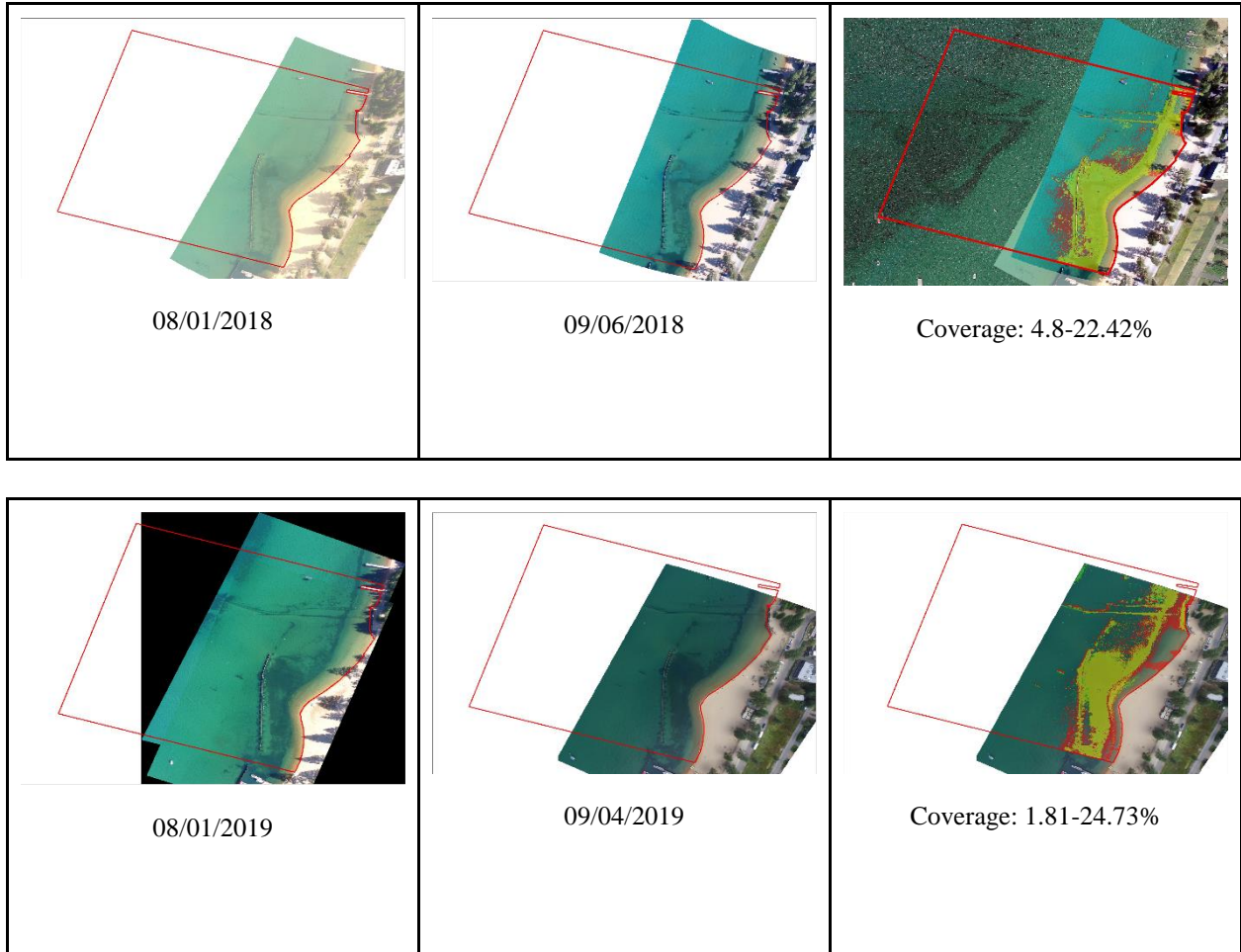


Figure 20. Lakeside images used for change detection method and graphic presentation of results for flights in 2018 and 2019. In right panel red shading indicates an 'object' that disappeared between two dates, yellow represents 'object' that appeared in both images, green represents newly emerged 'object'.

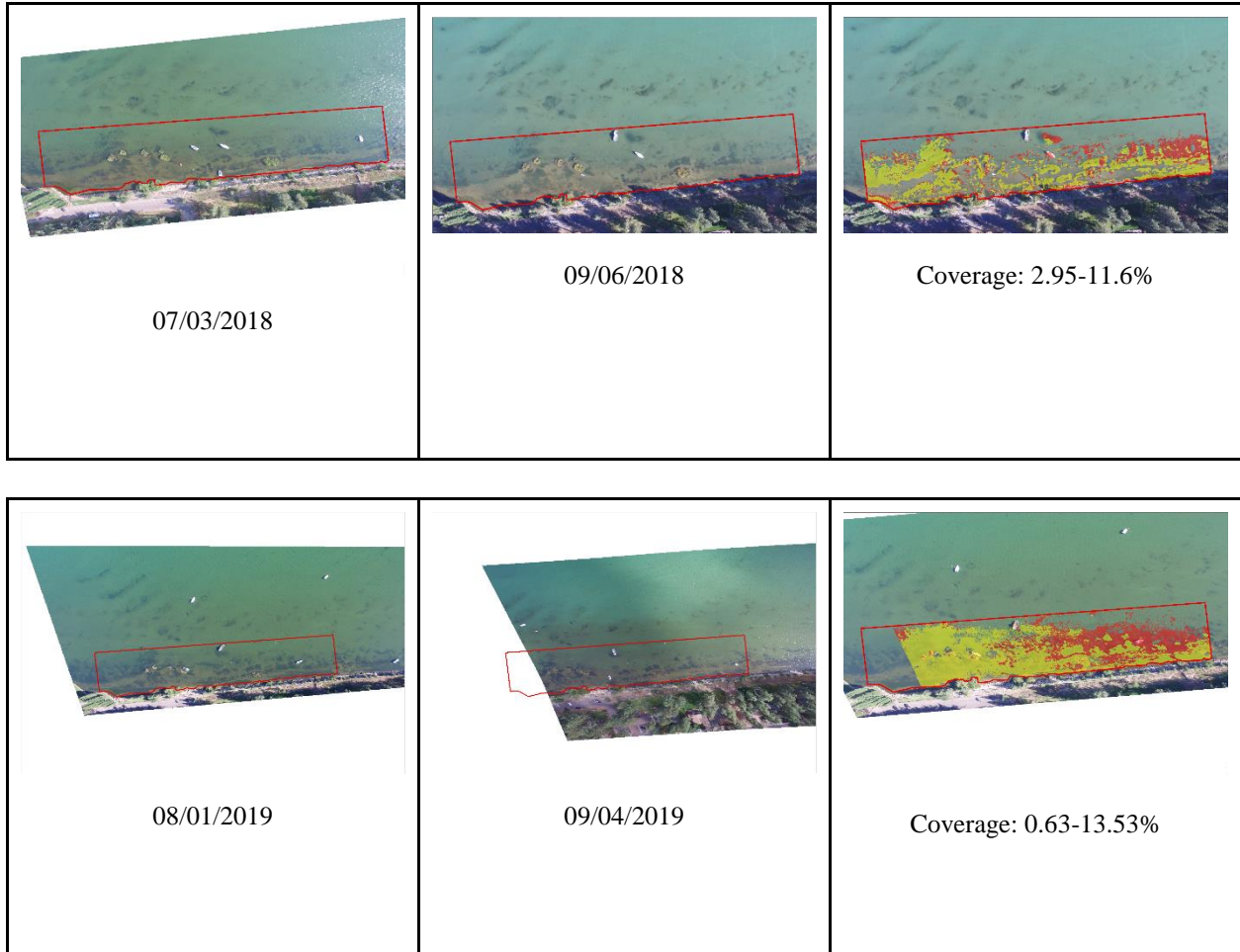


Figure 21. Regan Beach images used for change detection method and graphic presentation of results for flights in 2018 and 2019. In right panel red shading indicates an 'object' that disappeared between two dates, yellow represents 'object' that appeared in both images, green represents newly emerged 'object'.

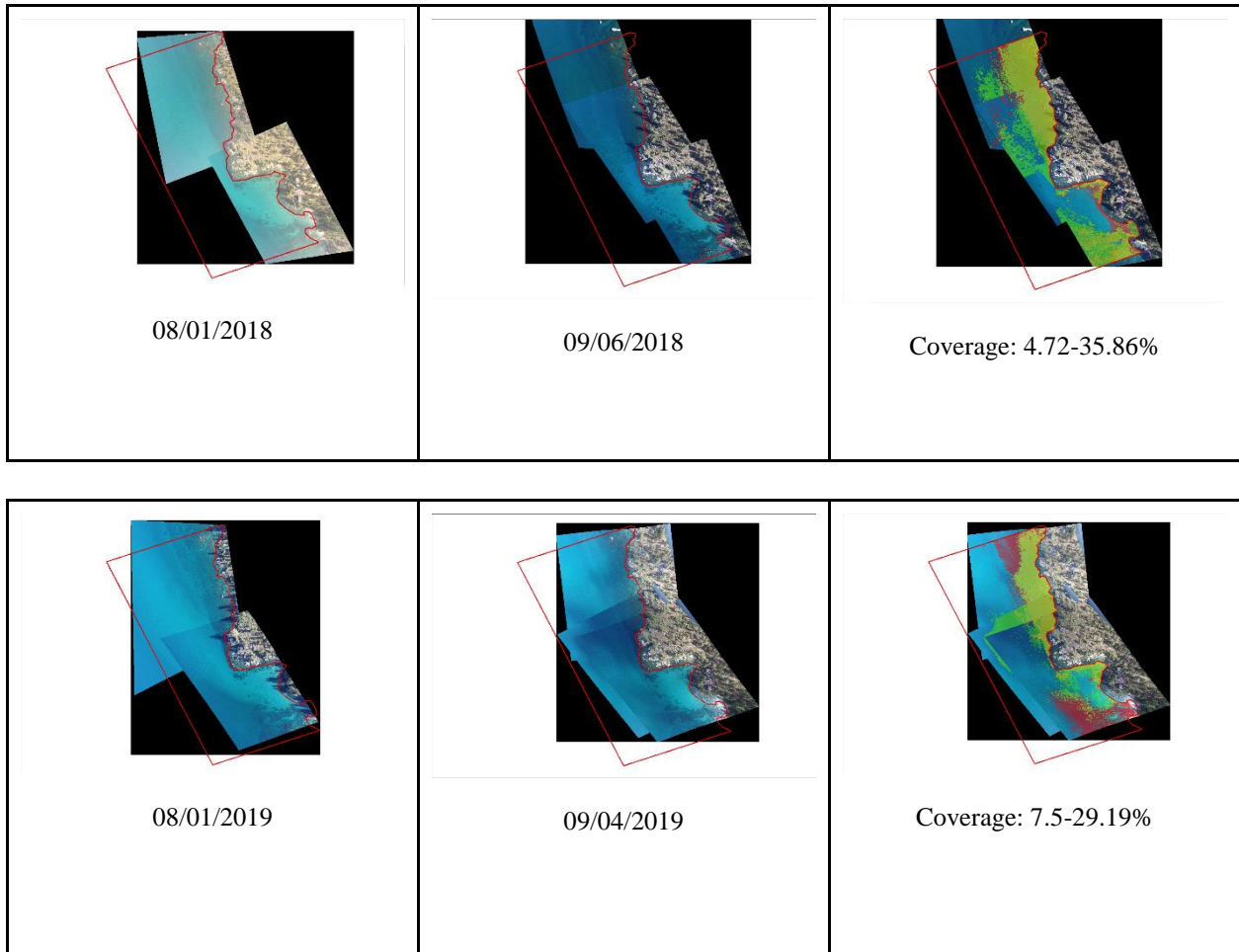


Figure 22. Skyland images used for change detection method and graphic presentation of results for flights in 2018 and 2019. In right panel red shading indicates an 'object' that disappeared between two dates, yellow represents 'object' that appeared in both images, green represents newly emerged 'object'.

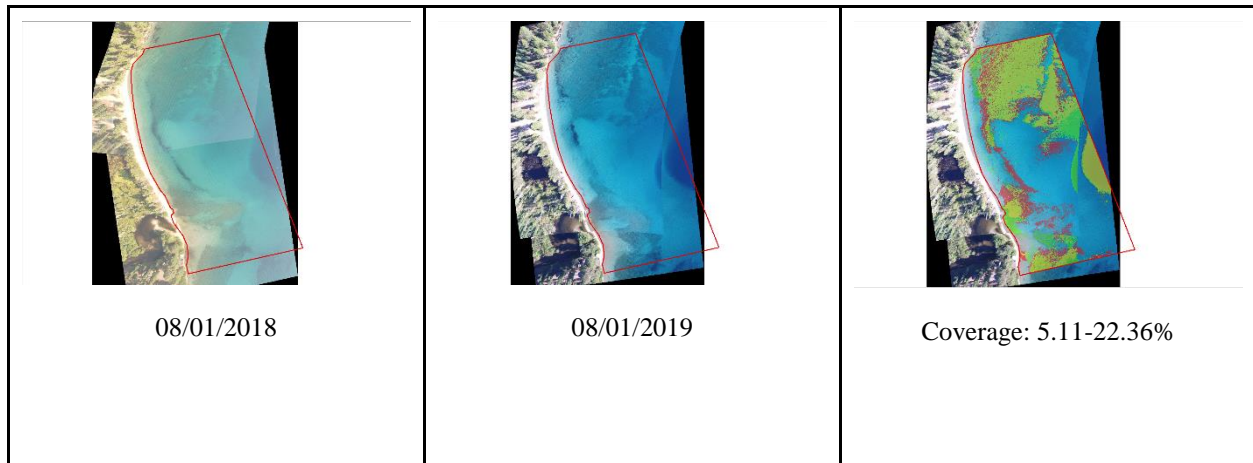


Figure 23. Sugar Pine Point images used for change detection method and graphic presentation of results for flights in 2018 and 2019. In right panel red shading indicates an 'object' that disappeared between two dates, yellow represents 'object' that appeared in both images, green represents newly emerged 'object'.

There are two major bottlenecks in implementing this work over the entire lake shore: (1) *Image geo-registration*: Geo-registration is extremely challenging. Pixels of an object may be misaligned between images, even when the images are manually geo-registered. One example is Sugar Pine Point's 2018 dataset shown below; we tried our best to align the shoreline using the bases of individual trees and other distinguishable features along the shore, but there is still misalignment of water pixels, especially over the deep water portion offshore (Figure 24). This problem would cause misidentification of disappeared/emerged submerged objects.

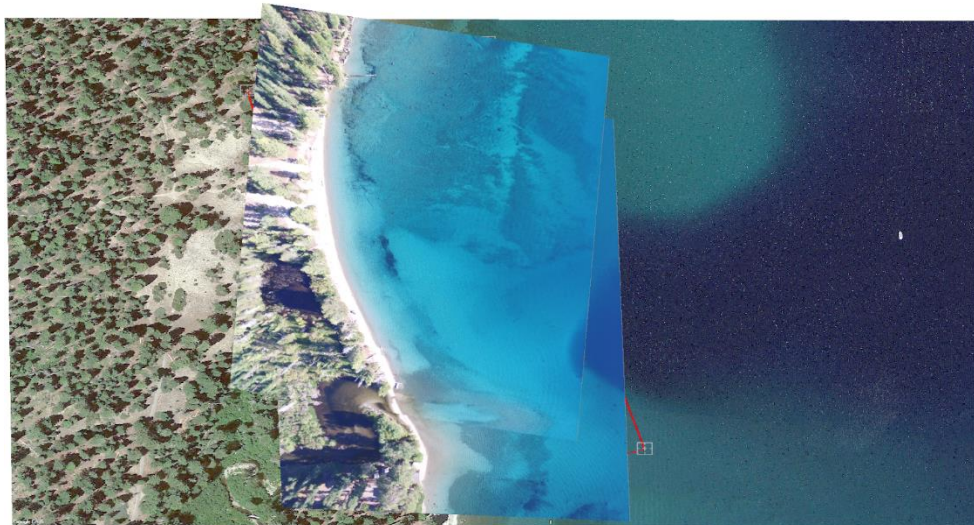


Figure 24. Sugar Pine Pt. 2018 images demonstrating difficulty in perfectly aligning water pixels offshore between images.

(2) *Shadow and Glare*: The color of tree shadows over clear water is often similar to that of metaphyton, so it would very likely be misidentified as submerged objects. Similarly, it is

impossible to discern whether there are objects underwater when the water surface has substantial glare.

We tried multiple approaches of mapping metaphyton. Given the limited time and resources, we picked one promising approach, analyzed, and presented it extensively on this report.

II.D. Conclusions

The helicopter flights were very valuable for identifying the location of metaphyton and aquatic vegetation patches around the lake. Most of the areas of metaphyton algae were found along the south and south east shores of the lake, extending from Tallac Point (east of Taylor Cr.) to Glenbrook Bay in the summers of 2018 and 2019. Along much of the rest of the lake shore, very few areas of metaphyton were observed. Aquatic plants and/or aquatic plants with associated algae, also contributed to some of the green or dark shading observed in images along the south shore from Tallac Point over to at least Lakeside at Stateline. Along the southeast section of shore primarily metaphyton was present both in shallow and deeper areas.

The helicopter imaging identified metaphyton in areas where we were previously unaware of its presence. For instance, at Skyland, NV., large patches of metaphyton were observed, as well as large patches of Asian Clam shells which also had associated algae. Other sites where metaphyton was detected included a site north of Cave Rock and an area of aquatic grasses, associated algae and metaphyton near Tahoe City. Large patches of bright green metaphyton were also observed in the buoy field at Round Hill Pines in September, 2019. Extremely thick filamentous algae growth was found to be growing off of the Upper Truckee River mouth in the summer of 2019 in association with aquatic vegetation. The helicopter proved an extremely valuable platform for visualizing and imaging the whole shoreline and identifying areas of potentially heavy metaphyton and vegetation growth in a short period of time (approximately an hour). However, imaging and image processing proved difficult and time consuming compared to that obtained by the UAV. The specific imaging platform (helicopter or UAV) should be determined by the desired areal coverage and the visual acuity required.

Extensive work and testing was done by researchers with the UCD LAWR remote sensing lab to develop methods and adapt equipment to images all along the shoreline of Lake Tahoe from the Eurocopter EC120B helicopter. Multiple cameras were tested, with a large volume of high quality images and imaging data generated for the Lake Tahoe shoreline in 2018 and 2019. The use of multispectral imaging cameras was tested to see if spectral characteristics could be used to separate metaphyton from plants and other substrates. However, the trials done using the multispectral camera showed that the spectral signature differences between these submerged substrates is very small. This phenomenon is driven by two factors. First, pure water absorbs most of the sunlight and reflects only 5-7% of it back to the sky. Second, the varying depth of water causes spectral signatures of different submerged objects to be indistinguishable on an image. It was not feasible to use the multispectral imaging to discern metaphyton from aquatic

vegetation. A change-detection method in which change through time in presence or absence of objects was also tested at 5 study sites to see if it could be used to assess percent metaphyton cover along the shoreline. Mixed results were obtained using this method, low and high range estimates for percent cover were generated. Values for some high range estimates of percent cover using the method were similar to estimates of percent cover obtained using UAV with determination of percent cover of metaphyton for each site evaluated using ArcGIS Pro[®] (see the next Section in this report). However, at some sites with little or no metaphyton estimates using the change detection method were too high. Presence of woody substrate (which may drift) as well as challenges with dereferencing and perfectly aligning images from different dates create challenges for this approach.

The use of helicopter-based surveys was shown to have great potential for rapidly visualizing the entire shoreline of Lake Tahoe. This would be particularly valuable for providing an early detection capability for new populations of metaphyton, Asian clams, periphyton and rooted plants, or for identifying rapidly changing conditions in areas that are not part of routine monitoring (i.e. the majority of the shoreline). We recommend helicopter observations of the whole shoreline and imaging be included in summer metaphyton and spring periphyton monitoring around the lake. With continued efforts to develop the helicopter imaging equipment and methodology, the remaining technological challenges are considered to be readily solvable.

The next section describes use of UAV for assessing metaphyton distribution. It employed a different method for assessing percent cover of metaphyton for each site (use of ArcGIS Pro[®]). The results using UAV for determination of metaphyton percent cover indicate it is suitable for tracking metaphyton at select regional sites.

III. Aerial Imaging by UAV

III.A. Introduction

Developments in unmanned aerial vehicles (UAV), commonly known as drones, have delivered countless new opportunities in remote sensing. UAVs provide a new and innovative approach to monitoring natural environments. As a cost and resource efficient alternative to aerial photography using manned vehicles, UAVs are quickly becoming the industry standard in aerial imagery.

The quantification of metaphyton distribution in Lake Tahoe requires the ability to observe areas of lake bottom on the order of hectares (100m x 100m). TERC utilized a UAV as an intermediary survey platform between a high elevation, fast flying helicopter and a surface based boat to evaluate the most efficient method of surveying large benthic areas with precision and a high level of visual acuity.

Due to Tahoe's very clear water, UAV imagery had a high likelihood of success in providing a visual assessment of the benthic (subsurface) algae community to depths appropriate for metaphyton. However, water depth, particulate matter, and dissolved organic matter (DOM) all play a role in how quickly the visual light spectrum is absorbed. Surface reflection can also create "blind spots" obscuring visual data collection.

Despite Tahoe's renown clarity, the nearshore is higher in both particulate matter and DOM than the center of the lake. High quality aerial imagery requires a wide range of the visual spectrum to be reflected back to the image sensor. Since water absorbs light quickly with long wavelengths (warm colors) being absorbed at the shallowest depths, differentiating material with similar color characteristics can prove difficult. For this reason, it was suspected that the ability of UAV imaging to distinguish metaphyton from sand or rock substrate and submerged aquatic vegetation would vary from location to location based on water depth, turbidity, and the color of the underlying substrate.

UAV surveys are relatively quick to execute. However, processing composite images, geo-referencing the surveyed area, and identifying target features (metaphyton) can be time consuming. A key question researchers faced was whether through-water images would allow automated processing of survey composite images while preserving detail and spectral separation such that metaphyton coverage could be calculated using colorimetrics.

III.B. Methods

The UAV employed for metaphyton monitoring in the nearshore of Lake Tahoe was the DJI Phantom 4 Pro[®]. The Phantom 4 Pro is a quadcopter format consumer/professional grade UAV. The integrated 20 megapixel camera provides detailed imagery with a sufficient ground sample distance (GSD) for data acquisition. GSD is the distance between two consecutive pixel centers measured on the ground. Flight planning and image capture was collected through Pix4dcapture[®] software. The standard 'lawnmower' flight path was executed to maximize coverage for mapping each site. Flight path parameters were consistent between sites unless noted otherwise (Regan Beach). Flight parameters can be found in Appendix 3. Metaphyton monitoring missions

were flown at a height of 350 feet. The 350-foot altitude allows for a larger area to be photographed while retaining a GSD of 3 inches/pixel. Regan Beach flight altitudes were flown at a 100 ft. altitude due to the proximity to the Lake Tahoe Airport. UAV speed during metaphyton flights was selected through the flight planning software and set to 'Normal+.' The 'Normal+' flight speed with the Phantom 4 Pro was equivalent to 12.5 m/s. Sufficient image overlap parameters were required to ensure effective 'stitching' of successive images. Metaphyton monitoring flights used a front overlap of 80% and a side overlap of 70%. Employing high percentage overlaps delivers a higher probability of stitching images together and reconstructing a large scale geo-referenced image, or orthomosaic map, of the site. Visual reference markers (1m² white squares) were deployed at specific sites to aid in the post processing of orthomosaic images. UC Davis UAV pilots were required to have a FAA Part 107 small unmanned aircraft pilot certification. Preflight checks and necessary flight permissions were obtained before UAV missions, ensuring safety to operators and the public alike during UAV operations.

Coordinated monitoring events were conducted at five sites during summer months to monitor peak metaphyton growth. Regan Beach, Lakeside Marina, Skyland, Hidden Beach, and Sugar Pine Pt. were used for coordinated in-lake monitoring events. Regan Beach, Lakeside Marina, and Skyland were selected based on significant observed metaphyton growth at each site. Hidden Beach was employed as a control site, with metaphyton yet to be observed at the location. A second control site, Sugar Pine Pt. with little or no past metaphyton growth, was added along the west shore, during the study to include in UAV imaging. Figure 25 shows the locations of the five sites. The monitoring events included aerial imaging with the UAV combined with in-lake sampling for metaphyton coverage and biomass, Asian clam abundance and water chemistry sample collections (see section V). UAV monitoring and in-lake monitoring were completed on the same day to ensure accurate correlations between data.

UAV flight grids were established at selected metaphyton sites around the nearshore of Lake Tahoe. Grid files for each site were saved in Pix4dcapture software ensuring accurate reproduction over time. Flight grids were designed to encompass metaphyton growth and movement within designated boundaries of each site. Typical flight grids included the shoreline to a depth of up to 10 meters. Specific site boundaries are shown in red for images in Appendix 4 (and also in images 32-36).

Post processing of aerial imagery involved calibrating and stitching UAV images together using photogrammetry to create an orthomosaic. Orthomosaics are geo-referenced large-scale aerial images of an area composed of multiple photographs. Analysis of UAV aerial images and processing of orthomosaics was completed using Pix4D Fields[®] software. Images collected by the UAV were individually calibrated and geo-referenced in the initial pre-processing of the software. Images were then 'stitched' together using generated keypoints by the Pix4D software. Keypoints were matched up between consecutive images, allowing for a seamless stitching of images into one large image. Generally, orthomosaic processing is difficult to complete over water because of the homogeneity of a water body. However, due to the clarity of Lake Tahoe's water, images of the nearshore can be successfully processed. Natural environmental factors such

as submerged rocks and woody debris can positively affect the ability to successfully recreate an orthomosaic (additional reference points) while surface glare, turbidity, and DOM hinder the process. Therefore, the natural characteristics of each site in addition to weather and time of day can impact orthomosaic generation. Visual reference markers were deployed at Regan Beach, Lakeside Marina, and Skyland to aid in the processing of images. The reference markers were utilized in order to provide additional keypoints due to the sandy, homogeneous bathymetry associated with these sites.

Resolution of completed orthomosaics is represented by the ground sample distance (GSD). GSD is the distance between two consecutive pixel centers measured on the ground. GSD is affected by camera quality and flight altitude. The GSD is the effective minimum detection limit for classifying parameters, such as metaphyton, at a site. The GSD determines the detection limit, any metaphyton area less than the GSD would represent less than a pixel in the imagery. Image classifications and percent cover estimates are calculated on a pixel by pixel basis. The GSD for flight grids utilized during the project averaged 3 in/pixel for processed orthomosaics. The 3 in/pixel GSD was sufficient resolution to map metaphyton growth at each site with a high degree of accuracy.

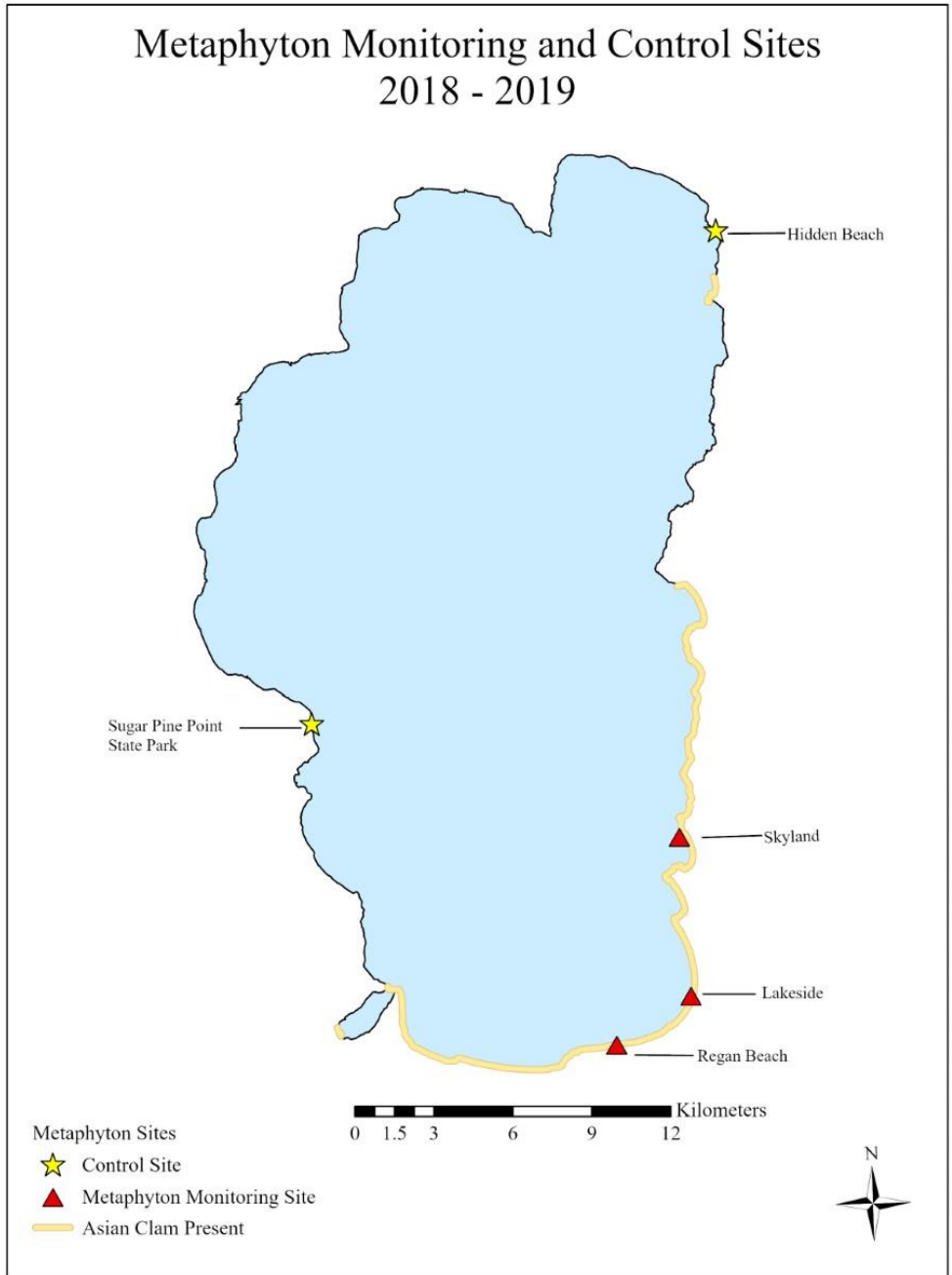


Figure 25. Locations of the five sites where UAV imaging was conducted. At Regan, Lakeside and Skyland and Hidden Beach, UAV imaging was coordinated with in-lake monitoring for metaphyton biomass, percent cover and predominant algal types, Asian clam numbers and sediment and water column chemistry. At Sugar Pine Pt. primarily UAV imaging was done.

Determination of percent cover of metaphyton for each site was evaluated using ArcGIS Pro®. Completed orthomosaics for each site were assessed in ArcGIS Pro and used to determine metaphyton coverage in the established site area. An example of a completed orthomosaic image is shown in Figure 26. Orthomosaics were evaluated using a machine-based learning tool known as image classification. Image classification is the process of extracting information classes from multiband remote sensing images. Supervised image classification is used to assign specific class categories to image pixels. Designated classes of metaphyton, sand, infrastructure, etc. were created to complete classification at each site. Class designations were site dependent and based on natural environmental constituents and substrates at the site. These class categories were defined as the classification schema. The classes were then ‘trained’ by referencing training samples to a specific spectral characteristic (see Figure 27). The samples were trained on a per-pixel basis, where the spectral characteristics of the individual pixel determines the class to which it is assigned. A new layer was produced displaying each pixel assigned to its classification with each classification represented by a different color (see Figure 28).

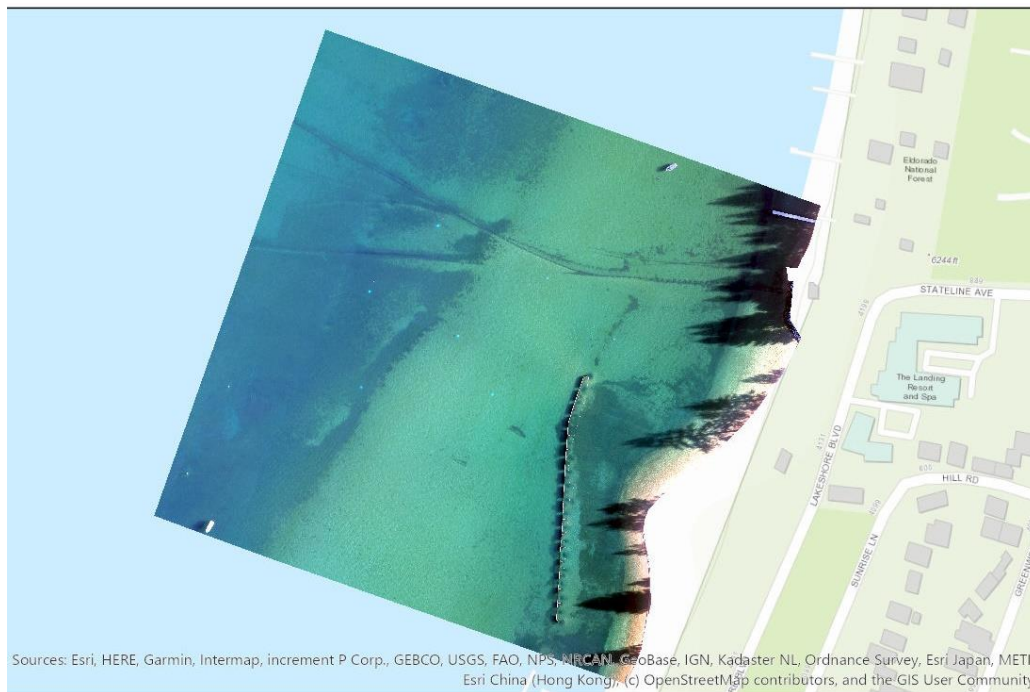


Figure 26. Original orthomosaic imported into ArcGIS Pro for image classification.

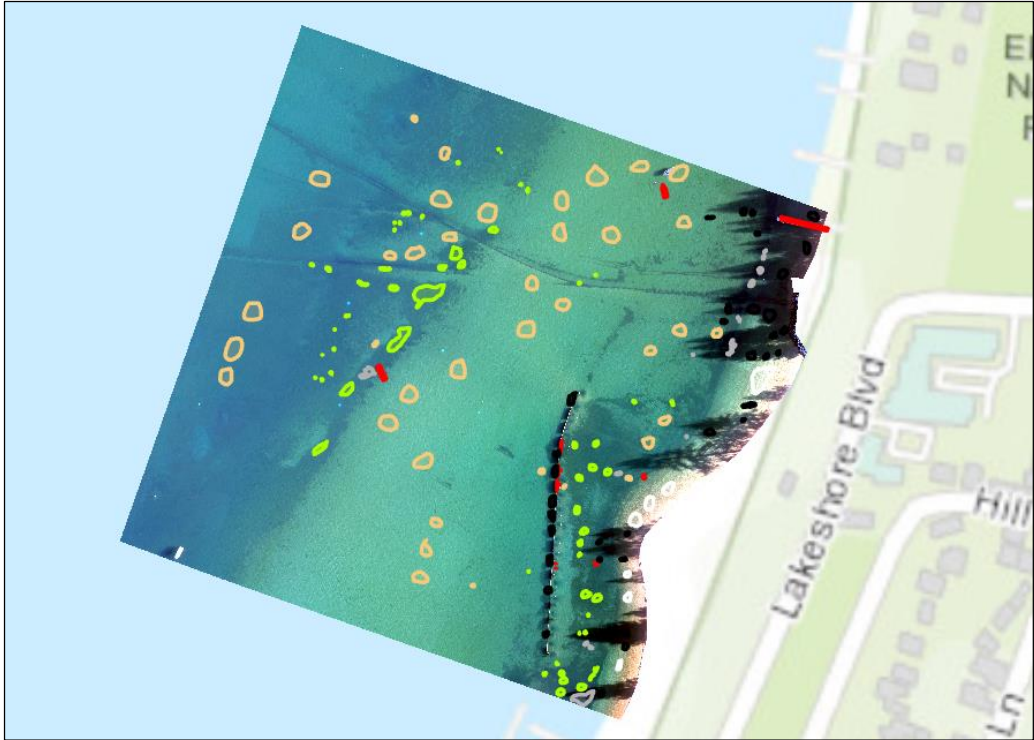


Figure 27. Training samples selected for classification to train ArcGIS which pixels represent types of substrate (i.e. green = metaphyton, tan = sand, red = infrastructure, etc.)



Figure 28. Pixels after classification by ArcGIS.

Percent cover and area were then determined for each classification. Both percent cover and area were evaluated based on the number of pixels representing each classification. Area was calculated using the GSD, or ground distance per pixel. Metaphyton percent cover calculations were evaluated using the in-lake (wet) area of each site boundary. Land areas encompassed in the site boundary were not included in percent cover calculations.

Accuracy assessments were applied to image classifications for each site. Accuracy assessments employ a reference dataset to determine the accuracy of classified results. A number, ≥ 100 , of random points were selected throughout the image to assess accuracy at each point. The points were selected by the ArcGIS program using a stratified random strategy, creating points that were randomly distributed throughout each class (see Figure 29).

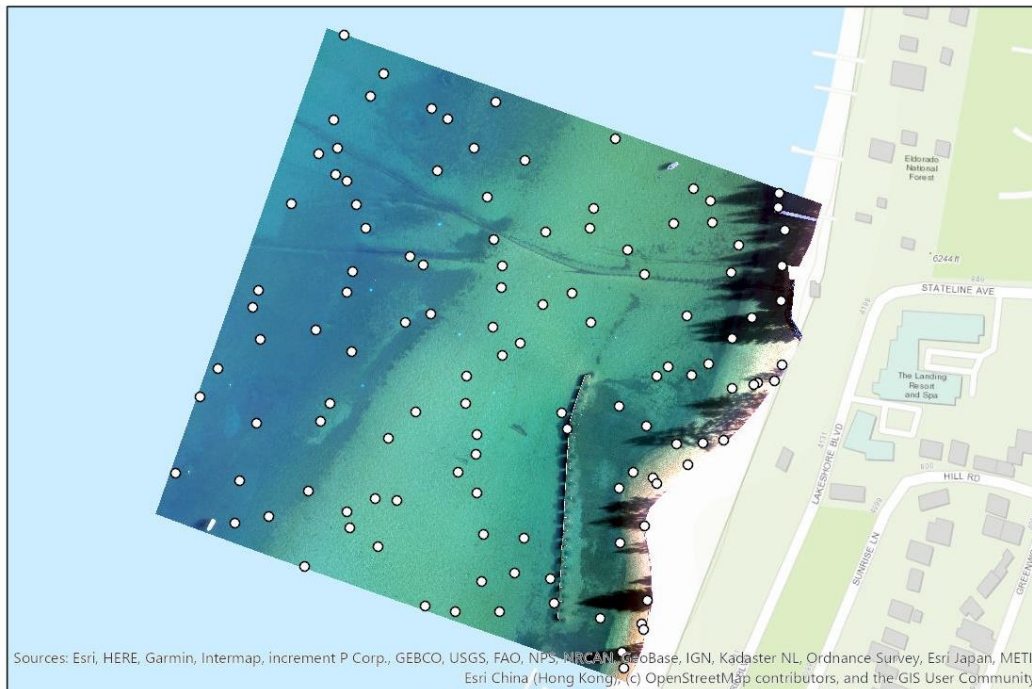


Figure 29. Example of 100 randomly generated accuracy assessment points in ArcGIS Pro. Each point is examined to determine if the pixel was correctly classified to the appropriate substrate.

Each point was then manually evaluated to determine the correct class it should be assigned. A confusion matrix, or accuracy table, was generated from these points to evaluate class errors during the classification process. An example accuracy table for Lakeside is shown below in Table 7.

Table 7: Accuracy table for Lakeside 08/01/2019.

ClassValue	Metaphyton	Sand	Infrastructure	Shadows	Beach Sand	Total	U_Accuracy	Kappa
Metaphyton	40	1	0	0	0	41	97.6%	0
Sand	3	46	0	0	0	49	93.9%	0
Infrastructure	4	2	0	2	2	10	0.0%	0
Shadows	0	0	0	10	0	10	100.0%	0
Beach Sand	0	0	0	0	10	10	100.0%	0
Total	47	49	0	12	12	120	0.0%	0
P_Accuracy	85.1%	93.9%	0.0%	83.3%	83.3%	0.0%	88.3%	0
Kappa	0	0	0	0	0	0	0%	82.9%

The accuracy table provides accuracy values for each class. False positives were associated with the U_Accuracy column, and false negatives were associated with the P_Accuracy row. A kappa value representing the overall statistic of agreement for the image is included. However, metaphyton accuracies were best evaluated through the accuracy assessments for the individual metaphyton class. Metaphyton accuracy values above 70% indicated a well classified image and provided confidence in the percent cover and biomass estimates for the given site. Accuracy values below 70% indicated some uncertainty in the metaphyton percent cover and biomass estimates.

Regan Beach was the only site with accuracy values consistently below the 70% threshold. The low accuracy values at Regan were predominantly due to the environmental factors at the site. The Regan Beach site contained significant areas of aquatic plants in addition to metaphyton inside the site boundary (see Figure 30). Often the metaphyton areas were intermixed with aquatic plants causing difficulty in differentiating plants from metaphyton, even to divers in the water (Figure 31). The swim area at Lakeside also contained a small area consisting of metaphyton mixed with aquatic plants. Similar challenges were observed in that area as well. Image classification proved difficult to distinguish between aquatic plants and metaphyton in these areas as spectral signatures overlapped. Abundance of aquatic vegetation should be considered when selecting future metaphyton monitoring sites.

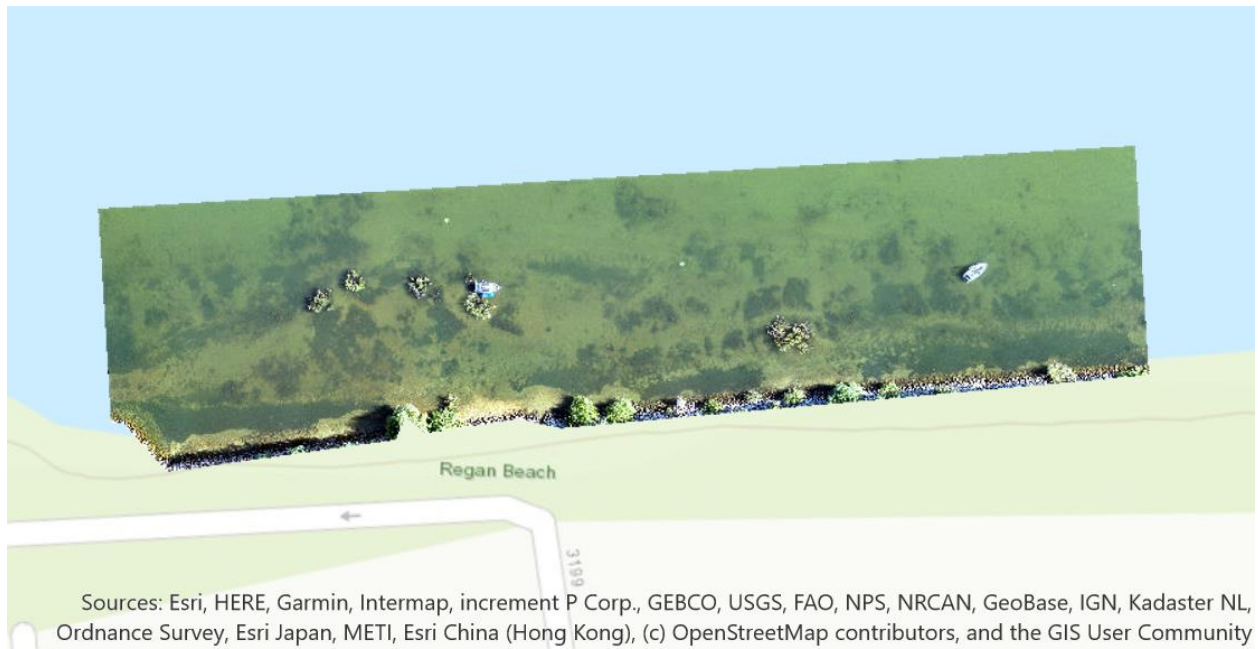


Figure 30. Orthomosaic image of Regan Beach site. Metaphyton patches intermixed with aquatic plants are difficult to distinguish between from aerial images.

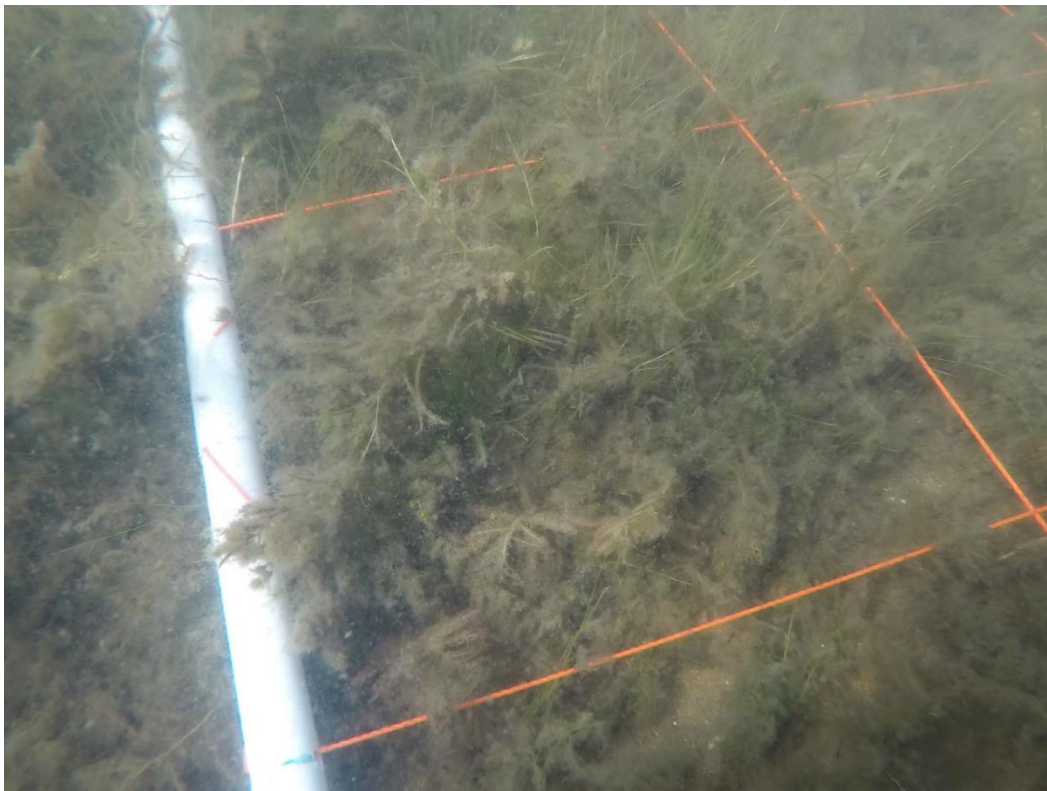


Figure 31. Aquatic plants and metaphyton mix at Regan Beach.

III.C. Results

Orthomosaics and image classifications were completed for UAV imaging data collected at each site. Each site was monitored during peak metaphyton growth as well as during minimal growth in winter. An example of completed orthomosaics with site boundaries for each site during peak growth are displayed in Figures 32 – 36.



Figure 32. Regan Beach orthomosaic 08/01/2019.



Figure 33. Skyland orthomosaic 09/06/2018.



Figure 34. Lakeside orthomosaic 09/04/2018.



Figure 35. Hidden Beach orthomosaic 07/22/2019.



Figure 36. Sugar Pine Pt. orthomosaic 07/22/2019.

UAV monitoring flights and dates can be found in Table 8. A monitoring flight was conducted at Regan Beach in January of 2019 however, an orthomosaic was not produced. Images were unable to stitch together due to unstable surface conditions and decreased water clarity. For successful UAV image data collection, monitoring flights must be conducted under favorable conditions. Favorable conditions include calms winds, good water clarity, low sun angle, and minimal surface vessel traffic.

All monitoring events were evaluated to determine estimated percent cover of metaphyton and area of metaphyton at each site. Estimated percent cover was calculated using the in-lake (wet) area inside each site boundary. Area represents the area of metaphyton in square meters inside the site boundary. U_Accuracy, P_Accuracy, Estimated Percent Cover and Coverage Area for each monitoring event and classification results can be found in Table 8 and a complete summary of accuracy tables with original images and images after classification of pixels is in Appendix 4. The U_Accuracy and P_Accuracy columns represent the accuracy associated with the specific metaphyton class. False metaphyton positives are associated with U_Accuracy, and false metaphyton negatives are associated with the P_Accuracy. Hidden Beach was used as a control site and monitoring events there were not processed for classification of percent cover or biomass, as no metaphyton was present at the site.

Table 8: Metaphyton UAV classification results

Flight Date	Site Name	Class	U_Accuracy	P_Accuracy	Est. % Cover	Area (m ²)
20180801	Regan Beach	Metaphyton	35	86	17.4*	2336*
20180906	Regan Beach	Metaphyton	50	55	12.1	1972
20190502	Regan Beach	Metaphyton	55	86	10.7	1764
20190801	Regan Beach	Metaphyton	50	63	7.0	1159
20190904	Regan Beach	Metaphyton	25	100	12.1	2035
20180906	Skyland	Metaphyton	88	86	36.7	57117
20190125	Skyland	No metaphyton	-	-	-	-
20190731	Skyland	Metaphyton	77	90	27.6	43364
20190904	Skyland	Metaphyton	74	84	31.1	48714
20180723	Lakeside	Metaphyton	84	89	17.0	5228
20180801	Lakeside	Metaphyton	97	82	32.9	26308
20180904	Lakeside	Metaphyton	83	66	23.4	18273
20190125	Lakeside	No metaphyton	-	-	-	-
20190801	Lakeside	Metaphyton	98	85	40.7	34181
20190904	Lakeside	Metaphyton	94	75	35.2	29231
20180801	Hidden Beach	No metaphyton	-	-	-	-
20180910	Hidden Beach	No metaphyton	-	-	-	-
20190503	Hidden Beach	No metaphyton	-	-	-	-
20190722	Hidden Beach	No metaphyton	-	-	-	-
20190905	Hidden Beach	No metaphyton	-	-	-	-
20180910	Sugar Pine Pt	No metaphyton	-	-	-	-
20190502	Sugar Pine Pt	No metaphyton	-	-	-	-
20190722	Sugar Pine Pt	No metaphyton	-	-	-	-
20190905	Sugar Pine Pt	No metaphyton	-	-	-	-

* Orthomosaic image does not include entire site area inside boundary due to sun glare in images

Corresponding UAV monitoring flights coordinated with in-lake sampling for metaphyton coverage and biomass provided a record of total biomass for each site. UAV flights and in-lake sampling were executed on the same day to ensure accurate correlations between metaphyton area and biomass samples. Total site biomass estimates were calculated for each site using the area of metaphyton inside the site boundaries and the ash free dry weight (AFDW) of biomass samples (Table 9). See section IV for AFDW information.

Table 9: Metaphyton biomass estimates

Flight Date	Site Name	Est. % Cover	Area (m ²)	AFDW (g/m ²)	Total Site Biomass (kg)
20180801	Regan Beach	17.4	2336	32.8	76.6
20190904	Regan Beach	12.1	2035	40.0	81.4
20190731	Skyland	27.6	43364	5.2	225.5
20190904	Skyland	31.1	48714	17.2	837.9
20180801	Lakeside	32.9	26308	40.6	1068.1
20180904	Lakeside	23.4	18273	42.7	779.7
20190801	Lakeside	40.7	34181	25.4	868.2
20190904	Lakeside	35.2	29231	31.8	929.5

III.D. Periphyton Monitoring with UAV

The same UAV monitoring process could potentially be applied to periphyton (attached algae) monitoring as well. UAV imagery data was collected in Spring 2019 to test the capabilities for periphyton monitoring. Data was collected at a site outside Tahoe City marina on March 29, April 17, April 25, and June 3. Periphyton data was processed using the same methods as developed for metaphyton monitoring.

The UAV aerial imagery data collected proved successful in quantifying periphyton distribution in the nearshore of Lake Tahoe. When compared with the same methods used for metaphyton monitoring, the periphyton data resulted in similar to higher accuracies during the classification process. This is most likely attributed to the location of periphyton growth compared to where metaphyton proliferates. Seasonal periphyton growth is abundant in shallow (<3m) nearshore areas with fixed substrates (rocks) for attachment. Aerial imagery data is much ‘cleaner’ in shallower depths with less of the water column to penetrate. The presence of rocks and other benthic substrates also aids in the ability to stitch images together in the creation of orthomosaics.

Metaphyton monitoring using the UAV successfully produced visual assessments of metaphyton in the nearshore correctly determining spatial distribution. Based on preliminary monitoring of periphyton at the Tahoe City site, it is estimated that UAV monitoring for periphyton would prove equally successful. The periphyton monitoring process using the UAV has the potential to be an integral part of future routine periphyton monitoring and should be considered for such programs moving forward.

III.E. Conclusions regarding UAV imaging of metaphyton

Remote sensing for metaphyton in the nearshore of Lake Tahoe using a UAV system was a new and effective approach to monitoring efforts for metaphyton. The UAV data successfully provided a visual assessment of benthic metaphyton areas in the nearshore appropriate to its spatial distribution. Images were then processed and classified, leading to accurate estimates of metaphyton coverage at selected sites. By coupling this data with measured biomass from in lake collections, an accurate assessment of the standing biomass of metaphyton could be calculated.

Due to the advancement in UAV camera technology and the relatively low flight elevation, UAV imagery can produce higher resolution composite images than helicopter or airplane imagery, allowing for metaphyton quantification on a site by site basis. The drawback to UAVs is their limited flight time, while helicopter and airplanes are capable of surveying the entire Tahoe shoreline in a single flight. However, the UAV provided a fast and cost-efficient alternative to surveying nearshore areas appropriate in scale to metaphyton growth, with high visual accuracy. The UAV monitoring process developed in this study would prove an instrumental resource to future metaphyton monitoring programs and may be able to be expanded to periphyton (attached algae) monitoring as well.

IV. In-lake work: Metaphyton Biomass, Percent Cover, Predominant Algal Types

IV.A. Introduction

In-lake work was coordinated with the aerial imaging done by the helicopter and UAV. This section describes the work done to quantify metaphyton biomass at the sites and measure algal percent cover over the bottom. Predominant algal types in the metaphyton were also assessed by examining samples under the microscope.

IV.A.1. Description of the in-lake study sites

The primary sites selected for in-lake monitoring work included Regan Beach, Lakeside offshore and Skyland along the south and southeast shores and Hidden Beach on the northeast shore. The sites locations were described in previous sections and are indicated on the map in Figure 25. This section provides some additional description of the sites.

The sites selected had differences in the levels of metaphyton growth, aquatic vegetation and Asian clam presence. Three sites had substantial metaphyton growth (Regan, Lakeside and Skyland) but different degrees of Asian clam presence. Hidden Beach had minimal metaphyton and no Asian clams present. One other site Sugar Pine Pt. was also monitored by UAV imaging, with either snorkeling or on-board boat checks for presence of Asian clams and metaphyton. The sites were easily distinguishable from the air and we were able to collect both helicopter images and UAV images. All sites were accessed by boat (R/V Bob Richards) for in-lake work. Some additional characteristics of the sites include:

Hidden Beach – This site is located in the northeast corner of the lake. It is a gently sloping, southwest facing cove, bounded by a rocky point to the northwest and sand and boulders along the shoreline to the east. It has a small tributary (Hidden Creek) entering in the northeast corner. The nearshore area is characterized by white sand, cobble and boulders. It has little algae growth, and no Asian clams or aquatic plants. It is exposed to south -southwest wind and waves created over a long fetch oriented from south west to north east. It is a popular summer area for both boaters and beach users.

Regan Beach Park - This site is located along the south shore, adjacent to the Al Tahoe urban area, between the Upper Truckee marsh to the west and El Dorado Beach to the east. It frequently has metaphyton present and is a popular area for use by the public. The bottom is relatively shallow at this site (a little over 2 m deep at maximum lake level for an extensive distance offshore (~125+ meters at high lake level). During periods of very low lake elevation such as in the summer of 2015, expansive areas of flat, sandy lakebed become flat beach area with very shallow lake water offshore. Lake levels during this study were relatively high (between 6226-6229 ft.), which resulted in the lake being present up to the boulders lining the shore around the beach park. The nearshore is quite complex with a mix of emergent vegetation, aquatic plants, metaphyton algae, boulders, with algae occurring also as periphyton on the boulders (epilithic periphyton) and attached to or associated with the aquatic vegetation. With such complexity it is a challenging site to discern the metaphyton from the other substrate present in aerial images. This area is potentially influenced by inflow from two large tributaries to the west (Upper Truckee River and Trout Cr.) and runoff from urban outfalls. There is some Asian clam presence but the numbers are very low compared with numbers at the Lakeside and Skyland sites.

Lakeside – The main metaphyton patch at this site is located about 175m offshore of Lakeside Beach in the southeast corner of the lake, just west of Stateline. It is on the south shore shelf area starting at a transition in depth from about 4.5m, to deeper shelf (approx. 7m deep, under full lake conditions). This area has been a site of summer metaphyton accumulation, with patch size of approx. 75m X 200m and a patch thickness that can reach 30 cm thick. There is a substantial Asian clam population and also a large accumulations of Asian clam shells. The bottom topography and lake currents may contribute to the accumulation of metaphyton and Asian clam shells in depressions. Its location well offshore necessitated extra offshore overflights by the helicopter in this study. The boundaries of the area at Lakeside also included the swim area protected by a metal wall offshore. Metaphyton and aquatic vegetation are found in this area.

Skyland- This site is located along the southeast shoreline adjacent to the Skyland subdivision in the north and section of USFS land just to the south. The shoreline has a north-south orientation and there is an area of shelf paralleling the shoreline. There is a small tributary which enters the lake south of the site (North Zephyr Cr.). Metaphyton was located on an area of shelf, at depth of about 6-7 m deep, from about 40-140 m offshore depending on the shoreline curvature. There are also large patches of Asian clam shells at this site near the outer edge of the shelf. The area is impacted by alongshore currents at times. Model simulations of currents done by Schladow et

al. (2014) showed that south to north currents can occasionally impact this site. Metaphyton was observed by divers to drift along the bottom during some of the sampling during this study.

Sugar Pine Pt. - This site is located along the central west shore of the lake in Sugar Pine Pt. State Park. The site is north of the General Cr. inlet. The substrate is composed of white sand and darker gravel and cobble over a shallow shelf area nearshore. There is no Asian clam presence here and very little or no metaphyton.

IV.B. Metaphyton Biomass Measurements

Samples of metaphyton were collected while snorkeling or SCUBA diving from areas of lake bottom with known dimensions and coverage, to estimate biomass present. These estimates could then be applied to estimates of percent cover from aerial images to estimate biomass in a region.

IV.B.1. Metaphyton Algae Biomass Collection and Ash Free Dry Weight Determination Methods

Samples of metaphyton were collected while snorkeling or SCUBA diving. Areas representative of the biomass were selected; or areas on pre-determined sampling grids were sampled. A sampling quadrat, usually 1 m² subdivided into .0625 m² squares with string was used to define the collection area in relatively light metaphyton. A 5-gallon bucket with the bottom cut off, was used to surround the metaphyton when the metaphyton layer was very thick. The quadrat or bucket was placed carefully over an area of metaphyton and coverage noted (usually an area with 100% cover was selected). In areas of light metaphyton, the algae were collected by scooping it into a hand-held aquarium fish net (approximate mesh 400-500 μm) from one or more squares of the quadrat and transferring the collected algae to a 1 gallon Ziploc® bag.

In very thick filamentous algae metaphyton, the metaphyton tended to be easily disturbed and nearly impossible to collect in a net without substantial loss of sample. A method was developed where the open-ended 5-gallon bucket (cross-sectional area of bucket at open bottom end determined in m²) was inserted into the metaphyton patch down to the sediment surface to enclose the algae (usually algae was hovering just above the bottom). A submersible electric bilge pump powered by electric cords extending to a battery at the surface, was used to suction the algae from the enclosed area into collection netting. A length of tubing was attached to the exhaust end of the pump. A cut-off section of nylon stocking (No Nonsense® regular size, approximate mesh opening size= 100μm non-stretched, 400-500μm stretched) was zip-tied to the end of the exhaust tubing to act as collection netting. The intake portion of the pump was moved through the algae enclosed by the bucket to suction off the algae which was discharged into the stocking. There was slight loss of material which passed through the stocking, but this appeared to be a small proportion relative to the total amount of sample collected. Once collected the stocking was removed from the pump hose and tied off and returned to the boat. Usually duplicate or triplicate samples were collected for biomass measurement.

Following sampling, metaphyton algae samples were placed in a cooler and returned to the lab at Incline Village, NV. Small subsamples of metaphyton were removed from the sample and

examined under the microscope to determine predominant algae types. After examination and photographs, the algae were returned to the main sample. Water in algae samples collected in Ziploc bags® (samples collected with a fish net) was poured off to leave a slurry of wet algae. When a slurry of water and algae could not be easily separated, water and algae were centrifuged for 10 minutes to settle the algae and the water decanted. For samples of metaphyton in nylon stockings, the algae were squeezed to remove excess water. Then the full sample of damp metaphyton was placed on a pre-tared piece of weighing paper. The samples were allowed to evaporate and dry to damp consistency for a short period (about an hour). A wet weight of the sample was obtained and a portion of the sample was split off into a pre-combusted (at 500° C for 1 hr.), pre-tared, aluminum pan for drying and Ash Free Dry Weight (AFDW) determination. AFDW was used to estimate biomass based on recommendations in our initial studies of metaphyton (Hackley et al., 2018). For a portion of the 2019 samples, another portion was split off into a pre-combusted pan for drying and saved for potential analysis of stable isotopes of ¹⁵N and ¹³C.

Ash Free Dry Weight Determination

Damp samples for dry weight were weighed in a pre-tared, pre-combusted aluminum tin to give a Sample Wet Weight (SWW) then dried overnight at a temperature of 60°C, allowed to cool in a desiccator, then weighed to determine 60°C dry weight (SDW 60°):

60°C Dry weight (g/m²) = (TSWW/SWW)*(SDW60°)/A
 [“TWW” is Total Wet Weight of metaphyton sample collected; “SWW” is subsample wet weight; “SDW60°” is sample 60°C dry weight; “A” is area sampled in m²; all weights in grams].

After determination of 60°C dry weight, samples were combusted at 500°C for one hour. The loss in weight at this high temperature was assumed to be primarily due to combustion of organic material present in the sample. AFDW was calculated as:

$$\text{AFDW (g/m}^2\text{)} = (\text{TWW}/\text{SWW}_{\text{afdw}}) * (\text{SDW}_{\text{afdw}60^\circ} - \text{SCW}_{\text{afdw}500^\circ}) / \text{A}$$

Where:

“TWW” is Total Wet Weight (g) of metaphyton field sample collected (all weights in grams)

“SWW_{afdw}” is AFDW subsample wet weight (g)

“SDW_{afdw} 60°” is sample 60°C dry weight (g)

“SCW_{afdw} 500°” is weight (g) of subsample after combusting at 500°C for 1 hour

“A” is area sampled in m²

IV.B.2. Metaphyton AFDW Results

The results for AFDW biomass are reported in Table 10. Values for individual replicates from a sampled area at the site, along with mean values for the area are presented. Mean AFDW levels for 100% cover are also presented. These values are the actual AFDW per m² when 100% cover was present in the area sampled. When less than 100% cover, these values were either

estimated from an association between AFDW and percent cover for multiple samples with varied percent cover (Figure 37 shows an example of such data from Regan); or by dividing AFDW/ m² by the sample percent cover. The AFDW per m² with 100% cover values were used to estimate regional biomass.

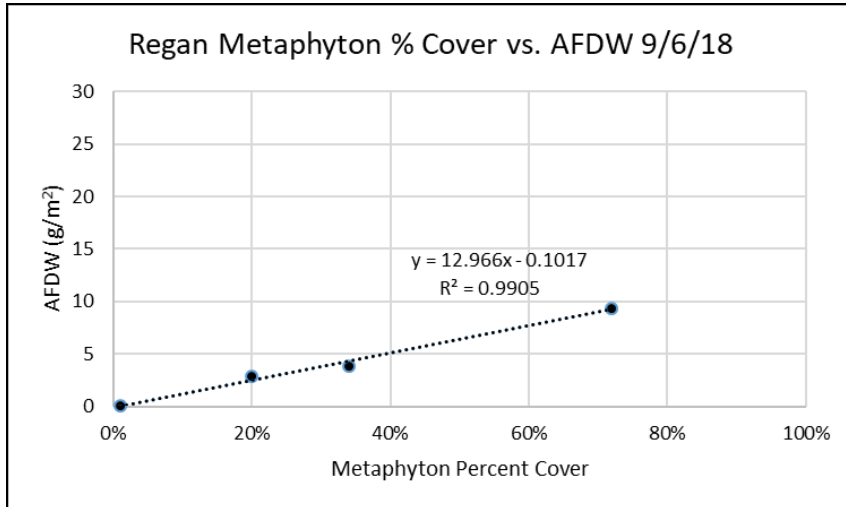


Figure 37. Association between metaphyton percent cover and AFDW at Regan on 9/6/18. Symbols represent AFDW of samples collected from quadrats with known percentage of metaphyton cover. The regression equation was used to estimate AFDW for 100% cover on this date.

The main metaphyton patch at Lakeside had 100% cover where sampled on most dates. Mean metaphyton AFDW for 100% cover ranged from 25.37 to 42.67 g/ m². Replicates from within the patch were similar to each other in 2018, but showed variability in 2019 samples (i.e. AFDW replicates for Aug. 1, 2019 at Lakeside were 10.81/16.59/48.70 g/m² and for 9/4/19 were 37.58/44.73/13.09 g/m²). This variation may reflect natural heterogeneity in the metaphyton layer, such as variation in the density, thickness and particular mix of algae, aquatic plant fragments and detritus in the patch.

At Regan, sampling was done both within patches with about 100% cover and patches with variable percent cover. Samples from nearshore patches with 99% and 100% cover had mean AFDW ranging from 32.78 to 62.32 g/m². There was also quite a bit of variation among replicates for these samples (i.e. AFDW replicates for Aug. 1, 2018 at Regan were 29.05/51.23/18.06 g/m² and for 9/4/19 were 49.56/75.07 g/m²). To give some reference for comparison, the median AFDW during the 2019 spring synoptic monitoring of *attached* algae around the lake (periphyton collected as part of the long-term monitoring program) was 50 g/ m², with a range from 6 to 194 g/ m².

On 8/1/18 at Regan, samples for AFDW were collected later in the morning when the winds increased and the lake began to be churned up by wave activity. The nearshore area where much of the metaphyton had accumulated was shallow and the layer of metaphyton along the bottom was stirred up into the overlying water column by wave action. This may have contributed to the variation among samples on that date. The turbulent conditions also made it difficult to collect

the sample on that date. As the bottom substrate was relatively hard, it was difficult to maintain a seal between the bottom of the open-ended bucket and sediments in the waves, causing some interchange of water and algae underneath the bucket as well as loss of algae from the open top portion of the bucket. Similar conditions were encountered during sampling at Regan on 9/6/18 making sampling difficult using the pump method. AFDW estimates on that date were obtained from net samples collected earlier in the morning when the metaphyton layer was still relatively undisturbed. The samples collected on 9/6/18 showed a good linear association ($r^2 = 0.99$) between percent cover and AFDW, which allowed AFDW for 100% to be estimated at 12.86 g/m^2 . This underscored the need to sample biomass and collect measurements of percent cover early in the day under calm conditions.

Samples collected on 8/1/19 from patches with variable percent cover also showed a good association between percent cover and AFDW. A sample with 50% cover had a AFDW of 12.79 g/m^2 and a sample with 5% cover had proportionally less AFDW at 1.28 g/m^2 . The AFDW for 100% cover was estimated at 25.58 g/m^2 .

AFDW samples were collected at different areas within the Regan site on 9/4/19 and these showed variation as well. Sampling done within a thick patch nearshore with 100% cover was done with the fish net and this gave an estimate of 62.32 g/m^2 . While sampling in areas along a 2X2 grid nearshore gave a mean of 17.74 g/m^2 . So it is evident there can be much variation in metaphyton AFDW biomass within a localized area at a site and between different areas at a site. This points out a need to collect many replicates at a site and also to potentially sample different regions of a site that may be representative of different levels of metaphyton presence.

At Skyland sampling for AFDW was done both within large patches and along sampling grids on a couple of dates. AFDW within the large patches tended to be greater than measured along the sampling grids. On 7/31/19 mean AFDW for 100% cover in a large patch was 5.21 g/m^2 while along the sampling grid mean biomass for 100% cover was estimated at 2.85 g/m^2 . On 9/3/19, the biomass within a large patch of metaphyton was 17.21 g/m^2 while along a sampling grid, mean AFDW for 100% cover was estimated to be 4.61 g/m^2 .

The sampling for AFDW showed that variation can occur both for replicates from the same site and at different areas within a regional site. Figure 38 summarizes AFDW values at 100% cover for individual sampling points which shows how at times there can be quite a bit of variation among samples. To compare data among sites and through time, it will be necessary to collect more replicates to get a better estimate of the mean. This may greatly add to the cost of a monitoring program. However, by using UAV measurements to quantitatively determine the spatial variability and then using ground-truth sampling for AFDW on specific patches of growth, it may be possible to quantify the biomass within the very heterogeneous distribution.

Table 10. AFDW values and AFDW for 100% cover for metaphyton samples collected from the different sampling sites. Sample areas of 0.0506 m² were sampled with bucket and pump, all others with net.

Site	Date	Area Sampled (m ²)	% Cover In Area Sampled	Patch AFDW (Replicate means, n=2/rep.) (g/m ²)	Patch AFDW Mean ± SD (g/ m ²)	AFDW for 100% Cover* Mean±SD (g/ m ²)
Lakeside						
Inside Main Patch	8/1/18	0.0506	100%	39.47/41.2/41.09	40.59 ± 0.97	40.59 ± 0.97
Inside Main Patch	9/4/18	0.0506	90%	34.59/42.21	38.40 ± 5.39	42.67 ± 5.99
Inside Main Patch	8/1/19	0.0506	100%	10.81/16.59/48.70	25.37± 20.41	25.37± 20.41
Inside Main Patch	9/4/19	0.0506	100%	37.58/44.73/13.09	31.80± 16.59	31.80± 16.59
Outside Main Patch	8/1/19	0.0625	100%	21.88	21.88	21.88
Skyland						
Large Patches	7/31/19	0.0506	100%	9.51/2.57/3.54	5.21± 3.76	5.21± 3.76
Subsamples from 3x3 grid of 1m ² quadrats, 50ft spacing:						
A1 (¼ quadrat)	7/31/19	0.25	15%	0.42	0.42	2.85 ³
B3 (¼ quadrat)	7/31/19	0.25	5%	0.14	0.14	“
C2 (¼ quadrat)	7/31/19	0.25	10%	0.44	0.44	“
Large Patches	9/3/19	0.0506	100%	10.68/25.42/15.53	17.21± 7.51	17.21± 7.51
Subsamples from 2x2 grid of 1m ² quadrats, 50ft spacing:						
A1 (¼ quadrat)	9/3/19	0.25	20%	1.42	1.42	7.1 ⁴
B1 (¼ quadrat)	9/3/19	0.25	15%	0.32	0.32	2.13 ⁵
Mean ± Std. Dev.	9/3/19					4.61± 3.51
Regan (nearshore)						
Nearshore Patch ⁶	8/1/18	0.0506	99%	29.05/51.23/18.06	32.78± 16.90	32.78 ± 16.90
Nearshore Patch ⁷	9/6/18	0.0506		NA	NA	
Nearshore quadrats with different levels of % Cover:						
#1 (1m ² quadrat)	9/6/18	1.0	34%	3.79	3.79	12.86 ⁸
#2 (1m ² quadrat)	9/6/18	1.0	72%	9.37	9.37	“
#3 (0.25 m ² quadrat)	9/6/18	0.25	<1%	0.02	0.02	“
#4 (1m ² quadrat)1.28	9/6/18	1.0	20%	2.88	2.88	“
Subsamples from 2x2 grid of 1m ² quadrats, 50ft spacing:						
A1 (¼ quadrat)	8/1/19	0.25	50%	12.79	12.79	25.58 ⁹
B2 (¼ quadrat)	8/1/19	0.25	5%	1.28	1.28	“
Nearshore Patch	9/4/19	0.0625	100%	49.56/75.07	62.32±18.04	62.32±18.04
Subsamples from 2x2 grid of 1m ² quadrats, 50ft spacing:						
A1 (¼ quadrat)	9/4/19	0.25	100%	18.87	18.87	18.87
B2 (¼ quadrat)	9/4/19	0.25	5%	0.83	0.83	16.6 ¹⁰
Mean ± Std. Dev.	9/4/19					17.74 ± 1.61
Regan (~ 180m offshore)	8/1/19	0.25	10%	2.34	2.34	23.4 ¹¹

³ Calculated AFDW for 100% Cover based on association of AFDW (y) and % Cover (x) for 3 replicates ($y=2.8x+.0533$), $r^2=0.697$.

⁴ Divided AFDW/Percent Cover to estimate AFDW when 100% Cover

⁵ Divided AFDW/Percent Cover to estimate AFDW when 100% Cover

⁶ Rough lake conditions likely resulted in variation.

⁷ Rough lake conditions, no data.

⁸ Calculated AFDW for 100% Cover based on association of AFDW (y) and % Cover (x) for 4 replicates ($y=12.966x-.1017$), $r^2=0.991$.

⁹ Calculated AFDW for 100% Cover based on association of AFDW (y) and % Cover (x) for 2 replicates ($y=25.578x+.0011$).

¹⁰ Divided AFDW/Percent Cover to estimate AFDW when 100% Cover

¹¹ Divided AFDW/Percent Cover to estimate AFDW when 100% Cover

Figure 38 summarizes the values for AFDW biomass per unit 100% cover for sites on different dates. Values from Regan showed more variability (range 13-75 g/m²) than Lakeside (range 11-49 g/m²), and Skyland had the lowest range (3-25 g/m²) despite sampling in some of the large patches present at the site. Many of the values from the Lakeside patch were close to 40 g/m².

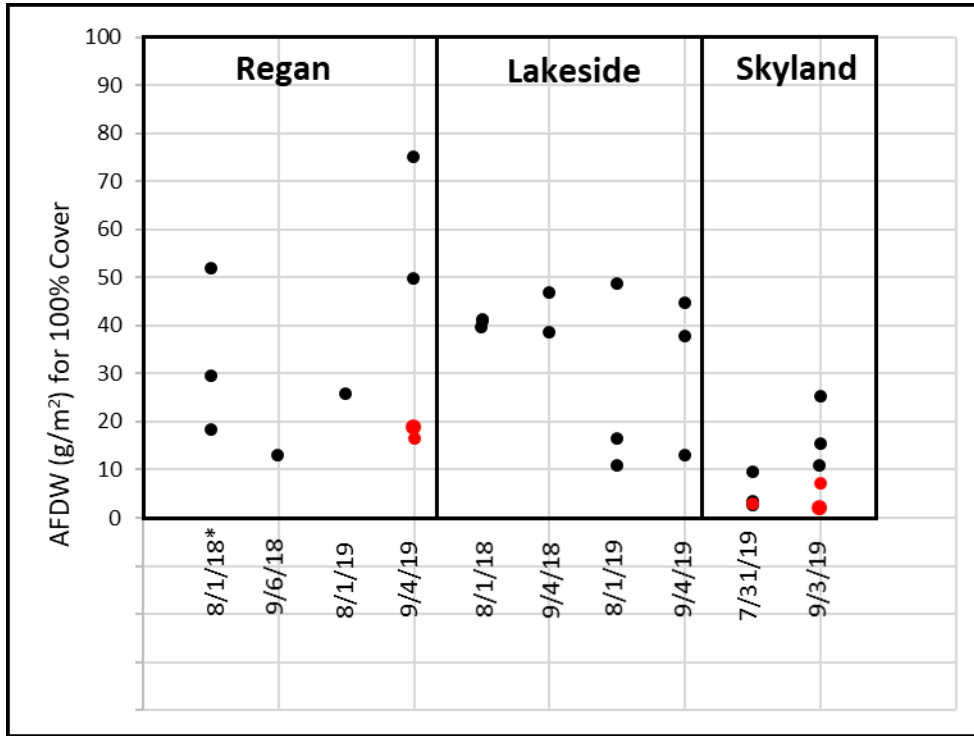


Figure 38. AFDW/ m² (actual or estimated) for 100% metaphyton coverage at Regan, Lakeside and Skyland sites. Red symbols indicate samples collected from sampling grids on 9/4/19 at Regan, and 7/31/19, 9/3/19 at Skyland. On 9/4/19 samples were also collected in a thick nearshore patch at Regan, shown in black. At Skyland on 7/31/19 and 9/3/19, samples collected with bucket method are shown in black. *-Regan 8/1/18 samples had 99% cover and was sampled under rough conditions which may have contributed to variability.

Regional biomass was estimated from the AFDW biomass per 100% cover and estimates of areal coverage from aerial imaging. Mean AFDW per unit area with 100% cover was multiplied by the total area covered with metaphyton within a defined boundary. Values for calculated regional biomass on sampling dates are presented in Table 9 in the UAV section. The highest regional biomass associated with metaphyton was found at Lakeside (range 780-1068 kg). Skyland biomass ranged from 226 kg on 7/31/19 to 838 kg on 9/4/19 using estimates for AFDW from sampling with the bucket and pump method. The regional biomass at Regan was lower than the other two sites. Regan regional metaphyton biomass was 77 kg on 8/1/18 and regional biomass on 9/4/19 was 81 kg using the mean AFDW biomass collected from a thick patch nearshore to represent the regional biomass in samples.

IV.C. Metaphyton percent cover

Snorkeling and SCUBA surveys were conducted at select sites to assess the amount of lake bottom covered with algae, viewed underwater.

IV.C.1. Underwater Percent Cover Measurement Methods

Estimates of percent cover were made using a 1 m² PVC pipe quadrat. The quadrat was subdivided into 16 reference squares of 0.0625 m² using nylon strung from opposing sides of the quadrat. Percent metaphyton cover over the bottom was estimated for each group of four squares on a corner of the 1 m² quadrat to create four 0.25 m² estimates of percent cover. The average of these provided an estimate of percent cover for the full 1 m² quadrat.

Estimates of percent cover were made along defined grids in the nearshore for some of the sites. 3x3 (9 point) and 2x2 (4 point) sampling grids with points located 50 ft. (15.2 m) apart, were used at Skyland on different dates. The 1 m² quadrat was placed in the standard way at each sampling point. Due to time constraints and lake conditions the 3x3 grid was the maximum number of sites feasible (taking 1.5 hours of dive time to complete). A 2x2 grid was more feasible (4 sites) and was employed at Regan on two dates. A more random sampling of seven 1 m² points 15-25 m offshore at Regan was done on one date (Aug. 1, 2018) while snorkeling. Coverage in the main patch at Lakeside typically was estimated when biomass sampling was done and generally found to be near 100% cover. Multiple samplings on sampling grids were not done there.

IV.C.2. In-lake Estimates of Metaphyton Percent Cover Results

Table 11 presents a summary of the percent cover estimates collected. Data for mean percent cover for the full 1m² quadrat is shown, with individual measurements for each 0.25m² portion of the quadrat below immediately below the mean value. Figure 39 summarizes the mean and standard deviation for sites with multi-point samples collected.

Percent cover showed a large amount of variation at Regan Beach. 2x2 sampling grids (4 points) measured at Regan on 8/1/19 and 9/4/19 showed much variability, with ranges from 12.5-68.8% (mean =29.7% ± 26.4% (n=4)) on 8/1/19 and from 2.5% to 100% (mean =35.0% ± 45.0% (n=4)) on 9/4/19. The estimates on these dates were made relatively close to shore (6-10 m away). This area was very heterogeneous with patches of accumulated metaphyton, algae and metaphyton associated with aquatic plants. Some of the coverage estimates included algae over aquatic plants.

Somewhat less variation was observed for seven measurements made on 8/1/18 slightly further offshore (10-20 m offshore) which ranged from 1.5-22.5% cover. Even further from shore at Regan, the levels of metaphyton percent cover were lower. Measurements of metaphyton percent cover were made at Regan about 180 m offshore on 8/1/19. There, small patches of metaphyton were observed with a mean percent cover of 5.4% ±1.9% for triplicate samples.

To characterize the average percent cover in the nearshore at Regan, a large number of replicates are needed. Hackley et al., (2018) estimated about 12 nearshore, small, 0.25 m² quadrats were

needed to characterize nearshore percent cover with a reasonable level variation in that study. Due to time constraints, we limited sampling to 4 points at Regan but with the larger 1m² quadrat. Four 0.25m² sub-quadrat percent cover measurements were obtained at each point for 16 measurements. With substantial variation still observed among replicates, when underwater percent cover is desired, sampling of a greater number of points, i.e. along a 3X4 sampling grid may be required.

At Skyland, the metaphyton percent cover showed a range of patch conditions from thin layers of algae on the sand, to large patches (2m x2 m) of filamentous algae extending 0.5m above the bottom (see Figures 13,14). On 7/31/19 percent cover ranged from 3.1-15% (mean 9.9±3.8% std. dev.) for measurements made along a 3x3 grid with points spaced 15.2 m apart. On 9/3/19 the coverage was less ranging from 1.3-6.9% (mean 4.0±3.2%) for measurements made along a 2x2 grid with points similarly spaced. The larger patches of metaphyton over the shelf at Skyland were spaced far enough apart that they were not captured in the grid sampling design. Coverage measured was primarily associated with smaller clumps of metaphyton. The UAV images on some dates showed relatively extensive patches slightly further offshore at Skyland. Future monitoring might take advantage of known distributions of algae along the shelf and at its edges, to estimate percent cover and biomass in representative areas.

At Lakeside, estimates of percent cover were made based on divers' observations while sampling algal biomass. The large metaphyton patch offshore generally had fairly uniform coverage with a thick layer (4-6 inches thick) of metaphyton. Coverage was estimated to be 100% on three dates and 90% on a fourth date. Smaller patches of metaphyton were observed outside the main patch but the levels of percent cover were not measured. There is also an area of metaphyton, aquatic plants and aquatic plants with associated algae, at Lakeside in the swim area shoreward of the metal wall. This area was ground-truthed with variable amounts of metaphyton and algae associated with aquatic plants observed. In-lake estimates of percent metaphyton cover were not made.

At Hidden Beach very little metaphyton was present. In 2018 coverage was estimated to be near 0% based on snorkel observations. On 7/22/19 there was a very small amount of algae and detritus observed on the bottom estimated to be 2% based on snorkeling the area. The algae was present in very small clumps, much of which was detritus with little associated color. It was too small to be seen in UAV and helicopter images and was not similar in composition to the metaphyton observed on the south shore. On 9/3/19, measurements of percent cover around the boat ranged from 0-1.4% based on 4 casts of the quadrat around the boat.

At Sugar Pine Pt. no metaphyton was observed. Observations were made while snorkeling on 7/22/19 with no metaphyton observed, and some woody debris present. No metaphyton was observed from the boat in Sept. 2019.

Table 11. Estimates of percent metaphyton percent cover at sites 2018 and 2019. For most sites a 1 m² quadrat was used, values for 0.25 m² sub-quadrat are given below the overall 1 m² quadrat percent cover.

Site	Date	Sampling Design	Station- Percent Cover in 1m² Quadrat (Percent Cover in each 0.25m ² sub-quadrat)	Mean % Cover±S.D.
Skyland	7/31/19	3x3 grid, 50 ft. (15.2 m) between sampling points starting with row "A" 30-40 m offshore	A3-12.5% (20,10,10,10) A2-15% (10,25,10,15) A1-6.25% (15,<5,<5,5) B3-3.13% (<5,5,<5,<5) B2-10% (10,5,15,10) B1-8.75% (10,10,5,10) C3-13.3% (5,20,<5,25) C2-7.5% (10,5,5,10) C1-12.5% (5,10,15,20)	9.9% ± 3.8% (n=9)
Skyland	9/3/19	2x2 grid, 50 ft. (15.2 m) between sampling points starting with row "A" 30-40 m offshore	A2-1.25% (0,0,0,5) A1-6.88% (<5,<5,<5,20) B2-1.25% (5,0,0,0) B1-6.75% (7,<5,<5,15)	4.0% ± 3.2% (n=4)
Regan	8/1/18	3 Reps. within patch with near 100% cover 3-4 m offshore	#1-98.75% (95,100,100,100) #2-98.75% (100,100,100,95) #3-98.25% (100,100,96,97)	98.6% ± 0.3% (n=3)
Regan	8/1/18	Quadrat drops from surface at sites: #2,3~10 m offshore #6,7~15 m offshore #1,4,5~20 m offshore (~10-15 m between adjacent points)	#3-12.5% (25,0,20,5) #2-4.5% (5,0,3,10) #7-2.75% (5,2,2,2) #6-1.5% (1,1,1,3) #5-20% (35,10,10,25) #4-17.5% (20,15,20,15) #1-22.5% (25,20,30,15)	11.6% ± 8.7% (n=7)
Regan	8/1/19	2x2 grid, 50 ft. (15.2 m) between sampling points starting with row "A" 8-10 m offshore.	A1-68.75%* (50,75,75,75) A2-15% (20,20,15,5) (*A1-many plants) B1-22.5% (5,10,25,50) B2-12.5% (15,25,5,5)	29.7% ± 26.4% (n=4)
Regan	8/1/19	Transect parallel to shore, ~200 yds (180 m) offshore, 50 ft. (15.2 m) between points	C3-3.75% (5,<5,<5,5) C1-5% (<5,<5,10,5) C2-7.5% (10,5,10,5)	5.4% ± 1.9% (n=3)
Regan	9/4/19	2x2 grid, 50 ft. (15.2 m) between sampling pts. starting with row "A" 6-8 m offshore.	A2-30% (10,50,10,50) A1-100% (100,100,100,100) B2-7.5% (10,10,5,5) B1-2.5% (<5,<5,<5,<5)	35.0% ± 45.0% (n=4)
Hidden	9/3/19	4 random casts of quadrat, ~120 ft (37 m) offshore	#1- 1.4% (4,<1,0,1) #2-0% (0,0,0,0) #3- 0.1% (0,<1,0,0) #4-0.1% (0,<1,0,0)	0.4% ± 0.7% (n=4)
Hidden	8/1/18	Snorkel Area	Estimate 0%	0%
Hidden	9/4/18	Snorkel Area	Estimate 0%	0%
Hidden	7/22/19	Snorkel Area	Estimate 2%	2%
Lakeside	8/1/18	Inside collection bucket, metaphyton patch ~200 m offshore	Estimate 100%	100%
Lakeside	9/4/18	"	Estimate 90%	90%
Lakeside	8/1/19	"	Estimate 100%	100%
Lakeside	9/4/19	"	Estimate 100%	100%
Sugar Pine	7/22/19	Snorkel Area	Estimate 0%	0%
Sugar Pine	9/5/19	Viewed from boat	Estimate 0%	0%

Note for 0.25m² sub-quadrat % cover estimates of "<5" used 2.5% and "1" used 0.5% for calculation of mean

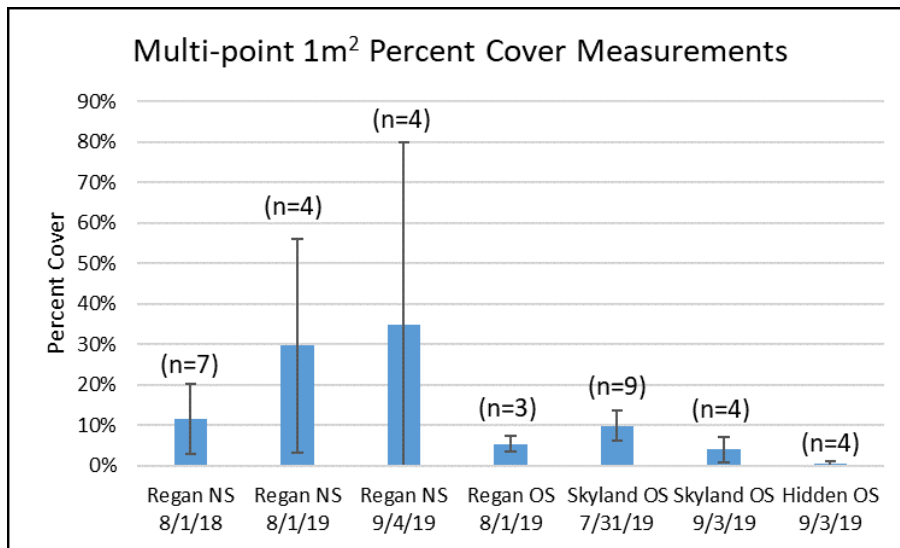


Figure 39. Sites where multiple points were sampled at a site for percent cover using a 1 m² quadrat. Error bars are standard deviation with “n” number of 1 m² samples. “NS” is nearshore site, “OS” is offshore site.

IV.C.3. Comparison of In-lake Measures of Percent Cover with Estimates from Helicopter and UAV

Levels of percent cover from in-lake measurements are compared with levels determined from imaging from the helicopter and UAV in Table 12. At Regan on 8/1/18 the percent cover estimates made in-lake 10-20 yards offshore (11.6±8.7%) were fairly close to the regional estimate from the UAV (17.4 %). No helicopter estimate was made at Regan. In contrast, in-lake mean percent cover levels at Regan on 8/1/19 and 9/4/19 were higher than regional estimates from aerial imaging. On 8/1/19 the mean in-lake percent coverage estimate was 29.7±26.4% while the UAV estimate was 7%. On 9/4/19, the in-lake estimate 35.0±45.0%, while the UAV estimate was 12.1 % and the helicopter estimate was 0.6-13.5%. The higher values for in-lake estimates on these dates appeared to be due to: (1) the limited number of replicates (n=4) for the in-lake estimate; and (2) high percent cover estimates for at least one of the in-lake replicates.

At Skyland there were also differences in in-lake estimates compared with helicopter or UAV imaging estimates of percent cover. For instance, on 7/31/19 the in-lake estimate of percent cover was 9.9 ± 3.8% while the UAV estimate was 27.6%. On 9/3/19 the in-lake estimate was 4.0±3.2% while the next day the UAV coverage estimate was 31.1% and the estimate based on helicopter images was 7.5-29.2%. The 3x3 and 2x2 sampling grid designs used for in-lake percent cover measurements on 7/31 and 9/3/19 did not capture any of the larger isolated patches on the shelf and the in-lake sampling may also have missed some of the contiguous metaphyton patches further offshore. These data show the challenges of trying to characterize metaphyton coverage over a large area with a limited number of localized observations. A larger number of replicates would be needed to better characterize regional coverage. Also UAV images might be examined to focus percent cover and biomass measurements on specific, representative areas.

Table 12. Comparison of metaphyton percent cover estimates from UAV, Helicopter and In-lake measurements.

	Regan			Lakeside		Skyland			Hidden	
	UAV % Cover	Helicopter % Cover	In-Lake % Cover	UAV % Cover	Helicopter % Cover	UAV % Cover	Helicopter % Cover	In-Lake % Cover	Helicopter % Cover	In-Lake % Cover
7/23/2018				16.0%						
8/1/2018	17.4 %		11.6±8.7%	32.9%						0%
9/4/2018				23.4%						0%
9/6/2018	12.1%	3.0-11.6%			4.8-22.4%	36.2%	4.7-35.9%		1.5-16.4%	
1/25/2019				0%		0%				
5/2/2019	10.7%									
7/22/2019										2%
7/31/2019						27.6%		9.9±3.8%		
8/1/2019	7.0%		29.7±26.4%	40.7%						
9/3/2019								4.0±3.2%		
9/4/2019	12.1%	0.6-13.5%	35.0±45.0%	35.2%	1.8-24.7%	31.1%	7.5-29.2%		4.9-28.5%	0.4±0.7%

IV.D. Onshore Deposition of Metaphyton algae and Aquatic Plant Fragments

Deposition of metaphyton onshore was observed at the monitoring sites on a limited number of dates during summer of 2018 and 2019. These dates were coordinated with wind events which either were occurring at the time of observation or preceded observations. At Regan Beach on 9/20/18, a north wind and associated waves caused deposition of metaphyton algae along parts of the shoreline there at the time of observations. The water turbulence stirred up metaphyton from the bottom near the steps to the lake (east end of parking area), creating a thick slurry of algae right near shore. As this washed over the boulders along the shoreline, algae and plant material was left on top of the boulders (Figure 40). The area was noted to have a high odor due to the algae and plant material deposited onshore. Similarly, metaphyton algae and fragments of aquatic plants were observed to be deposited on the small beach on the west side of Regan Beach Park (Figure 41). On 9/17/19 El Dorado Beach was observed to have fragments of aquatic plants with associated algae (*Cladophora*) washed up on boulders. This was after a strong southwest wind event the previous two days. The area had a slight vegetative smell.

Deposition of fragments of aquatic plants along the shoreline was more frequently observed during studies in 2018 and 2019 along the small beach at Regan and the broader beach at El Dorado Beach. Observations while snorkeling on various dates showed fragments of aquatic plants floating off the bottom. These floating fragments of aquatic plants can drift inshore and be deposited along the shoreline.

Very little or no metaphyton was observed washed up along the shore during in-lake monitoring. The low levels of metaphyton deposition apparent along shore in summers of 2018 and 2019 contrasted with greater amounts of deposition onshore as observed at Regan and El Dorado Beaches during studies 2015 and 2016 (Hackley et al., 2018). During 2015 the lake surface elevation was much lower, dropping to nearly 6222 ft. (a foot below the natural rim) by the end of summer. Under conditions of low lake level with minimal slope between the beach and offshore along portions of the south shore, metaphyton may accumulate close to the shoreline and be deposited onshore through wave activity or as the lake level recedes. Under conditions of higher lake level, as occurred in 2018 and 2019 (with lake level ranging between approximately 6227.5 ft. to 6229 ft.) the metaphyton algae was observed to accumulate along the bottom, slightly offshore, often at a transition area from relatively flat lakebed to a steeper slope to the beach. The data from our earlier metaphyton study (Hackley et al., 2018) and the present study suggests that nearshore slope and lake level may play a role in the degree to which metaphyton accumulates along the shoreline and is deposited on the beach. Lowered lake levels and minimal slope to the shoreline, seemed to favor movement of metaphyton algae to the water's edge and deposition on shore at Regan and El Dorado beaches.



Figure 40. Wave activity stirred up metaphyton algae and plant fragments creating a slurry of material in the water with some being deposited on boulders at east end of Regan Beach Park 9/20/18.

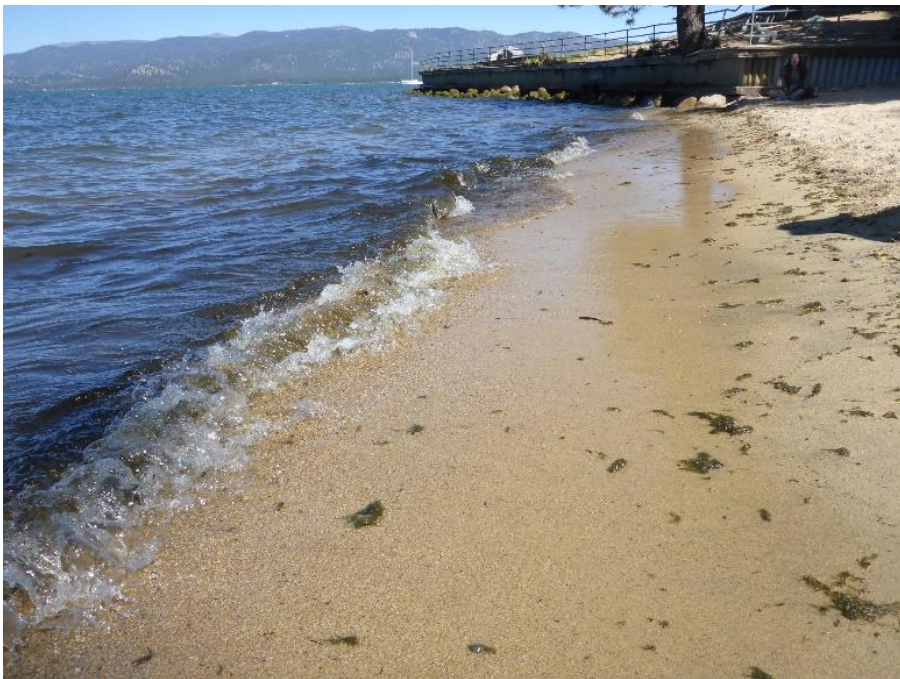


Figure 41. Deposition of mostly plant fragments along the beach at the west end of Regan Beach Park 9/20/18.

IV.E. Predominant Algal Types

IV.E.1. Predominant Algal Types Methods

Samples of algae collected from the sites were examined under the microscope to determine predominant types present. A glass slide containing fresh material was quickly scanned and the predominant algae were identified to the genus level when possible and photos were taken. After examination, the algae were returned to the main sample. A formal count of the cells and algae types was not performed.

IV.E.2. Predominant Algal Types in Metaphyton Results

A summary of predominant algal types observed in samples is presented in Appendix 5. Table 13 below presents a summary of the frequency at which various types of algae were predominant. Metaphyton was composed predominantly of filamentous green algae. The most predominant filamentous green algae genera were *Zygnema* and *Spirogyra*. Other filamentous green types were also predominant in samples from specific sites. For example, *Mougeotia* was prevalent in algae from deeper sites at Round Hill Pines and Skyland. *Oedogonium* was present in samples from Regan nearshore. Figure 42-47 shows microscope images of several of the predominant algal types present in the metaphyton.

The Regan nearshore and Lakeside sites had quite heterogeneous algal compositions, with different types of algae predominant in different samples. At the Regan nearshore site, *Oedogonium*, *Zygnema* and *Spirogyra* were frequently predominant in samples, however there were also other types of filamentous green algae including *Bulbochaete* and *Mougeotia*. Cyanobacteria, *Cladophora* and diatoms were also present. Lakeside metaphyton also had quite heterogeneous algal types including prevalence of *Zygnema* and *Spirogyra*. Charophytes were also prevalent in the metaphyton samples collected from Lakeside.

The heterogeneity of the different algal types at Regan may have resulted from either favorable conditions to support a diverse algal assemblage and/or multiple sources of algae which contribute to the metaphyton. At Regan, large tributaries (Upper Truckee and Trout Creeks) and urban runoff sources nearby add nutrients which may contribute to the productivity of the nearshore. Algae may be contributed to the metaphyton from periphyton (such as *Cladophora*) growing on rocks in the region, and from epiphytic algae growing attached to plentiful submerged vegetation in the area.

At some sites, the predominant algae in the metaphyton patches was limited to a small number of genera. At Elk Pt. on 7/24/19, metaphyton was mostly (95%) *Spirogyra*. At the Regan site about 180 m offshore, the metaphyton was primarily *Zygnema* and *Spirogyra*.

At Skyland and Round Hill Pines, an interesting form of *Mougeotia* was prevalent in many of the samples. Many of the *Mougeotia* cells were genuflexing (bending at contact points with other *Mougeotia*). This was different from conjugation (which is one of the reproductive processes for

these type of algae). The genuflexing may have contributed to the mass of algal cells holding together as a cloud or mass for a period. It is interesting to note that *Mougeotia* are considered to do well in deeper water with less light (Zohary et al., 2019). This would be consistent with observations of patches in deeper water at Skyland and Round Hill Pines.

At Hidden Beach very little metaphyton was present. Observation of the metaphyton from that area showed it to consist of mainly detritus including what appeared to be a large number of animal hairs (possibly from dogs as this is a popular beach). There were also cyanobacteria prevalent in some of the samples and diatoms similar to those present in the spring periphyton growth on rocks, in the late July 2019 sample.

Table13. Predominant algal types in metaphyton samples collected from select sites. Predominant algal type identified to genus level for most types, “Other Grn fil” indicates unidentified other green filamentous genera, “*Mougeotia**” – indicates genuflexing form of *Mougeotia*. “# Smp” indicates number of samples in which algae type was predominant.

Regan Inshore		Regan Offshore		Lakeside		Elk Pt.		Round Hill Pines		Skyland		Hidden Beach	
Predominant Algae	# Smp	Predominant Algae	# Smp	Predominant Algae	# Smp	Predominant Algae	# Smp	Predominant Algae	# Smp	Predominant Algae	# Smp	Predominant Algae	# Smp
<i>Oedogonium</i>	11	<i>Zygnema</i>	1	<i>Zygnema</i>	15	<i>Spirogyra</i>	4	<i>Mougeotia</i> *	1	<i>Zygnema</i>	9	<i>Cyano.</i>	4
<i>Spirogyra</i>	10	<i>Spirogyra</i>	1	<i>Spirogyra</i>	8	<i>Zygnema</i>	4	<i>Zygnema</i>	1	<i>Mougeotia</i> *	7	<i>Diatoms</i>	2
Other Grn fil	7			Charophytes	8	<i>Mougeotia</i>	1	<i>Spirogyra</i>	1	<i>Spirogyra</i>	5	<i>Zygnema</i>	1
<i>Zygnema</i>	5			<i>Bulbochaete</i>	6	Other Grn fil	1			<i>Oedogonium</i>	2	*Detritus	7
<i>Bulbochaete</i>	4			<i>Cyanobacteria</i>	5					Other Grn fil	1		
<i>Cyanobacteria</i>	4			<i>Oedogonium</i>	4								
<i>Diatoms</i>	4			Other Grn fil	3								
<i>Cladophora</i>	3			<i>Mougeotia</i>	1								
<i>Mougeotia</i>	1			<i>Cladophora</i>	1								
				<i>Diatoms</i>	1								
Total Samples	13		1		15		4		1		9		7

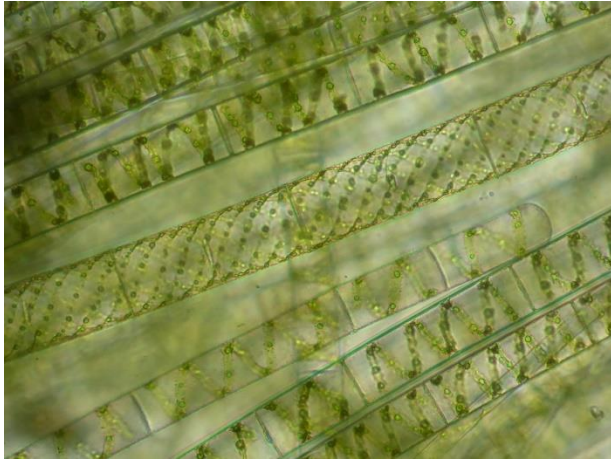


Fig. 42. *Spirogyra* Elks Pt. 7/23/19.

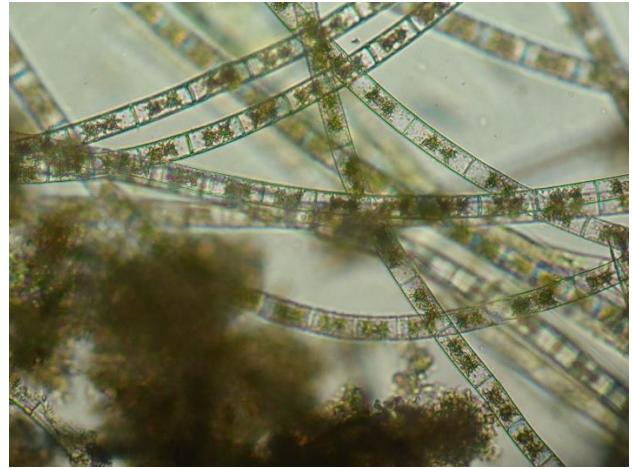


Fig. 43. *Zygnema* Regan offshore site C-2 8/1/19

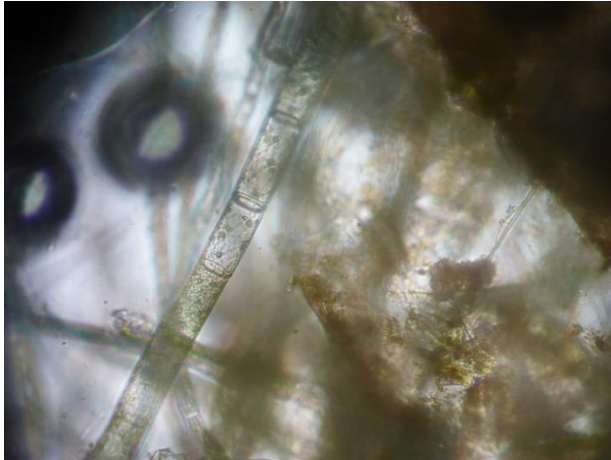


Fig. 44. *Oedogonium* from Regan #2, 9/6/18



Fig. 45. *Mougeotia* (genuflexing) Skyland, 9/3/19



Fig. 46. *Bulbochaete* El Dorado Beach 9/20/18.



Fig. 47. Charophyte Lakeside, 8/1/18.

V. Assessing Linkages between Metaphyton and Asian Clams: Sediment Pore Water and water column Nutrients, Asian Clam excretion, Asian Clam Abundance, Algae Stable Isotopes

Several past studies have provided data which suggests a linkage between Asian Clams and metaphyton algae growth. Filamentous algal blooms were observed in 2008 in areas with Asian clam populations along portions of the south east shore of Lake Tahoe (Wittmann et al., 2008). Schladow (2010) found “filamentous algae growth to be highly correlated with Asian clam presence, but there are other factors/ nutrient inputs that can contribute to the presence of filamentous algal growth, further research was needed. Forrest et al. (2012) found that Asian clams and filamentous green algae were co-located in 2009 along portions of the south and south east shore by imaging around the lakeshore at depths <10m using an autonomous underwater vehicle (AUV), the UBC-Gavia. Though co-located, causality could not be demonstrated. Wittmann et al. (2011) visually monitored filamentous green algae (*Zygnema* sp. and *Spirogyra* sp.) in areas with Asian clams 2009 –2010. They also deployed an in situ fluorometer to study filamentous algae levels along the bottom at Lakeside, Marla Bay and Glenbrook. The deployments of the *in situ* fluorometer combined with visual field observations in both 2008 and 2009 show that filamentous algal blooms are occurring in Marla Bay and Lakeside but not at Glenbrook in Lake Tahoe. Laboratory experimental work showed that excretion from Asian clams could stimulate the growth of Lake Tahoe filamentous algae. Results from their experiments in Lake Tahoe suggested that there is potential for the relationship between Asian Clams and alterations to algal concentrations. Further monitoring and experimentation was recommended.

One of the goals of this study was to further examine linkages between the invasive Asian Clam (*Corbicula fluminea*) and metaphyton/ filamentous green algae. In addition to the studies of metaphyton algal biomass, percent cover and predominant algal types already discussed, we looked at sediment pore water and water column nutrients at the sites within and outside of patches of metaphyton. We also looked at excretion of nutrients from Asian clams. The nutrients in excretion can potentially impact pore water and water column nutrients which may stimulate algae growth. We also collected information on Asian Clam abundance and shell numbers at the study sites inside and outside of patches of metaphyton. With support from a small pilot study grant from the UC Davis Stable Isotope facility, we also looked at stable isotopes of ^{13}C and ^{15}N in metaphyton algae from different locations to see if there were any patterns associated with Asian clam presence. The following section presents the results of these investigations.

V.A. Sediment Pore Water and Water Column Nutrients

V.A.1. Sediment Pore Water and Water Column Nutrients Methods

Water column samples were collected from mid-water column or surface and near the bottom just above the sediment surface. These samples were collected in areas with and without

metaphyton algal patches. Nutrients in sediment pore water both inside and outside metaphyton patches were also examined.

Water column samples were collected by opening pre-cleaned 250 HDPE sampling bottles at depth either by a diver or when surface samples were collected, from the boat. Sediment pore water samples were collected from the sediments beneath the water column samples. A 2-3 ft. length of pre-cleaned vinyl tubing (1/8 in. I.D.) with a small piece of nylon stocking material placed over the tip to act as a screen, was attached to a small piece of rebar and used to directly withdraw sediment pore water from the sediments. The rebar and attached tubing were pushed or hammered into the sediments to a depth of several inches. The sediment pore water was withdrawn into pre-cleaned 60 ml syringes. Typically, at least three syringes of pore water were collected from a site. The syringes from a sampling site were returned to the boat where the pore water was expelled and composited into a 250 ml pre-cleaned HDPE sampling bottle. The samples were returned to the lab. There the water was filtered through 0.45 Magna® Nylon filters to remove particles. Pore water from several sites developed an orange precipitate after sitting in bottles for several hours. This was likely a result of exposure of anoxic pore water to air and formation of iron precipitates. The precipitate and sediment particles were removed by the filtration process. Water column and pore water samples were analyzed for NO₃-N, NH₄-N and SRP (soluble reactive phosphorus) by the UC Davis TERC lab. Standard QA/QC employed by TERC for water chemistry was used.

V.A.2. Sediment Pore Water and Water Column Nutrients Results

Table 14 summarizes the values for NO₃-N, NH₄-N and SRP and specific conductance for samples collected. Sediment pore water concentrations and lake water column concentrations for samples are plotted for NO₃-N, NH₄-N and SRP in Figures 48 a-c (when replicates were collected, mean values are plotted). Levels of lake water column NO₃-N, NH₄-N and SRP were generally very low at the sites. NO₃-N was consistently low (≤ 2 $\mu\text{g/l}$) in all but one sample (Skyland, near sediment surface, 9/6/18, 9 $\mu\text{g/l}$). Water column NH₄-N ranged from 0-6 $\mu\text{g/l}$. Three water column samples from Skyland had slightly elevated NH₄-N. Two of these were mid-water column samples outside the metaphyton patch (5 and 6 $\mu\text{g/l}$) and another was a near sediment surface sample (5 $\mu\text{g/l}$). SRP levels were also low (≤ 2 $\mu\text{g/l}$) with the exception of two samples collected near the sediment surface from Lakeside (SRP= 4, 7 $\mu\text{g/l}$) and a Skyland sample collected near the sediment surface (SRP=6 $\mu\text{g/l}$). Specific conductance (SC) was analyzed on a portion of the samples. Water column SC was generally close to 92 $\mu\text{S cm}^{-1}$. An exception was at Regan on 8/1/19 when the water column samples had an SC of 83 $\mu\text{S cm}^{-1}$. This lowered SC likely was the result of inflow from the Upper Truckee River to the west (which was shown to have a SC of 63 $\mu\text{S cm}^{-1}$ on 8/7/19). The Upper Truckee River influence on this site was apparent from the air on several dates showing up as darker-colored water (due to presence of dissolved organic material (DOM)) in the nearshore at Regan.

Levels of NO₃-N, NH₄-N and SRP in pore water showed a greater range. NO₃-N in pore water (including values inside and outside algal patches) ranged from 1-64 $\mu\text{g/l}$, with most samples < 30 $\mu\text{g/l}$. NH₄-N concentrations in pore water spanned three orders of magnitude from 2- 4172 $\mu\text{g/l}$ at the sites. The NH₄-N in pore water at Lakeside was lower in early August samplings

(range 104-420 $\mu\text{g/l}$) and much higher a month later in September samplings (range 3138-4172 $\mu\text{g/l}$). SRP in pore water ranged from 1-21 $\mu\text{g/l}$, with all but one sample having concentrations \leq 12 $\mu\text{g/l}$. One pore water sample from Elk Pt. had a concentration of 21 $\mu\text{g/l}$. SC in pore water samples ranged from 121 $\mu\text{S cm}^{-1}$ in a sample from Skyland to 312 $\mu\text{S cm}^{-1}$ in a sample from Lakeside. All pore water samples had SC elevated above the typical lake SC of near 92 $\mu\text{S cm}^{-1}$.

The samples of pore water were typically collected from a relatively shallow depth in the sediments (a few inches). This is relatively close to the sediment water interface and may represent nutrients which can be released into the water column. Asian clams were also found to be concentrated mostly in the upper few inches of lake sediments (Wittmann et al., 2011). Wittmann et al. (2011) also looked at nutrient concentrations in sediment pore water from sediment cores at sites Asian Clams, including Lakeside in March, 2009. They found average pore water concentrations of $\text{NO}_3\text{-N}$ generally to be less than about 30 $\mu\text{g/l}$; the median $\text{NH}_4\text{-N}$ concentration was near 200 $\mu\text{g/l}$, which was near the lower range for Aug. 2018, and 2019 samples collected for this study; SRP concentrations in pore water in their study were higher than observed in the present study (median SRP > 100 $\mu\text{g/l}$) at Lakeside.

There were no readily apparent associations between water column and pore water $\text{NO}_3\text{-N}$, $\text{NH}_4\text{-N}$ and SRP for samples from individual sites. The surface water concentrations were generally low with isolated incidences where the lake water had elevated N or P either just above the sediment surface or higher in the water column. The uniformity and low levels of water column nutrients is expected as lake currents are constantly moving water, and there should be no expectation of a correlation between surface and pore water concentrations. Any nutrients entering surface waters from the pore water would be occurring at a low rate and would not have a detectable impact on surface water concentrations. It may be possible that nutrients entering the lake from the sediments could be taken up by algae (either metaphyton or algae and bacteria near the sediment water interface) which spend a protracted time at specific locations.

We compared pore water nutrients inside and outside of metaphyton patches (Figures 49 a-c) to see if presence of algae patches was associated with areas in which pore water nutrients were elevated. Concentrations were relatively similar in sediment pore water inside and outside metaphyton patches for many of the paired samplings. This was the case for $\text{NO}_3\text{-N}$ in 5 of 8 paired samples, for $\text{NH}_4\text{-N}$ in 4 of 8 samples, and for SRP in 4 of 8 paired samples. However, some sites did show differences in pore water nutrients inside patches of metaphyton compared to outside patches. $\text{NO}_3\text{-N}$ was higher in the pore water beneath metaphyton patches for 3 of 8 sample pairs; NH_4 was higher inside metaphyton patches in 3 of 8 sample pairs, with one instance where $\text{NH}_4\text{-N}$ was higher in sediments outside the patch. SRP was generally similar in sediment pore water inside and outside patches.

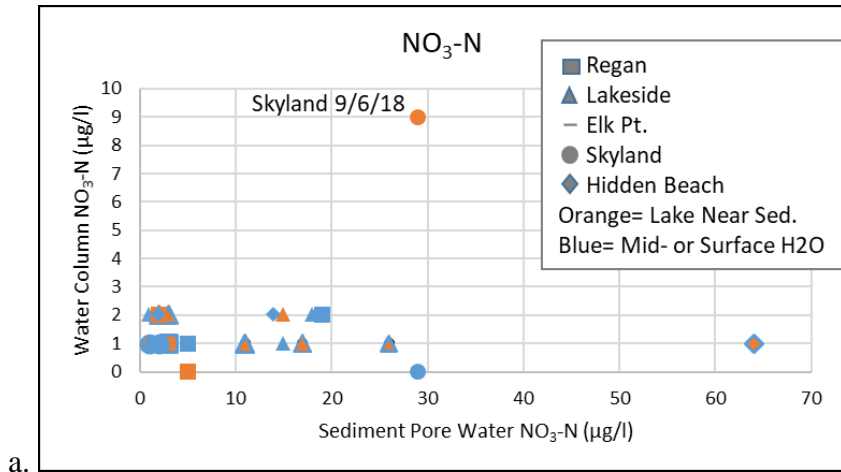
These results leave open the possibility that presence of some metaphyton patches may be associated with elevated nutrients in the sediment pore water at some sites. Metaphyton may also drift and not necessarily reflect nutrient levels in pore water over which it is found at any one point in time. But metaphyton may take advantage of nutrients released by pore water in a general region as it drifts along.

Table 14. Summary of NO₃-N, NH₄-N and SRP analyses for water samples collected at metaphyton monitoring sites. “Sed. Pore” is sediment pore water, “Above Sed.” is water column sample just above sediment surface and “Mid” is mid-water column sample, “Surface” is water column sample at surface. Select samples were also analyzed for Specific Conductance “Sp. Cond.” (“*” indicates Sp. Cond. value several months after collection). Data for stream samples collected at the Upper Truckee River (near USGS UT-1 site) and North Zephyr Cr. (downstream of highway 50) on one sampling date is also shown.

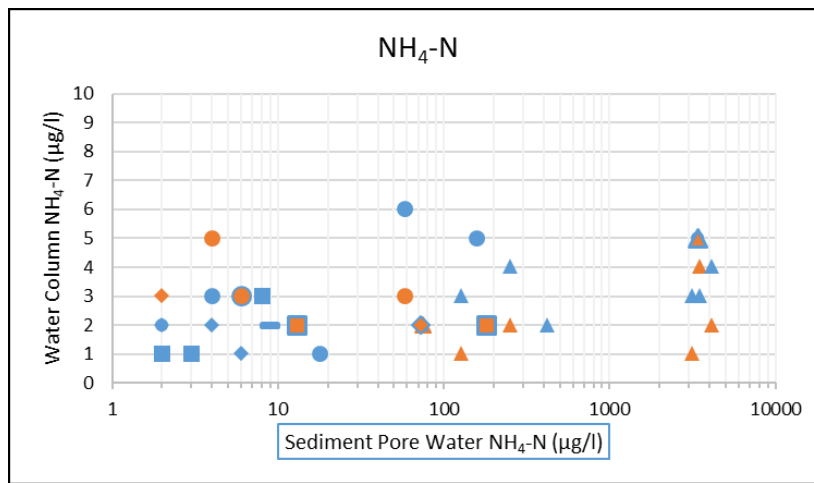
Site Name	Date	Samp. Point	In Patch				Out Patch				Notes
			NO ₃ -N (µg/l)	NH ₄ -N (µg/l)	SRP (µg/l)	Sp. Cond. (µS/cm)	NO ₃ -N (µg/l)	NH ₄ -N (µg/l)	SRP (µg/l)	Sp. Cond. (µS/cm)	
Lakeside	8/1/18	Sed. Pore-1	25	41	2	NA	6	409	3	NA	
Lakeside	8/1/18	Sed. Pore-2	28	218	3	NA	17	96	2	NA	
Lakeside	8/1/18	Mean	26.5	129.5	2.5		11.5	252.5	2.5		
Lakeside	8/1/18	Above Sed.-1	1	2	6	NA	1	2	2	NA	
Lakeside	8/1/18	Above Sed.-2	1	0	2	NA	1	3	1	NA	
Lakeside	8/1/18	Mean	1	1	4		1	2.5	1.5		
Lakeside	8/1/18	Mid-H2O-1	1	3	2	NA	1	4	1	NA	
Lakeside	8/1/18	Mid-H2O-2	NA	NA	NA	NA	1	4	1	NA	
Lakeside	8/1/18	Mean	1	3	2		1	4	1		
Lakeside	9/4/18	Sed. Pore-1	10	4211	2	NA	24	3587	2	NA	
Lakeside	9/4/18	Sed. Pore-2	19	4133	2	NA	11	3212	2	NA	
Lakeside	9/4/18	Mean	14.5	4172	2		17.5	3399.5	2		
Lakeside	9/4/18	Above Sed.-1	2	2	7	NA	NA	5	1	NA	
Lakeside	9/4/18	Mid-H2O-1	1	4	1	NA	1	5	NA	NA	
Lakeside	7/24/19	Sed. Pore-1	NA	NA	NA	NA	1	76	3	188/187*	
Lakeside	7/24/19	Mid-H2O-1	NA	NA	NA	NA	1	2	1	90*	
Lakeside	8/1/19	Sed. Pore-1	18	420	2	177	8	104	4	174	
Lakeside	8/1/19	Mid-H2O-1	2	2	2	NA	NA	NA	NA	NA	
Lakeside	9/4/19	Sed. Pore-1	1	3138	2	312	3	3508	1	210	
Lakeside	9/4/19	Above Sed.-1	1	1	0	88*	2	4	0	91*	
Lakeside	9/4/19	Mid-H2O-1	2	3	0	94/94*	1	4	0	89*	

Site Name	Date	Samp. Point	In Patch				Out Patch				Notes
			NO ₃ -N (µg/l)	NH ₄ -N (µg/l)	SRP (µg/l)	Sp. Cond. (µS/cm)	NO ₃ -N (µg/l)	NH ₄ -N (µg/l)	SRP (µg/l)	Sp. Cond. (µS/cm)	
Regan B.	8/1/18	Sed. Pore-1	NA	NA	NA	NA	NA	NA	NA	NA	
Regan B.	8/1/18	Above Sed.-1	1	0	2	NA	1	1	1	NA	
Regan B.	8/1/18	Above Sed.-2	1	0	2	NA	NA	NA	NA	NA	
Regan B.	8/1/18	Mid-H2O-1	1	1	1	NA	1	1	1	NA	
Regan B.	9/6/18	Sed. Pore-1	5	124	1	NA	4	12	3	NA	
Regan B.	9/6/18	Sed. Pore-2	4	240	1	NA	3	14	2	NA	
Regan B.	9/6/18	Mean	4.5	182	1		3.5	13	2.5		
Regan B.	9/6/18	Above Sed.-1	0	2	1	NA	1	2	1	NA	
Regan B.	9/6/18	Mid-H2O-1	1	2	1	NA	1	2	1	NA	
Regan B.	8/1/19	Sed. Pore-1	19	8	6	169	NA	NA	NA	NA	Near B2
Regan B.	8/1/19	Mid-H2O-1	2	3	1	83	NA	NA	NA	NA	Near B2
Regan B.	8/1/19	Sed. Pore-1	NA	NA	NA	NA	2	3	5	149	Offshore
Regan B.	8/1/19	Surface H2O	NA	NA	NA	NA	2	1	2	83	Offshore
Regan B.	9/4/19	Sed. Pore-1	NA	NA	NA	NA	2	2	3	155/159*	
Regan B.	9/4/19	Above Sed.-1	NA	NA	NA	NA	2	2	1	NA	
Regan B.	9/4/19	Mid-H2O-1	NA	NA	NA	NA	1	1	1	90/91*	
Skyland	9/6/18	Sed. Pore-1	40	5	9	NA	2	6	7	NA	
Skyland	9/6/18	Sed. Pore-2	1	6	8	NA	19	2	6	NA	
Skyland	9/6/18	Mean	20.5	5.5	8.5		10.5	4	6.5		
Skyland	9/6/18	Above Sed.-1	9	5	6	NA	1	3	1	NA	
Skyland	9/6/18	Mid-H2O-1	0	3	0	NA	1	3	1	NA	
Skyland	7/31/19	Sed. Pore-1	2	158	12	121	2	18	10	108	
Skyland	7/31/19	Above Sed.-1	NA	NA	NA	NA	NA	NA	NA	NA	
Skyland	7/31/19	Mid-H2O-1	2	5	1	94	NA	NA	NA	NA	
Skyland	7/31/19	Surface H2O	NA	NA	NA	NA	2	1	1	93	Offshore
Skyland	9/3/19	Sed. Pore-1	2	58	3	NA	2	29	3	NA	
Skyland	9/3/19	Above Sed.-1	1	3	1	NA	NA	NA	NA	NA	
Skyland	9/3/19	Mid-H2O-1	1	6	1	NA	NA	NA	NA	NA	

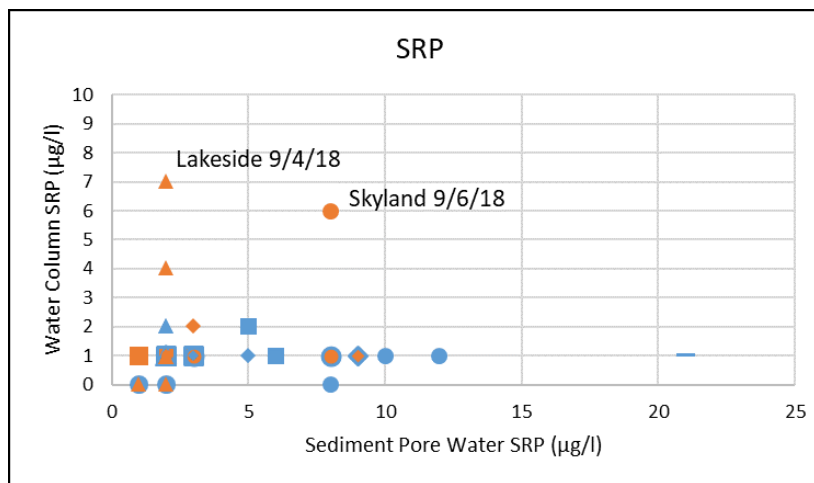
Site Name	Date	Samp. Point	In Patch				Out Patch				Notes
			NO ₃ -N (µg/l)	NH ₄ -N (µg/l)	SRP (µg/l)	Sp. Cond. (µS/cm)	NO ₃ -N (µg/l)	NH ₄ -N (µg/l)	SRP (µg/l)	Sp. Cond. (µS/cm)	
Elk Pt.–Marla Bay	7/23/19	Sed. Pore-1	NA	NA	NA	NA	2	9	21	167/165*	
Elk Pt.–Marla Bay	7/23/19	Mid-H2O-1	NA	NA	NA	NA	2	2	1	92*	
Elk Pt.–Marla Bay	7/23/19	Under Barrier	NA	NA	NA	NA	2	73	2	104	Bottom barrier
Hidden B.	8/2/18	Sed. Pore-1	NA	NA	NA	NA	60	85	16	NA	
Hidden B.	8/2/18	Sed. Pore-2	NA	NA	NA	NA	68	61	2	NA	
Hidden B.	8/2/18	Mean					64	73	9	NA	
Hidden B.	8/2/18	Above Sed.-1	NA	NA	NA	NA	1	2	1	NA	
Hidden B.	8/2/18	Above Sed.-2	NA	NA	NA	NA	1	1	1	NA	
Hidden B.	8/2/18	Mean					1	1.5	1	NA	
Hidden B.	8/2/18	Mid-H2O-1	NA	NA	NA	NA	1	2	1	NA	
Hidden B.	8/2/18	Mid-H2O-2	NA	NA	NA	NA	1	2	1	NA	
Hidden B.	9/5/18	Sed. Pore-1	NA	NA	NA	NA	6	4	2	NA	
Hidden B.	9/5/18	Sed. Pore-2	NA	NA	NA	NA	4	3	3	NA	
Hidden B.	9/5/18	Mean					5	3.5	2.5	NA	
Hidden B.	9/5/18	Mid-H2O-1	NA	NA	NA	NA	0	2	1	NA	
Hidden B.	7/22/19	Sed. Pore-1	NA	NA	NA	NA	11	5	7	128	
Hidden B.	7/22/19	Sed. Pore-2	NA	NA	NA	NA	17	8	3	147/139*	
Hidden B.	7/22/19	Mean					14	6.5	5	137.5	
Hidden B.	7/22/19	Mid-H2O-1	NA	NA	NA	NA	2	1	1	89*	
Hidden B.	9/3/19	Sed. Pore-1	NA	NA	NA	NA	1	2	3	148	
Hidden B.	9/3/19	Above Sed.-1	NA	NA	NA	NA	1	3	1	NA	
Hidden B.	9/3/19	Mid-H2O-1	NA	NA	NA	NA	1	2	1	91*	
<u>Site Name</u> (Streams)	<u>Date</u>		<u>NO₃-N (µg/l)</u>	<u>NH₄-N (µg/l)</u>	<u>SRP (µg/l)</u>	<u>Sp. Cond. (µS/cm)</u>					
Upper Truckee	8/7/19 12:00		20	1	7	63					
North Zephyr	8/7/19 12:40		13	1	7	123					
(Urban Runoff)											
Pasadena Ave.	12/2/19		134	2285	247						



a.



b.



c.

Figure 48 a-c. Sediment pore water concentrations and lake water column concentrations of $\text{NO}_3\text{-N}$, $\text{NH}_4\text{-N}$ and SRP for sites (indicated different symbols) in summer of 2018 and 2019. Colors: orange = water column sample collected just above lake sediment surface; blue = sample either was collected in mid-water column or at the surface.

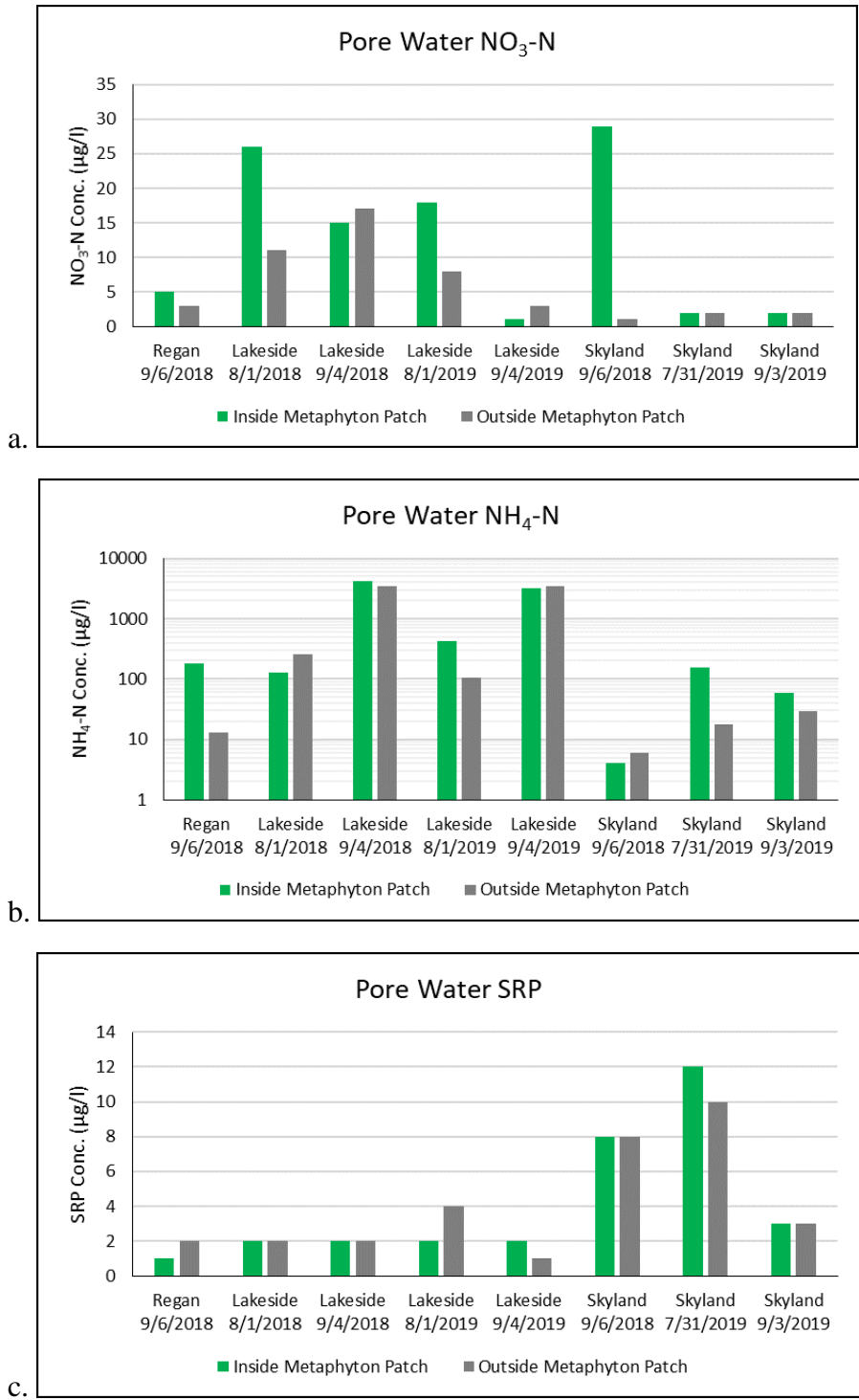


Figure 49 a-c. Concentrations of NO₃-N, NH₄-N and SRP in sediment pore water collected inside and outside of metaphyton patches.

V.B. Nitrogen and Phosphorus in Asian Clam (*Corbicula fluminea*) Excretion

We measured the amount of clam excretion collected over a short period of time to estimate the rates of nutrients released and also collected samples of the excretion for stable isotope analyses. The methods and results for this test are reported below.

V.B.1. Nitrogen and Phosphorus in Asian Clam Excretion Methods

On 7/23/19 the dive team collected samples of Asian clams from the sandy bottom sediments at a depth of approximately 5m slightly offshore of Elk Pt., NV. (near the south end of Marla Bay). Small shovels with slotted openings were used to scoop the clams located near the sand surface into a Ziploc bag. A sufficient number of clams was collected to provide 80 clams of similar size (a subsample of 20 clams was measured and had mean size of 2 cm across). The clams were lightly scrubbed with a toothbrush to remove any adhering dirt or algae, and rinsed in filtered lake water (GF/F filtered, collected from Mid-lake the previous day), and placed briefly in a bag of filtered lake water. A subsample of the filtered lake water was saved to determine initial concentrations of $\text{NO}_3\text{-N}$, $\text{NH}_4\text{-N}$ and SRP. 40 clams each were added to duplicate 1 liter Erlenmeyer flasks containing 720 ml of GF/F filtered Mid-lake water at 10:40 am on 7/23/19 to start the excretion test. The flasks were kept in the shade in a cooler and returned to the lab at TERC by 12:30 pm. In the lab the flasks with clams were kept at room temperature (20°C), with aeration applied equally to both flasks. The clams were held in the flasks for 11.33 hours over which time their excretion accumulated in the water. Since the lake water in the container was filtered, they did not feed on phytoplankton during this period. Excretion was assumed to be associated with feeding at the site prior to collection. After 11.33 hours, water from the flasks was removed and filtered through a 0.45 micron Magna® nylon filter and the water saved for nutrient ($\text{NO}_3\text{-N}$, $\text{NH}_4\text{-N}$ and SRP) analysis. A portion of the water containing excretion was also saved for possible stable isotope analysis.

V.B.2. Nitrogen and Phosphorus in Asian Clam Excretion Results

The results of the excretion test indicated the Asian clams excreted primarily $\text{NH}_4\text{-N}$ and SRP, with no detectable $\text{NO}_3\text{-N}$ excreted (Table 15). The average $\text{NH}_4\text{-N}$ excretion rate was $2.637 \mu\text{g NH}_4\text{-N}$ per clam per hour and the average SRP excretion rate was $0.361 \mu\text{g SRP clam}^{-1} \text{ hr}^{-1}$. These rates are very similar to excretion rates reported for Asian clams in Marla Bay in 2009 (McNair, 2010): $\text{NH}_4\text{-N}$ of 89 ppb/clam/day (which is equivalent to $2.67 \mu\text{g NH}_4\text{-N}$ per clam per hour for 720ml water volume as used in our tests) and SRP of 12.35 ppb/clam/day (which is equivalent to $0.371 \mu\text{g SRP clam}^{-1} \text{ hr}^{-1}$ for 720 ml volume used in our tests). These excretion rates for Tahoe Asian clams are about an order of magnitude lower than rates found for Asian clam excretion in a North Carolina River (Lauritzen and Mozley, 1989), which were $28.84 \mu\text{g NH}_3\text{-N}$ and $11.15 \mu\text{g PO}_4\text{-P}$.

Excretion from large numbers of clams in the sediments would result in elevated levels of $\text{NH}_4\text{-N}$ and SRP in the sediment pore waters. High concentrations of $\text{NH}_4\text{-N}$ were found in sediment pore water both within and outside the metaphyton patch at Lakeside (reaching as high as 3138-4172 $\mu\text{g/l}$ in the Sept. samples). A portion of this $\text{NH}_4\text{-N}$ may have been contributed by clam excretion, some may also result from other biological and chemical reactions in the sediments. It

was interesting that the levels of $\text{NH}_4\text{-N}$ in the sediment pore water appeared be lower earlier in the August samples and to increase at Lakeside later in the summer. This was true for pore water both from inside and outside the metaphyton patch.

Since the clams also excrete SRP it might be expected pore water concentrations of SRP would also be elevated. Interestingly though, the amount of SRP in pore water was relatively low for most samples, ranging to 7 $\mu\text{g/l}$.

We estimated the amount of $\text{NH}_4\text{-N}$ and SRP that could be released associated with clam excretion. For a patch of lake bottom 100m x 100m (1 hectare), with 800 clams/ m^2 (near the median number of clams at Lakeside (see section V.C. on clam abundances)), the excretion contribution of $\text{NH}_4\text{-N}$ from the clams would be 506 g/ha/day and the SRP contribution would be 69 g/ha/day. In comparison, the median contribution of DIN ($\text{NO}_3\text{-N} + \text{NH}_4\text{-N}$) in atmospheric deposition to the lake surface at mid-lake is around 4 g/ha/day and the contribution of SRP is about .05 g/ha/day. The nutrients in excretion represent recycled nutrients generated from feeding on phytoplankton in the water column and organic material in the sediments.

These results need to be considered with knowledge of the inherent patchiness of Asian clam populations at Lake Tahoe. During extensive sampling at the height of the Marla Bay Asian clam occurrence (Wittmann et al., 2008), dozens of grab samples of sediment were taken to estimate clam density. The clam densities ranged from over 1000 clams/ m^2 to zero, with the majority showing zero clams present. It is expected that even in a known area of clam presence, the pore water samples will show a similar patchiness.

Table 15. Clam excretion experiment results.

<u>Test Sample</u>	<u>Test Start Date Time</u>	<u>Collection Date Time</u>	<u># Asian Clams</u>	<u>Elapsed Time</u>	<u>Vol. (L)</u>	<u>NO3-N (µg/l)</u>	<u>NH4-N (µg/l)</u>	<u>SRP (µg/l)</u>	<u>Sp. Cond. µS/cm/sec</u>	<u>Excretion Rate NO3-N µg/clam/hr</u>	<u>Excretion Rate NH4-N µg/clam/hr</u>	<u>Excretion Rate SRP µg/clam/hr</u>
Replicate 1	7/23/19 10:40	7/23/19 22:00	40	11.33 hr	0.720	2	1779	236		-.003	2.823	.373
Replicate 2	7/23/19 10:40	7/23/19 22:00	40	11.33 hr	0.720	2	1544	221	89	-.003	2.453	.350
						2	1662	229		-.003	2.637	.361
Initial Lake H2O	-	7/22/19	-	-	-	4	2	1	92	-	-	-

Table 16. Pore Water, water column and under bottom barrier nutrients.

<u>Site Name</u>	<u>Date</u>	<u>Samp. Point</u>	<u>Out Patch</u>		<u>Sp. Cond. (µS/cm)</u>	<u>Notes</u>
			<u>NH4-N (µg/l)</u>	<u>SRP (µg/l)</u>		
Elk Pt.–Marla Bay	7/23/19	Sed. Pore-1	9	21	167/165*	
Elk Pt.–Marla Bay	7/23/19	Mid-H2O-1	2	1	92*	
Elk Pt.–Marla Bay	7/23/19	Under Barrier	73	2	104	Bottom barrier

These nutrient inputs could impact metaphyton algae growth at locations like Lakeside and Skyland. The combination of N + P as is present in clam excretion may be particularly beneficial for algal growth. In bioassays using Lake Tahoe phytoplankton through the years, the combination of N and P added together was nearly always stimulatory to the phytoplankton (Hackley et al., 2013). It's possible the filamentous algae in the metaphyton may similarly benefit from the combination of N and P contributed with clam excretion.

V.B.3. Nutrient Accumulation under Bottom Barrier

In addition to testing excretion levels using clams collected from Elk Point, we collected samples of water which might be seeping into the lake from the sediments there for nutrient analysis and stable isotope analysis. On 7/11/19, a 10 ft. X 10 ft. sheet of EDPM rubber pond liner anchored with heavy gage rebar, was placed over the sediments adjacent to the area where the clams for the excretion experiment were collected from. After 12 days (on 7/23/19) the water accumulated under the barrier was sampled to check for levels of nutrients. Pore water from sediments adjacent to the barrier was also sampled.

The results of sampling of sediment pore water adjacent to the barrier and sampling of the water accumulated underneath the barrier are presented in Table 16. Sediment pore water collected adjacent to the barrier was found to have slightly elevated $\text{NH}_4\text{-N}$ (9 $\mu\text{g/l}$) and elevated SRP (21 $\mu\text{g/l}$). The elevated $\text{NH}_4\text{-N}$ and SRP in the pore water at Elks Pt. may have been the result of Asian clam excretion. Water collected from underneath the bottom barrier which had been in place for 12 days also had an elevated $\text{NH}_4\text{-N}$ concentration 73 $\mu\text{g/l}$ compared with $\text{NH}_4\text{-N}$ in the water column (2 $\mu\text{g/l}$), while SRP levels under the barrier were only slightly elevated (2 $\mu\text{g/l}$) compared to the water column water from the same area (1 $\mu\text{g/l}$). Specific conductance (SC) of pore water adjacent to sediments capped by the barrier, was 167 $\mu\text{S cm}^{-1}$, while SC of water collected under the barrier was 104 $\mu\text{S/cm/sec}$. Typical lake surface water Sp. Cond. is near 92 $\mu\text{S cm}^{-1}$ which was observed in the mid-water column sample. The elevated Sp. Cond. in the water from under the barrier indicates there may have been transfer of pore water into the overlying water.

The elevated $\text{NH}_4\text{-N}$ under the barrier may have represented $\text{NH}_4\text{-N}$ contributed to surface water from clam excretion. Chemical changes in water quality under the barrier were also possible if the water and sediments became anoxic. We do not have information on the level of oxygen in water underneath the barrier for this sampling.

V.C. Asian Clam Abundance

Estimates of numbers of live Asian clams and dead (relic) clamshells were made at Regan, Lakeside, Skyland and Hidden Beach to relate to information on nutrients and metaphyton.

V.C.1. Asian Clam Abundance Methods

Two to three replicate samples of clams were collected by divers. Plastic scoops which retained clams and shells but let sand grains pass through were used to collect clams and shells to a depth of 3-4 inches in the sand, from within areas outlined by a 0.25 x 0.25m² (0.0625 m²) randomly placed quadrat. Clams and shells collected from the sand were placed in plastic bags and

returned to the boat. Live clams, relic shell pairs and single valves were counted to determine numbers at each sampling site.

V.C.2. Asian Clam Abundance Results

No Asian clams were found at Hidden Beach, and very low numbers of live clams were found at Regan Beach, while Lakeside and Skyland had relatively high numbers of clams. Table 17 summarizes the mean numbers of live Asian clams found at the sites on different dates and Figure 50 summarizes the data for all replicates collected from sites in a box and whisker plot.

Close to shore at Regan, mean numbers of live clams per sampling date ranged from 0-16 clams/m² inside metaphyton patches and 5-8 clams/m² outside patches. About 180 m offshore at Regan, Asian clam numbers were slightly higher (32 clams/m²).

At Lakeside, high numbers of Asian clams were found both inside and outside the metaphyton patch. Inside the patch, mean numbers per sampling date of clams ranged from 688 to 1016 clams/m² (overall: mean = 784 clams/m², median = 784 clams/m²). Outside the patch, mean numbers ranged from 632 to 1016 clams/m² (overall: mean = 856 clams/m², median = 888 clams/m²). These numbers are higher than reported in Wittmann et al. (2011) for Lakeside (median number of clams of approximately 200 clams/m² with a maximum of 800 clams/m² in 2009).

At Skyland, the mean numbers of live clams collected per sampling date ranged from 224 – 2608 clams/m² inside metaphyton patches (overall: mean = 1290.7, median = 1040) and from 416-1224 clams/m² outside patches (overall: mean = 776, median = 688 clams/m²).

The numbers of dead clam or relic shells was also counted in samples. Generally low numbers of shells were observed in the nearshore area at Regan (mean of 0-24 paired shell valves per m² in patches, 0-40 paired shell valves per m² outside patches), with slightly more (168 paired shell valves per m²) approximately 180 m offshore. At Lakeside, there were large numbers of shells within the metaphyton patch area mean range (560-3240 paired shell valves per m²) and generally fewer numbers outside the patch (range 8-1048 paired shell valves per m²). At Skyland, relatively low numbers of shells (0-56 shell pairs per m² inside and outside patches) were found for several of the samplings. However, on one date, 7/31/19, there was a large number of shells (2752-4736 paired shell valves per square meter) associated with a patch of metaphyton. There were also a large number of live clams associated with this patch (2032-3084/m²). From aerial images at Skyland we know there are many large patches of shells towards the outer portion of the shelf along shore.

Table 17. Summary of number of live Asian clams and shells at sites on sampling dates (Mean \pm std. deviation with (n) collection replicates). “Inside Patch” is inside metaphyton patch; “Outside Patch” is outside metaphyton patch; “Shells” are dead (relic) clam shells.

<u>Site</u>	<u>Date</u>	Inside Patch Live Clams (#/ m ²)	Inside Patch Shells (Valve pairs) (#/ m ²)	Inside Patch Shells (Non- paired valves) (#/ m ²)	Outside Patch Live Clams (#/ m ²)	Outside Patch Shells (Valve pairs) (#/ m ²)	Outside Patch Shells (Non- paired valves) (#/ m ²)
Regan Nearshore	8/1/18	0 \pm 0 (3)	0 \pm 0 (3)	0 \pm 0 (3)	5 \pm 9 (3)	0 \pm 0 (3)	5 \pm 9 (3)
Regan Nearshore	9/6/18	0 \pm 0 (2)	8 \pm 11 (2)	0 \pm 0 (2)	8 \pm 11 (2)	40 \pm 34 (2)	8 \pm 11 (2)
Regan Nearshore	8/1/19	8 \pm 11 (2)	24 \pm 34 (2)	56 \pm 11 (2)	-	-	-
Regan Nearshore	9/4/19	16 \pm 0 (2)	8 \pm 11 (2)	144 \pm 23 (2)	-	-	-
Mean		5.3	8.9		6.4	16	
Median		0	0		0	0	
n		9	9		5	5	
Regan Offshore	8/1/19	32 \pm 0 (2)	168 \pm 57 (2)	88 \pm 11 (2)	-	-	-
Lakeside	8/1/18	744 \pm 11 (2)	3240 \pm 11 (2)	-	1016 \pm 260 (2)	1048 \pm 125 (2)	-
Lakeside	9/4/18	688 \pm 272 (2)	1160 \pm 419 (2)	-	632 \pm 487 (2)	96 \pm 0 (2)	-
Lakeside	8/1/19	688 \pm 543 (2)	2008 \pm 1120 (2)	864 \pm 656 (2)	880 \pm 91 (2)	648 \pm 34 (2)	168 \pm 102 (2)
Lakeside	9/4/19	1016 \pm 283 (2)	560 \pm 249 (2)	184 \pm 57 (2)	896 \pm 339 (2)	8 \pm 11 (2)	24 \pm 11 (2)
Mean		784	1742		856	450	
Median		784	1336		888	360	
n		8	8		8	8	
Skyland	9/6/18	224 \pm 23 (2)	16 \pm 23 (2)	0 \pm 0 (2)	416 \pm 113 (2)	0 \pm 0 (2)	-
Skyland	7/31/19	2608 \pm 815 (2)	3744 \pm 1403 (2)	3920 \pm 1471 (2)	688 \pm 23 (2)	48 \pm 0 (2)	8 \pm 11 (2)
Skyland	9/3/19	1040 \pm 656 (2)	48 \pm 45 (2)	40 \pm 34 (2)	1224 \pm 464 (2)	56 \pm 11 (2)	48 \pm 0 (2)
Mean		1290.7	1269.3		776	34.7	
Median		1040.0	56		688	48	
n		6	6		6	6	
Hidden	9/4/18	-	-	-	0 \pm 0 (2)	-	-
Hidden	7/22/19	-	-	-	0 \pm 0 (2)	-	-
Hidden	9/3/19	-	-	-	0 \pm 0 (6)	-	-
Mean					0		
Median					0		
n					10		

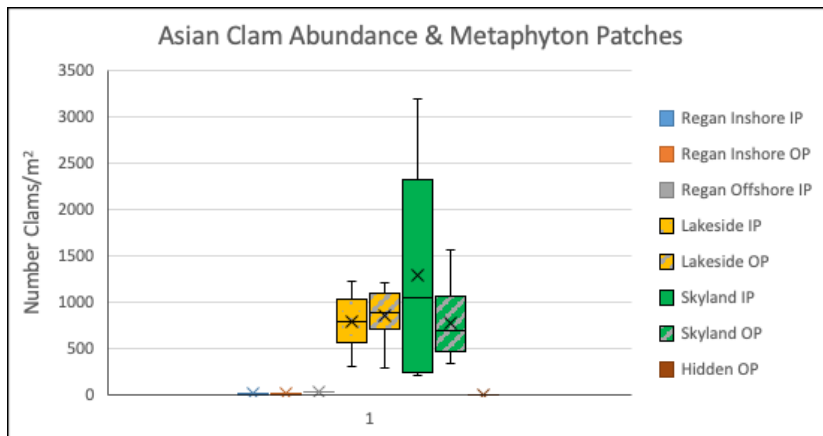


Figure 50. Abundance of live Asian Clams at sites inside metaphyton patches (IP) and outside metaphyton patches (OP). Whisker and box plot, horizontal lines are quartiles, center line is median, “X” is average of all values, whiskers are minimum and maximum values.

V.C.3. Asian Clam Abundance Discussion

There were no Asian Clams or shells found at Hidden Beach. There was a small amount of algae along the bottom which included detritus, cyanobacteria and some algae which appeared to be derived from the periphyton on nearby boulders. The algae was only visible when swimming underwater and was not similar to the bright green metaphyton patches observed along the south and southeast shore. Low to moderate levels (using mean when replicates were collected) of $\text{NO}_3\text{-N}$ (1-64 $\mu\text{g/l}$), $\text{NH}_4\text{-N}$ (2-73 $\mu\text{g/l}$) and SRP (2-9 $\mu\text{g/l}$) were found in pore water at Hidden Beach. Asian Clams are not impacting this site.

At Regan Beach there were very few live clams and shells in the nearshore. Low –moderate levels of nutrients were found in pore water $\text{NO}_3\text{-N}$ (2-19 $\mu\text{g/l}$) including samples inside and outside patches, $\text{NH}_4\text{-N}$ (2-182 $\mu\text{g/l}$), and SRP (1-6 $\mu\text{g/l}$). There were relatively large patches of metaphyton near the shore there, a large amount of aquatic vegetation, much of it with algae and metaphyton filamentous green algae, as well as thick growth of attached periphyton *Cladophora* along the boulder breakwater lining the park.

The substantial metaphyton green filamentous algae growth, algae and periphyton at Regan may be supported by nutrient inputs from sources other than Asian Clams. There are few live clams in the nearshore. The Upper Truckee River and Trout Creek flow into the lake through the Upper Truckee marsh west of this site. The inflow from these streams typically hugs the shore to the east and can impact Regan. Evidence of stream impact on this site was seen during aerial observations as darker colored plume of water along shore. Also, specific conductivity in the

mid-water column at Regan on 8/1/19 (83 $\mu\text{S cm}^{-1}$) was lower than typical lake value of 92 $\mu\text{S /cm}$. The Upper Truckee River contributes nutrients which may impact algae growth (for instance on 8/7/19, it had a $\text{NO}_3\text{-N}$ concentration of 20 μl , $\text{NH}_4\text{-N}$ of 1 $\mu\text{g/l}$, SRP of 7 $\mu\text{g/l}$. Storm water and urban runoff also enter the lake near this site, which can have high concentrations of nutrients. A sample of storm water discharging to the lake at Pasadena Ave. on 12/2/19 had quite high levels of nutrients (i.e. $\text{NO}_3\text{-N}$ 134 $\mu\text{g/l}$, $\text{NH}_4\text{-N}$ 2285 $\mu\text{g/l}$, SRP 247 $\mu\text{g/l}$). The productive aquatic plant and algae growth at Regan Beach may be due to nutrient inputs associated with surface runoff there.

At Lakeside there were large numbers of live clams and a large patch of metaphyton present. The data collected in this and previous studies suggest a potential linkage between Asian Clams and metaphyton at this site. There may be additional factors contributing to the development of the metaphyton patch there as well though. The presence of high levels of $\text{NH}_4\text{-N}$ in pore water concentrations inside and outside of the metaphyton patch and also high numbers of clams inside and outside the patch suggests a possible linkage between the clams and $\text{NH}_4\text{-N}$ concentrations. The increase in $\text{NH}_4\text{-N}$ from August to Sept. in pore water samples may indicate contribution of $\text{NH}_4\text{-N}$ by the clams. Wittmann et al (2011) found veliger (clam larva) production to increase in late summer. Williams and McMahon (1989) found Asian Clam excretion may increase during spawning – *Corbicula fluminea* showed a 20–40-fold increase in excretion with spawning. Clams may be adding more $\text{NH}_4\text{-N}$ into the sediments associated with excretion later in the summer. Other chemical and biological processes in the sediments may also be contributing to the late summer increase in $\text{NH}_4\text{-N}$. Loeb (1987) looked at lake sediment pore water $\text{NH}_4\text{-N}$ along the south shore near Pope Beach and offshore of the Upper Truckee marsh and also observed seasonal fluctuation with highest values observed during the summer. Increased microbial activity in the sediments during the summer was thought to be a potential cause.

Relatively low levels of SRP (1-4 $\mu\text{g/l}$) were observed in Lakeside sediment pore water despite large numbers of Asian clams. This is contrary to what might be expected since SRP is elevated in clam excretion. Wittmann et al., 2011 also looked at SRP in pore water from the Lakeside area and did find elevated SRP. We do not fully understand why the SRP was so low in the samples we collected at Lakeside. It is possible there may have been loss of SRP from solution in our samples when the samples became oxygenated see discussion in footnote.¹² It is possible

¹² Many of the pore water samples appeared to produce an orange precipitate after collection, an indication that the water was anoxic. The precipitates likely were complexes of insoluble iron oxides which formed as oxygen entered the water prior to filtration later in the day. $\text{PO}_4\text{-P}$ can also complex with iron oxides. The precipitates were removed during filtration with a 0.45-micron filter prior to analysis. Wittmann et al. (2011), also looked at SRP in sediment pore water in areas where clams were present at Lakeside in 2009. They used a different method in which sediment cores were collected and frozen, then the frozen core was divided into sections, thawed, and pore water filtered through a GF/C filter (~1.2-micron pore size), then the water was frozen again until analyzed. They found much higher SRP concentrations in pore water (> 100 $\mu\text{g/l}$) at Lakeside and even higher concentrations at Marla Bay (~200-600 $\mu\text{g/l}$ in a majority of samples). The larger pore size filter they used may resulted in more particulate-associated P passing through the filter and being picked up in their analysis as SRP.

that the SRP was taken up rapidly by microorganisms in the sediments. Or that other chemical reactions were occurring in the sediments resulting in low SRP in the pore water.

NO₃-N was also relatively low in sediment pore from Lakeside. It is possible the clams are having some impact on loss of NO₃-N through denitrification. *Corbicula* has been shown to increase denitrification in sediments in some systems (Turek and Hollein, 2015).

The filamentous green algae metaphyton patch at Lakeside was very interesting. The layer of algae observed by divers was 4-6 inches thick on one date and there was nearly 100% cover over the bottom in the area where it was located. The patch appeared to mostly disappear in the winter based on UAV images. There were greater numbers of clam shell coincident with the patch location compared with the area outside it. The patch appears to be in a transition area from shallower to slightly deeper bottom area along the shelf offshore. Currents may naturally deposit the shells in this transition area. (Historical images from Google Earth show the presence of shell patches in this area in recent years). It is possible the metaphyton similarly tends to accumulate or stay in place in this depression area. The presence of shells may also provide substrate for filamentous algae to attach to or become entangled within and so be held in place. It is possible that a combination of nutrient inputs from clams, topography, current effects as well as physical roughness provided by shells along the bottom, may contribute to the development of the metaphyton patch at Lakeside.

At Skyland, the number of live clams inside and outside patches was more variable and the association with presence of metaphyton patches was not consistent. There were slightly more live clams outside metaphyton patches than inside patches for samplings done in Sept. 2018 and 2019. However, for the 7/31/19 sampling there were very large numbers of live clams (mean = 2608/m²) and shell pairs (mean=3744/m²) associated with a filamentous green metaphyton patch. The metaphyton in the patch at this site, may have resulted from attachment sites afforded by the shells, and/or nutrients contributed by the live clams or both.

Both the helicopter and UAV images show dark patches of metaphyton over the sandy bottom at Skyland. These patches were fairly large (up to 3m x 5m) and extend up off the bottom about 0.5 m. Underwater photos collected during sampling also show there were also areas of bottom with variable coverage with small patches of metaphyton. The divers also observed thin coating of algae over the bottom on at least one. The metaphyton was also observed to move along the bottom in this area.

The images from the helicopter of Skyland show an area with substantial white patches of offshore of Skyland. These represent large patches of clamshells. Inspection from just below the surface indicated algae over portions of the shell beds. Forrest et al (2012) in their surveys with an AUV, also noted the presence of clams off of this area in 2009. Currents may play a role in moving both clamshells and metaphyton algae at Skyland. Model simulations of currents along the southeast shore by Schladow et al. (2014) have shown the currents do affect the shelf area there. Currents likely play a role in the accumulation of large patches of shells on the sloping shelf offshore there.

Currents may also move metaphyton out of this shelf area at Skyland. On 9/6/18 during monitoring at Skyland, large patches of metaphyton were observed. When we returned to the site later in September after a strong south west wind event, the metaphyton patches were gone. They apparently had been either moved or dispersed by currents associated with a period of strong winds.

Overall at Skyland, pore water levels of $\text{NH}_4\text{-N}$ were low to moderate (5-158 $\mu\text{g/l}$) and SRP slightly elevated (3-12 $\mu\text{g/l}$). There were areas with substantial live clams, and shells. The nutrients produced by the clams and the association of algae with shell patches, suggest there is potential for a linkage between the algae growth and presence of clams either due to nutrient inputs or physical impacts of the shells or both. Currents can impact algae and distribution of shells at this site.

V.D. Stable Isotopes ^{13}C and ^{15}N in Metaphyton Algae

There is a growing body of evidence supporting linkages between the Asian clams and metaphyton/ green filamentous algal growth in Lake Tahoe. This would be evident through the co-location of metaphyton in areas with large numbers of live clams as well as shells (Wittmann et al., (2008); Schladow et al. (2010), Wittmann et al, (2011); Forest et al (2012). There have been demonstrations of the potential for clam excretion to stimulate filamentous algae growth (Wittmann, et al., 2011); elevated $\text{NH}_4\text{-N}$ in sediment pore water from sites with clams (Wittmann et al., 2011; this study); elevated SRP in pore water from sites with clams (Wittmann et al., 2011). There are also other factors that may contribute to the observed distribution of metaphyton at sites (i.e. currents and accumulation of metaphyton in depressions, other sources of nutrients including tributary inputs and storm water inputs, presence of aquatic vegetation and clam shells as attachment points for filamentous algae.

We were interested in whether there was a way to directly demonstrate a link between Asian Clam and growth of metaphyton at the sites and whether stable isotopes of ^{13}C and ^{15}N could be used to assess a linkage between nutrients in clam excretion and growth of the metaphyton.

We received a small pilot study grant from the UC Davis Stable Isotope Facility to apply to stable isotope sample analyses, to test whether stable isotopes could be used to demonstrate a linkage between clams and metaphyton growth.

The approach we took was to examine stable isotopes in metaphyton algae and algae from a range of sites around the lake, with and without presence of Asian clams. Then compare the range for values, and range for values in a specific source related to clams, i.e. excretion. This was similar to an approach recommended in Peterson and Fry (1987):

“It is often impossible to judge on theoretical grounds alone whether or not stable isotopes will be useful in solving a particular field research problem. However, by analyzing a few carefully selected samples, one can often determine whether further analyses will contribute significantly to a solution. One initial objective is to determine signal to noise ratio. If isotopic differences between pools are very large and the variation within pools is small, isotopes may provide a very powerful tool, and a few samples may be very effective”.

If the range for isotopic ratios were relatively low within algae from areas with little or no clams, and the levels noticeably different in algae from areas with a large presence of clams, this would be a first step in showing a linkage between presence of clams and metaphyton at the sites.

The next step was to look at stable isotopes in excretion products produced by the clams and compare to levels in clams from within clam-impacted areas. Our plan was to analyze stable isotopes both in excretion produced by the clams, along with stable isotopes in some potential natural waters which may supply nutrition to the clams (i.e. tributary water, storm water, ground water and pore water, precipitation). However, concentrations of $\text{NO}_3\text{-N}$ and $\text{NH}_4\text{-N}$ in many of the water samples as collected were too low for analysis of stable isotopes. A few samples did have sufficient $\text{NH}_4\text{-N}$ for stable isotope analysis of ^{15}N $\text{NH}_4\text{-N}$, these included (samples of clam excretion, Pasadena Ave. storm water and sediment pore water from Lakeside). With lab closures due to the COVID19 pandemic, stable isotope analyses of the water samples were not completed as of preparation of this report. However, analyses for ^{13}C and ^{15}N in algae samples were complete and we report the results here.

V.D.1. Methods

Metaphyton filamentous green algae and other algae samples were collected during site monitoring visits and associated with ground-truthing visits. Portions of samples were dried at 60°C and stored frozen. A portion of these samples were selected for analysis of ^{13}C and ^{15}N analysis, focusing on primary study sites, with select samples from other areas of the lake. The dried samples were ground to a powder using a cleaned mortar and pestle, and a small amount of the ground algae (usually ~3-5 mg) added to a tin capsule, the capsule folded and sealed and placed in a tray in preparation for analysis by the UC Davis Stable Isotope Facility. UCD SIF descriptions of procedures for ^{13}C and ^{15}N isotope analysis of the are presented below.

Samples were analyzed for ^{13}C and ^{15}N isotopes at UCD SIF using a PDZ Europa ANCA-GSL elemental analyzer interfaced to a PDZ Europa 20-20 isotope ratio mass spectrometer (Sercon Ltd., Cheshire, UK). Samples are combusted at 1000°C in a reactor packed with chromium oxide and silvered copper oxide. Following combustion, oxides are removed in a reduction reactor (reduced copper at 650°C). The helium carrier then flows through a water trap (magnesium perchlorate and phosphorous pentoxide). N_2 and CO_2 are separated on a Carbosieve GC column (65°C , 65 mL/min) before entering the IRMS.

During analysis, samples are interspersed with several replicates of at least four different laboratory reference materials. These reference materials have been previously calibrated against international reference materials, including: IAEA-600, USGS-40, USGS-41, USGS-42, USGS-43, USGS-61, USGS-64, and USGS-65) reference materials. A sample's provisional isotope ratio is measured relative to a reference gas peak analyzed with each sample. These provisional values are finalized by correcting the values for the entire batch based on the known values of the included laboratory reference materials. The long term standard deviation is 0.2 per mil for ^{13}C and 0.3 per mil for ^{15}N .

The final delta values, delivered to the customer, are expressed relative to international standards VPDB (Vienna Pee Dee Belemnite) and Air for carbon and nitrogen, respectively. For information on delta notation and the international references, please refer to a stable isotope reference such as Sharp, Z. (2005) *Principles of Stable Isotope Geochemistry* (Prentice Hall).

Samples of clam excretion water collected from the clam excretion test, samples of pore water collected from the sites and storm water was filtered on the day of collection through 0.45-micron pore size nylon Magna® filters. A portion of the water was refrigerated and analyzed for NO₃-N, NH₄-N and SRP at the UC Davis TERC lab. Another portion was frozen for potential later analysis by the UC Davis Stable Isotope Facility.

$\delta^{15}\text{N}$ in NH₄ in clam excretion, pore water from Lakeside and stormwater from Pasadena Ave. was also to be analyzed by the UCD SIF after the lab reopened following closure due to the COVID 19 pandemic. Samples had not yet been analyzed as of preparation of this draft report.

V.D.2. Results

The results for analysis of $\delta^{15}\text{N}$ and $\delta^{13}\text{C}$, Total Carbon, Total Nitrogen and Molar C: N ratios in metaphyton algae and other algae samples are presented in Table 18. Results for $\delta^{13}\text{C}$ and $\delta^{15}\text{N}$ in metaphyton algae are plotted by site in Figure 51 and 52 respectively.

$\delta^{13}\text{C}$ values for many of the sites ranged between -15 to -21 ‰. The exception was for the filamentous algae *Tribonema* collected from the mouth of the Upper Truckee River. The $\delta^{13}\text{C}$ for that site was much more negative -38 ‰. Comparing levels of $\delta^{13}\text{C}$ in algae between sites with no Asian Clam presence (Hidden Beach and Tahoe City) and little Asian Clam influence (Regan Beach), with sites with more Asian clam presence showed ranges were similar among sites. There was not a discernable difference in $\delta^{13}\text{C}$ between sites with clams and sites without or with low amounts of clams.

The one site with notably different $\delta^{13}\text{C}$ was in algae from the mouth of the Upper Truckee River. That site was in the inflow from the Upper Truckee River and impacted by stream flow, increased nutrients, likely increased dissolved organic carbon, high light at the surface and variable temperature. The filamentous algae primarily consisted of the Xanthophyte *Tribonema*.

$\delta^{15}\text{N}$ for the sites showed more variability by site. $\delta^{15}\text{N}$ in filamentous algae from the Upper Truckee mouth was quite elevated, near 5 ‰. Most of the other samples ranged from 0 to near -3 ‰. Two samples, an inshore and offshore sample from Hidden Beach had slightly positive $\delta^{15}\text{N}$ values between 0 and 2‰.

When sites with little or no presence of clams were compared with sites with presence of clams, some slight differences did appear. Sites with presence of clams had some of the lowest ranges for $\delta^{15}\text{N}$, i.e. Lakeside (range -1.6 to -2.6‰), Elk Pt. (range -1.5 to -1.7‰), Round Hill Pines (range -1.1 to -1.4‰) and Skyland (range -0.4 to -1.7‰). It should be noted these sites are also deeper sites (5m+) which may also potentially have an impact on $\delta^{15}\text{N}$. Sites with fewer numbers

of clams and closer to the Upper Truckee River had $\delta^{15}\text{N}$ closer to 0, i.e. Regan (range 0 to -0.6) and El Dorado Beach (range -0.2 to -0.7). However, Tahoe City, which had no clams had negative $\delta^{15}\text{N}$ levels (range -1.7 to -1.8) which are similar to some of the sites with clams. The sample there was collected in the fall of 2019 and came from a very small amount of algae that appeared to be a remnant of the summer growth there. Offshore samples from Hidden Beach had spanned a range of values from (range -1.4 to 0.5) while samples from nearshore, in shallower water, had a range of (range 1.5 to 1.6). The sample with a $\delta^{15}\text{N}$ of -1.4 was composed mostly of detritus and cyanobacteria. This is different from the composition of metaphyton along the south shore which is often composed of green filamentous algae. Therefore, a few of the algae samples from sites without clams had $\delta^{15}\text{N}$ similar to sites with clams. It would be desirable to have more samples analyzed from algae outside clam areas to better understand the variability in $\delta^{15}\text{N}$ for algae outside clam impacted areas. We may attempt this with some additional samples remaining from last summer's work.

The results for $\delta^{15}\text{N}$ suggest a possible association between more negative values and presence of clams, but a limited number of samples from sites without clams also had negative $\delta^{15}\text{N}$. It would be desirable to have a few more samples analyzed from algae outside clam areas to better understand the variability in $\delta^{15}\text{N}$ for algae outside clam impacted areas. It will be valuable to see what the values are for $\delta^{15}\text{N}$ $\text{NH}_4\text{-N}$ in excretion, pore water and storm water (analyses still pending), how they compare to levels in metaphyton nearby to see if the stable isotopes provide additional evidence of the link between clams and metaphyton growth.

Table 18. Results for analysis of stable isotopes $\delta^{15}\text{N}$ and $\delta^{13}\text{C}$, as well as Total Carbon, Total Nitrogen and Molar C: N ratios in metaphyton algae and other algae collected during the study.

<u>Algae Sampled At:</u>	<u>Date</u>	$\delta^{13}\text{C}_{\text{VPDB}}$ <u>(‰)</u>	$\delta^{15}\text{N}_{\text{Air}}$ <u>(‰)</u>	<u>Total C (μg)/ Sample Wt. (μg)</u>	<u>Total N (μg)/ Sample Wt. (μg)</u>	<u>C:N molar ratio</u>
U. Truckee R. mouth	8/20/2019	-37.76	4.94	0.289	0.0149	22.6
U. Truckee R dup.	8/20/2019	-37.76	4.78	0.288	0.0146	23.0
Regan ns. A1-2	8/1/2019	-19.92	-0.46	0.119	0.0097	14.3
Regan ns. A1-2	8/1/2019	-20.06	-0.45	0.122	0.0098	14.4
Regan ns. B2-2	8/1/2019	-21.23	-0.63	0.056	0.0041	16.0
Regan ns. 100% 1-2	9/4/2019	-20.08	-0.32	0.206	0.0150	16.0
Regan ns. 100% 2-2	9/4/2019	-18.45	-0.02	0.271	0.0186	17.0
El Dorado ns. 2	8/7/2019	-17.52	-0.66	0.336	0.0143	27.5
El Dorado ns. 3	8/7/2019	-17.19	-0.17	0.337	0.0157	25.0
Lakeside os. 1-1	7/24/2019	-17.83	-1.97	0.276	0.0111	29.1
Lakeside os.1-2	7/24/2019	-18.00	-1.85	0.284	0.0114	29.1
Lakeside os. 2-1	7/24/2019	-16.82	-1.62	0.128	0.0065	23.0
Lakeside os. 3-1	7/24/2019	-17.45	-2.03	0.180	0.0082	25.6
Lakeside os. 3-1 dup.	7/24/2019	-17.32	-2.04	0.169	0.0077	25.5
Lakeside os. 1-2	8/1/2019	-16.33	-1.67	0.166	0.0085	22.8
Lakeside os. 2-2 IP	8/1/2019	-16.40	-1.90	0.034	0.0020	19.9
Lakeside os. 1-2	9/4/2019	-15.21	-2.63	0.292	0.0193	17.7
Lakeside os. 2-2	9/4/2019	-17.22	-1.77	0.296	0.0192	18.0
Elk Pt. os. 1-1	7/23/2019	-14.80	-1.46	0.299	0.0157	22.2
Elk Pt. os. 1-2	7/23/2019	-15.12	-1.54	0.243	0.0130	21.9
Elk Pt. os. 2-1	7/23/2019	-15.71	-1.60	0.191	0.0116	19.2
Elk Pt. os. 2-2	7/23/2019	-15.62	-1.68	0.178	0.0100	20.7
Elk Pt. os. 2-2 dup.	7/23/2019	-15.70	-1.53	0.166	0.0098	19.8
Round Hill Pines os. 1	9/11/2019	-17.26	-1.05	0.272	0.0115	27.5
Round Hill Pines os. 1	9/11/2019	-17.28	-1.17	0.268	0.0112	27.9
Round Hill Pines os. 2	9/11/2019	-18.27	-1.38	0.162	0.0058	32.4
Skyland os. A-1	7/31/2019	-15.80	-0.43	0.218	0.0097	26.2
Skyland os. B3-2	7/31/2019	-15.11	-1.33	0.302	0.0173	20.4
Skyland os. C2-2	7/31/2019	-15.26	-1.67	0.269	0.0174	18.0
Skyland os. A2	9/3/2019	-18.75	-0.52	0.108	0.0068	18.5
Skyland os. B2	9/3/2019	-18.15	-0.99	0.194	0.0120	18.9
Skyland os. B2 dup.	9/3/2019	-18.22	-0.80	0.197	0.0122	18.8
Hidden ns. 4	7/22/2019	-18.62	1.55	0.234	0.0075	36.6
Hidden ns. 4 dup.	7/22/2019	-18.57	1.45	0.235	0.0071	38.8
Hidden os. 3	7/22/2019	-17.19	-1.35	0.039	0.0024	19.1
Hidden os. 1	9/3/2019	-16.90	0.46	0.188	0.0154	14.3
Hidden os. 2	9/3/2019	-16.99	-0.53	0.082	0.0058	16.7
Tahoe City ns.	10/11/2019	-17.77	-1.88	0.184	0.0061	35.0
Tahoe City ns. dup.	10/11/2019	-17.80	-1.77	0.182	0.0061	34.7

Section VI. Conclusions and Recommendations for Regional Metaphyton Monitoring Program

This project had the primary goal of developing and demonstrating a regional (lake-wide) monitoring approach for the status and trend monitoring of summer metaphyton growth and distribution using a combination of aerial surveillance via a helicopter and an UAV, and a ground-truthing program. Through the project we have tested both aerial platforms and have refined our ground-truthing methodology.

In addition, the project wished to test the association of metaphyton blooms with the occurrence of the invasive clam, Asian clam, as these clams are known to excrete highly concentrated levels of nutrients and have been present in the lake for a similar amount of time for which metaphyton has anecdotally been of concern. Through funding obtained from UC Davis, we also experimented with the use of stable isotopes to quantitatively link metaphyton with Asian clam and other potential sources of nutrients.

Additionally, we experimented with the data to investigate the possibility of simultaneously detecting and quantifying the extent of periphyton coverage. Periphyton, or attached algae, are another important issue impacting nearshore quality.

It is now possible to draw the following conclusions:

1. The use of helicopter-based surveys was shown to have great potential for rapidly visualizing the entire shoreline of Lake Tahoe. Such a survey takes approximately one hour of flight time. A variety of cameras were used, with variable success for numerous technical reasons as described in the report. Currently the technical difficulties associated with vibration and accurately ortho-rectifying the imagery are the greatest drawbacks to using a helicopter-based approach. The speed and simplicity of the approach are its greatest attributes, making it in its current state ideal as a semi-quantitative, rapid surveillance tool. Most of the areas of metaphyton algae observed in helicopter images were found along the south and south east shores of the lake, extending from Tallac Point to Glenbrook Bay.
2. UAV, or drone-based surveys provided very high spatial resolution imagery (ground resolution < 3"). While limited in range compared to the helicopter, they were able to complete the quantitative surveillance of areas on the scale of 10 hectares (1 km x 100 m) in under 10 minutes. Using a combination of commercially available software and algorithms developed through this project, it was possible to identify different targets (metaphyton, periphyton, rooted plants, sand, rock, structures etc.) to a very high level of accuracy, repeatability and confidence. This post-processing can be accomplished in under 4 hours per site. This allowed for the very accurate calculation of the extent of cover by metaphyton. This was one of the primary goals of the project.
3. Ground-truthing techniques that had been developed through an earlier study were modified and refined. We now have the ability to rapidly collect metaphyton samples, and to process

them to determine biomass. What became apparent was that the high degree of patchiness or spatial variability in metaphyton distribution led to large standard deviations in the measured biomass. The only way to reduce this would be to utilize a great many more ground-truthing sites, something that would greatly add to the cost of a monitoring program. However, by using UAV measurements to quantitatively determine the spatial variability and then using ground-truthing on specific patches of growth, it is possible to quantify the biomass within the very heterogeneous distribution.

4. Spectral signatures of different types of algae and substrate had been collected by TERC as part of an earlier SNPLMA project. We experimented with using these spectral signatures as a way to identify different algal and plant types. However, the similarities of the signatures, combined with the low reflection of shortwave signals from water, and the interference produced by dissolved and suspended material in the nearshore led us to conclude that this approach is still not feasible.
5. The co-location of Asian clams and metaphyton was explored by taking nutrient measurements in the lake water and in the pore water, through quantifying the distribution of Asian clams (both live and dead) relative to the location of metaphyton patches, and measuring the nutrient flux produced by Asian clam excretion. The measurements of clam densities, nutrient excretion rates, and pore water nutrient concentrations were largely in agreement with earlier measurements. The clams were shown to excrete primarily $\text{NH}_4\text{-N}$ and SRP. In some cases, clam densities exceeded previous estimates, although these were highly variable. It was found that while there was a connection in the location of metaphyton patches and Asian clam populations, it was variable. The reasons for this were:
 - the inherent patchiness of Asian clam distribution makes it difficult to know where they are and what their areal concentration is;
 - the movement of metaphyton patches by lake currents means that while they may have been initiated in concert with an area of Asian clams, the day on which they were observed their location may have been different;
 - the effect of very localized bathymetric changes (e.g. depressions) in trapping metaphyton was an important factor in where they were found;
 - the availability of other enriched sources of nutrients, such as the Upper Truckee River and stormwater outfalls made Asian clam excretion just one potential source of nutrient supply.
6. The stable isotope measurements were only partially concluded due to Covid-19 restrictions on lab operations at UC Davis. However, the results to date suggest that the data may be of limited use.
7. Specific measurements and sites were used during this study, allowing us to build up a picture of metaphyton and Asian clams at those sites. The sites were chosen as they were areas where metaphyton and Asian clams had been observed in the past or where metaphyton and Asian clams had not been observed (our control sites). The sites had the following characteristics:

- At Lakeside there were large numbers of live clams and a large (approx. 75m X 200m) patch of metaphyton present. The presence of high levels of $\text{NH}_4\text{-N}$ in pore water concentrations inside and outside of the metaphyton patch and also high numbers of clams inside and outside the patch suggests a possible linkage between the clams and $\text{NH}_4\text{-N}$ concentrations. An experiment done during the study showed the clams to excrete $\text{NH}_4\text{-N}$ and SRP. Currents may naturally deposit the shells in this area which is a transition area from shallow to a slightly deeper shelf area offshore. It is possible the metaphyton similarly tends to accumulate or stay in place in this depression area. A combination of nutrient inputs from clams, topography, current effects as well as physical roughness provided by shells along the bottom (which may provide sites for algae to attach to), may contribute to the development of the metaphyton patch at Lakeside.

- At Regan Beach there were very few live clams and shells in the nearshore. There were relatively large patches of metaphyton near the shore, a large amount of aquatic vegetation, much of it with algae and metaphyton filamentous green algae, as well as thick growth of attached periphyton *Cladophora* along the boulder breakwater lining the park. The productive aquatic plant and algae growth at Regan Beach may be due to nutrient inputs associated with surface runoff from the nearby Upper Truckee River, Trout Creek and urban drains, rather than nutrient inputs associated with Asian clams.

- At Skyland, both the helicopter and UAV images show isolated dark patches of metaphyton over the sandy bottom in water 6-7m deep (up to 3m X 5m) with a much more extensive area (approx. 350m long X 100m wide) of uniform algal coverage on at least one date. Smaller (several inches long) patches of algae or a thin coating of algae over the bottom were also observed by divers, the algae was also observed to drift. The number of live clams inside and outside patches was more variable and the association with presence of metaphyton patches was not consistent. There were slightly more live clams outside metaphyton patches than inside patches for samplings done in Sept. 2018 and 2019. One patch did have substantial numbers of live clams and shells associated with it. Sediment pore water levels of $\text{NH}_4\text{-N}$ were low to moderate (5-158 $\mu\text{g/l}$) and SRP slightly elevated (3-12 $\mu\text{g/l}$) above background lake levels. The nutrients produced by the clams and observations of algae associated with shell patches near the edge of the shelf, suggest there is potential for a linkage between the algae growth and presence of clams, either due to nutrient inputs or physical impacts of the shells or both. Currents can impact movement of algae along the shelf at this site.

- At Hidden Beach there were no Asian Clams or shells found. There was only a small amount of algae along the bottom which included detritus, cyanobacteria and some algae which appeared to be derived from the periphyton on nearby boulders. Asian Clams are not impacting this site.

8. Metaphyton types – Metaphyton was composed predominantly of filamentous green algae. The filaments of these algae are formed by long chains of cells. The filaments of one or more different types of algae can intertwine to form clouds or masses just above the bottom. The most predominant filamentous green algae genera observed were *Zygnema* and

Spirogyra. Other filamentous green types were also predominant in samples from specific sites. For example, *Mougeotia* was prevalent in algae from deeper sites at Round Hill Pines and Skyland. *Oedogonium* was prevalent in many samples from Regan nearshore.

The data also showed that a range of factors are responsible for the observed metaphyton distribution year-to-year. The fact that we do not know how the distribution changes limits our ability to evaluate the importance of the various sources and the potential for management actions to control them or to mitigate them. Clearly the local bathymetry in conjunction with lake level plays an important role in trapping metaphyton. Likewise, the lake currents play an important role in moving patches and in breaking apart patches. It is currently within our ability to actually model the movement and growth of metaphyton, and through that provide guidance on future actions. What is lacking, however, is the data on the location of the metaphyton. That critical piece of information is what a lake wide (regional) monitoring program will provide.

The monitoring of metaphyton using a UAV and helicopter in this trial project proved to be both efficient and effective in quantifying the distribution of metaphyton over large areas of Lake Tahoe's nearshore, particularly when it could be combined with ongoing TERC field operations. The UAV monitoring process developed by TERC, coupled with in-lake biomass sampling, would allow future metaphyton monitoring to assess the timing, distribution, and abundance of nearshore nuisance algae on both a seasonal and interannual basis, information critical to an agency response to public and stakeholder concerns.

We would recommend that consideration be given to establishing a limited metaphyton monitoring project. Ideally this could be combined with the existing periphyton monitoring program, as significant economies could be realized.

We proposed that UAV flights be conducted on four occasions during favorable weather. These will be in July, August and September to capture peak metaphyton abundance and one flight during winter (February) to establish a baseline minimum.

The proposed sites are Hidden Beach (a control site, where no metaphyton has been observed to date), Sand Harbor, Skyland, and Lakeside. Skyland and Lakeside are areas with seasonally abundant metaphyton accumulation, near popular recreation beaches, where Asian clam populations are thriving. Sand Harbor represents a recreationally important area where Asian clam has recently become established but metaphyton has yet to reach nuisance levels. There is the possibility that in the near future Asian clam may contribute to a proliferation of metaphyton at Sand Harbor. As Sand Harbor is an extremely valuable public recreation site, we believe early monitoring is justified. UAV monitoring of Sand Harbor will provide management agencies annual information regarding any changes in the aesthetic value of the area in the presence, or absence, of continued Asian clam treatment and add further evidence of the linkage between Asian clams and localized metaphyton blooms.

All metaphyton monitoring sites will be ground sampled on the same day aerial surveys are conducted. Using SCUBA, divers will collect triplicate biomass samples for later analysis in the laboratory (wet weight and ash free dry weight (AFDW)). These collections will enable site wide determination of biomass accumulation (on the order of km²) adjacent to popular recreation resources.

Biomass sampling will be done based on experience of the researchers with typical distribution of filamentous algae metaphyton at the sites. Areas with representative levels of metaphyton will be selected for measurement. Patches with 100% cover with metaphyton will be sampled from a known area using the bucket/ pump method described in this document. If the distribution of biomass is very heterogeneous (for instance large patches visible from the air with other areas of thin growth also visible from the air), samples of biomass representative of the different zones of algae will be collected for biomass measurement. Samples will be returned to the lab, dried to damp consistency and a wet weight determined. A portion of this sample will be split off, weighed in a pre-tared, precombusted tin, dried overnight, then weighed again for determination of Ash Free Dry Weight (as described in this report). If chlorophyll *a* is to be analyzed, a sample will also be split off, weighed and frozen for later analysis.

Helicopter surveys are proposed to be taken twice each year in April (peak periphyton) and in August (peak metaphyton). While these surveys do not yet have the quantitative resolution of the UAV surveys, they have the ability to image the entire nearshore of the lake in only one hour. They have proven to be very effective in identifying areas of “concern”, where suddenly changed conditions can be identified and noted for follow up investigation. Photographic images will be collected on the flights to provide a record of conditions observed and archived.

The proposed work also leverages ongoing basin investments. The Nearshore network data will be used to complement the findings, especially if the breakdown products from metaphyton turn out to be significant influencers of CDOM fluorescence. Similarly, planned 3-D lake modeling will be extremely useful in accounting for the distribution of metaphyton.

Proposed Schedule and Budget

The schedule below is for a two-year metaphyton monitoring program for the four sites recommended above. This presumes a July 1 start date.

		Jul	Aug	Sep	Oct	Nov	Dec	Jan	Feb	Mar	Apr	May	Jun	Jul	Aug	Sep	Oct	Nov	Dec	Jan	Feb	Mar	Apr	May	Jun
Task 1	Metaphyton Field and Lab																								
Task 2	UAV data acqu. and image analysis																								
Task 3	Helicopter all-lake																								
Task 4	Reporting																								

The budget to support the monitoring described above for the **full two year period** is \$74,100 in direct costs (approximately \$37,000 per year). Note that indirect costs would need to be applied,

which vary depending on the source of the funding or the limitations imposed by the funding agency.

VII. References

- Forrest, A.L., Wittmann, M.E., Schmidt, V., Raineault, N.A., Hamilton, A., Pike, W., Schladow, S.G., Reuter, J.E., Laval, B.E. and A.C. Trembanis. 2012. Quantitative assessment of invasive species in lacustrine environments through benthic imagery analysis. *Limnology and Oceanography: Methods* 10: 65-74.
- Forrest, A. L., Andradóttir, H. Ó., Mathis, T. J., Wittmann, M. E., Reuter, J. E., & Schladow, S. G. 2017. Passive transport of a benthic bivalve (*Corbicula fluminea*) in large lakes: implications for deepwater establishment of invasive species. *Hydrobiologia*, 797(1), 82-102.
- Heyvaert, A.C., Reuter, J.E., Chandra, S., Susfalk, R.B., Schladow, S.G., Hackley, S.H. 2013. Lake Tahoe Nearshore Evaluation and Monitoring Framework. Final Report prepared for the USDA Forest Service Pacific Southwest Research Station. 410 pp.
- Hackley, S.H., Allen, B.C., Hunter, D.A. and J.E. Reuter. 2013. Lake Tahoe Water Quality Investigations, algal bioassay, phytoplankton, atmospheric nutrient deposition, periphyton. Final report: July 1, 2010 – June 30, 2013. Prepared for State Water Resources Control Board, Lahontan Regional Water Quality Control Board. Tahoe Environmental Research Center, University of California, Davis. 106p.
- Hackley, S.H., Watanabe, S., Senft, K.J., Hymanson, Z., Schladow, S.G. and J.E. Reuter. 2016. Evaluation of trends in nearshore attached algae: 2015 TRPA threshold evaluation report. Final report submitted to Tahoe Regional Planning Agency, March 9, 2016. 113 pp.
- Hackley, S.H., Senft, K., Allen, B., Rettig, R. and G. Schladow. 2018. Pilot study: monitoring summer metaphyton growth along the south and southeast shore of Lake Tahoe. Final report submitted to the Nevada Division of State Lands, by the UC Davis Tahoe Environmental Research Center. March 1, 2018. 101 pp.
- Lauritzen, D.D. and S.C. Mozley, 1989. Nutrient excretion by the Asiatic clam *Corbicula fluminea*. *Journ. North American Benthological Soc.*, 8(2): pp. 134-139.
- Loeb, S.L. 1987. Groundwater quality within the Tahoe Basin. Report prepared for California State Water Resources Control Board. Institute of Ecology, Division of Environmental Studies, U.C. Davis. 265pp
- McNair, H. 2010. Asian clams *Corbicula fluminea* contribution to algal growth in Lake Tahoe. pdfs.semanticscholar.org/2eea/677c7f2be72e61b77dab6b06ca5f9e69f292.pdf Online report
- Peterson, B.J. and B. Fry. 1987. Stable isotopes in ecosystem studies. *Ann. Rev. Ecol. Syst.* 18:293-320.

- Schladow, S.G. 2010. Final report for Lake Tahoe Asian clam survey project. Prepared for Lahontan Regional Water Quality Control Board.
- Schladow, S.G., Hoyer, A., Rueda, F. and Anderson, M. 2014. Lake Tahoe Flow Modeling, Potential Pathogen Transport and Risk Modeling. Final Report to Nevada Division of Environmental Protection.
- Turek, K.A. and T.J. Hoellein. 2015. The invasive Asian clam (*Corbicula fluminea*) increases sediment denitrification and ammonium flux in 2 streams in the midwestern USA. *Freshwater Science* 34(2): pp 472-484.
- Wehr, J.D., Sheath, R.G. and J.P. Kociolek. 2015. *Freshwater Algae of North America Ecology and Classification*. Academic Press, Elsevier Inc., USA. 1150 pp.
- Williams, C.J and McMahon, R.F. 1989. Annual variation of tissue biomass and carbon and nitrogen content in the freshwater bivalve, *Corbicula fluminea*, relative to downstream dispersal. *Canadian Journal of Zoology*, 67: 82-90.
- Wittmann, M., Reuter, J., Schladow, G., Hackley, S., Allen, B., Chandra, S. and A. Caires. 2008. Asian clam of Lake Tahoe: preliminary scientific findings in support of a management plan. University of California at Davis, Tahoe Environmental Research Center and University of Nevada – Reno, Department of Natural Resources. 46p.
- Wittmann, M.E., Allen, B., Chandra, S., Reuter, J.E., Schladow, S.G. and K. Webb. 2011. Final report for the Lake Tahoe Asian clam Pilot Project. Report prepared for the Tahoe Resource Conservation District. 89pp.
- Zohary, T., Alster, A., Hadas, O. and U. Obertegger. 2019. There to stay: invasive filamentous green alga *Mougeotia* in Lake Kinneret, Israel. *Hydrobiologia*, 831: 87-100.

Appendix 1. Summary of follow-up observations or ground-truthing of areas with possible metaphyton or other substrate of interest identified in aerial photos.

Site	Flight/ Imaging Date	Ground- truthing Date	Meta- phyton Present	Aquatic Plants Present	Aquatic Plants w/ Associated Algae	Location	Description from Helicopter Image	Results (Detailed)
1	8/1/18	8/14/18	YES	YES	YES	Tahoe Keys nearshore east of pier	Large dark patches	Mix of aquatic plants with associated green filamentous algae (much <i>Bulbochaete</i>) small amount metaphyton near base of wall.
2	8/1/18	8/14/18	YES	YES	YES ¹³	Tahoe Keys nearshore west of pier	Tan shading just offshore	Metaphyton in sand riffles nearshore (green filamentous algae including much <i>Bulbochaete</i>)
3	8/1/18	8/14/18	NO	NO	NO	Camp Richardson	Black patch west of pier between boat slips	Small fragments of black woody debris
4	8/1/18	8/14/18	NO	NO	NO	Camp Richardson	Tan patch west of pier nearshore	Cobble over sand
5	9/4/19	9/11/19	NO	YES	YES	Tallac Point	Green patches on point	Low growing aquatic plants and associated green filamentous algae (<i>Zygnema</i> and some <i>Mougeotia</i>)
6	8/1/18	8/14/18	NO	NO	NO	Baldwin Beach	Black patch west of pier, west end of beach	Woody debris, pine needles, pine cones
7	8/1/18	8/14/18	NO	NO	NO	Baldwin Beach	Green patch northwest of beach	Low-growing aquatic plants or aquatic moss
8	8/1/18	8/24/18	YES Small amt.	NO	NO	Lester Beach, D.L. Bliss St. Park nearshore	Black patches just offshore of beach	Mostly woody debris, trash, small clumps metaphyton
9	8/1/18	8/24/18	YES Small amt.	NO	NO	North of Rubicon Beach	Black patches	Woody debris, some clumps metaphyton
10	8/1/18	8/24/18	YES Small amt.	NO	NO	North of Rubicon Beach	Black patches	Woody debris, thin band algae along nearshore edge of debris

¹³ Metaphyton may have been associated with aquatic plants and broken free.

Site	Flight/ Imaging Date	Ground- truthing Date	Meta- phyton Present	Aquatic Plants Present	Aquatic Plants w/ Associated Algae	Location	Description from Helicopter Image	Results (Detailed)
11	8/1/19	7/22/19	NO	NO	NO	Sugar Pine Pt.	Dark lines nearshore	Dark patches woody debris
11	9/4/19	9/5/19	NO	NO	NO	Sugar Pine Pt.	Some dark patches	Dark patches woody debris
12	9/4/19	9/6/19	YES	YES	YES	Near Truckee River Outlet, Tahoe City	Large bright green patches	Low growing aquatic grasses and associated green filamentous algae (<i>Zygnema</i>) metaphyton patches (<i>Zygnema</i>) in depressions
12	None	10/11/19	NO	YES	NO	Near Truckee River Outlet, Tahoe City	No Aerial Image	Aquatic grasses reduced in height and had no algae associated with them.
13	9/4/19	9/6/19	NO	YES	NO	Lake Forest, Tahoe City	Green patches near island	Low growing aquatic grasses creating underwater turf
14	8/1/19	7/25/19	NO	NO	NO	Near Incline Cr. mouth	Black patches	Woody debris, pine needles
15	8/1/18	8/2/18	NO	NO	NO	Hidden Beach	Dark rust color on bottom sands	Rust coloration on sand but not metaphyton.
15	9/6/18	9/4/18	NO	NO	NO	Hidden Beach	None visible in image	No Metaphyton
15	8/1/19	7/22/19	YES Small amt.	NO	NO	Hidden Beach	None visible in image	2% cover with algae and detritus offshore, some algae in depressions inshore
15	9/4/19	9/3/19	YES Small amt.	NO	NO	Hidden Beach	None visible in image	Small amount of algae and detritus
16	8/1/18	8/24/18	NO	NO	NO	Glenbrook Bay	Dark underwater objects	Old pier pilings and cribbing rocks
17	8/1/18	8/24/18	YES	NO	NO	Glenbrook Bay	Southeast bay dark material near shore	Woody debris, 20mx20m patch of metaphyton on shoreward side (Cyano- bacteria on detritus)
18	9/6/18	9/20/18	YES ¹⁴	NO	NO	North of Cave Rock	Green patches nearshore among buoys and boats	Algae gone when ground-truthed after strong winds (patches drifted or dispersed)

¹⁴ No algae present when ground-truthed 9/20/18, however there had been strong winds between time aerial imaging on 9/6/18 and ground-truthing on 9/20/18, suspect metaphyton patches drifted or dispersed.

Site	Flight/ Imaging Date	Ground- truthing Date	Meta- phyton Present	Aquatic Plants Present	Aquatic Plants w/ Associated Algae	Location	Description from Helicopter Image	Results (Detailed)
19	8/1/18	8/24/18	YES	NO	NO	Skyland	Green patches along bottom and among boulders; white patches	Green patches up to 2x2 m, 3-7 m deep (metaphyton was filamentous algae <i>Mougeotia</i> -g.; <i>Zygnema</i> , <i>Spirogyra</i>); white patches were Asian clam shells
19	9/6/18	9/6/18	YES	NO	NO	Skyland	Large green patches; large black patches	Large green patches of metaphyton and large black patches that appear to be dead algae. Unable to sample.
19	9/6/18	9/17	NO ¹⁵	NO	NO	Skyland		Returned to site, metaphyton gone likely as a result of strong winds and currents since visit 9/6/18
19	8/1/19	7/31/19	YES	NO	NO	Skyland	Green patches	Thin layer of algae coating bottom much of area, with clumps which may have pulled free; patches drifting; clam siphons protruding from sand surface
19	8/1/19	8/16/19	NA	NO	NO	Skyland	Dark and white patches offshore	~75-100 yds offshore large shoals of irregular patches of shells with irregular tan bottom, difficult to tell if metaphyton present
19	9/4/19	9/3/19	YES	NO	NO	Skyland	Many small dark patches	Green metaphyton filamentous algae (primarily <i>Mougeotia</i> -g, also some <i>Zygnema</i> , <i>Oedogonium</i>)
20	9/6/18	9/20/18	NO	NO	NO	Zephyr Cove near beach	Black patches nearshore	Woody debris, detritus, pine cones
20	9/6/18	9/20/18	YES	NO	NO	Zephyr Cove near beach	Tan patches nearshore	Lines of metaphyton between sand riffles (<i>Zygnema</i> , <i>Spirogyra</i> , <i>Mougeotia</i> . Cyanobacteria)
21	8/1/18	7/27/18	NO	NO	NO	Round Hill Pines, Marla Bay	Black patch south of pier	Woody debris, woody roots

¹⁵ No algae present when ground-truthed 9/17/18, however there had been strong winds between time of aerial imaging on 9/6/18 and ground-truthing date, suspect metaphyton patches drifted or dispersed.

Site	Flight/ Imaging Date	Ground- truthing Date	Meta- phyton Present	Aquatic Plants Present	Aquatic Plants w/ Associated Algae	Location	Description from Helicopter Image	Results (Detailed)
22	9/4/19	9/11/19	YES	NO	NO	Round Hill Pines, Marla Bay	Bright green patches in buoy field and near pier	Bright green metaphyton (primarily <i>Mougeotia</i> -g; some <i>Zygnema</i> , <i>Spirogyra</i>)
22		9/17/19	NO	NO	NO	Round Hill Pines, Marla Bay		Returned after strong S-SW winds on 9/15-9/16. No metaphyton along pier or along pipe visible from pier. No algae on beach. Algae may have been moved along bottom by currents and may have broken up or dispersed.
23	8/1/19	7/23/19	YES	NO	NO	Elk Pt.	No metaphyton visible, clamshells visible offshore	Some metaphyton present (filamentous greens: primarily <i>Spirogyra</i> ; some <i>Zygnema</i> and <i>Mougeotia</i>)
24	8/1/19	8/13/19	YES	NO	NO	Nevada Beach	Dark shaded areas	Possibly darker sediments between patches of shells, appears to be some green metaphyton over clam shells
25	8/1/19	8/13/19	YES	NO	NO	Pipe near Kahle Dr.	Dark shaded area along pipe	Metaphyton olive green on south side pipe; accumulation of shells too
26	8/1/18	8/1/18	YES	YES	?	Lakeside Beach and Marina, offshore	Large dark patch	Metaphyton (filamentous greens: Primarily <i>Zygnema</i> , also some <i>Spirogyra</i> , <i>Mougeotia</i> and others)
26	9/4/18	9/4/18	YES	YES	?	Lakeside Beach and Marina, offshore	Large dark patch	Metaphyton (mixed green filamentous (<i>Zygnema</i> , <i>Oedogonium</i> , <i>Spirogyra</i> , others))
26		7/24/19	YES	YES	?	Lakeside Beach and Marina, offshore	Large dark green patches	Metaphyton (mixed green filamentous: <i>Spirogyra</i> , <i>Zygnema</i> , <i>Mougeotia</i> , <i>Oedogonium</i> , others)
26	8/1/19	8/1/19	YES	YES	?	Lakeside Beach and Marina, offshore	Large dark green patches	Metaphyton (mixed green filamentous: <i>Zygnema</i> , <i>Spirogyra</i> , <i>Mougeotia</i> , others)
26	9/4/19	9/4/19	YES	YES	?	Lakeside Beach and Marina, offshore	Large dark patch	Metaphyton (mixed green filamentous: <i>Zygnema</i> , <i>Oedogonium</i> , <i>Spirogyra</i> , others)
27	8/1/19	8/16/19	YES	YES	YES	Lakeside Beach swim area inside of protective barrier	Large dark green patches	Metaphyton old and new and aquatic plants and plants with associated filamentous algae

Site	Flight/ Imaging Date	Ground- truthing Date	Meta- phyton Present	Aquatic Plants Present	Aquatic Plants w/ Associated Algae	Location	Description from Helicopter Image	Results (Detailed)
28	8/1/19	8/16/19	YES	YES	YES	Nearshore east of Ski Run Marina	Small dark green patches nearshore	Metaphyton, low-growing aquatic plants, some with associated filamentous algae;
29	6/25/17 ¹⁶	6/30/17	YES	YES		Ski Run Marina	Large Dark Patch in channel	Aquatic plants with some metaphyton.(green filamentous algae)
30		7/25/19	YES	?	?	Timber Cove Offshore of end of pier		Moderate patchy green metaphyton
31	8/1/19	8/20/19	YES			Timber Cove near pier	Dark patches nearshore both sides of pier	Metaphyton patches; no algae onshore.
31	9/4/19	9/17/19	YES			Timber Cove near pier		Checked after strong S-SW winds on 9/15-9/16, still some metaphyton near shore; no algae on beach, however were plant pcs. onshore.
32	8/1/18	7/27/18	YES			El Dorado Beach	Dark patch offshore	Line of metaphyton offshore, appears old, olive green
32	9/6/18	9/20/18	YES	YES	YES	El Dorado Beach	Dark line offshore of beach	Thick metaphyton patch offshore (filamentous greens: <i>Bulbochaete</i> , <i>Zygnema</i> , <i>Spirogyra</i> , <i>Oedogonium</i>). Aquatic plants with assoc. green filamentous algae.
33	8/1/19	8/7/19	YES	YES	?	El Dorado Beach	Lighter-colored blotches in swim area	Metaphyton patches of dark and bright green filamentous algae
33		9/17/19	YES	YES	?	El Dorado Beach		Checked after strong S-SW winds 9/15-9/16. Fragments of plants with some algae (<i>Cladophora</i>) washed up on cobble along shore. Line of metaphyton, plants present offshore.
34	8/1/19	8/7/19	YES	YES	YES	El Dorado Beach East, Offshore	Dark green patches offshore east of El Dorado	Aquatic plants, many with associated bright green filamentous algae; also some metaphyton patches including adjacent to pipe near Rufus Allen Dr.

¹⁶ Reconnaissance flight and ground check year prior to study

Site	Flight/ Imaging Date	Ground- truthing Date	Meta- phyton Present	Aquatic Plants Present	Aquatic Plants w/ Associated Algae	Location	Description from Helicopter Image	Results (Detailed)
35	8/1/19	8/7/19	YES	YES	YES	El Dorado Beach East nearshore	Dark line in nearshore	Mix of aquatic plants, associated filamentous algae and metaphyton.
36	8/1/18	7/27/18	NA			Regan Beach	Dark green on jetty boulders	Water too turbid for observing metaphyton; thick <i>Cladophora</i> on jetty rocks 6 inch strands.
36	8/1/19	7/26/19	NA			Regan Beach		Water turbid; thick <i>Cladophora</i> on jetty boulders
37	8/1/18	8/1/18	YES	YES	YES	Regan Beach	Dark Patches	Metaphyton Patches, Aquatic vegetation; Aquatic vegetation with algae.
37	9/6/18	9/6/18	YES	YES	YES	Regan Beach	Dark Patches	Metaphyton patches, aquatic vegetation; aquatic vegetation with algae.
37		9/20/18	YES	NA	NA	Regan Beach		Suspended metaphyton washing up on boulders along shore, smelly; <i>Cladophora</i> being exposed on boulders adjacent to east parking; suspended algae and plant fragments washing onshore on small beach west side park.
37	8/1/19	8/1/19	YES	YES	YES	Regan Beach inshore and offshore	Dark patches	Metaphyton (detritus, green filamentous algae <i>Spirogyra</i> , <i>Zygnema</i> , <i>Oedogonium</i>), aquatic plants with algae; metaphyton rolls 200 yds offshore (<i>Zygnema</i> , some <i>Spirogyra</i>)
37		8/13/19	YES	YES	YES	Regan Beach		Metaphyton Patches, Aquatic vegetation; Aquatic vegetation with algae.
37	9/4/19	9/4/19	YES	YES	YES	Regan Beach	Dark Patches	Metaphyton patches (heterogeneous mix of green filamentous:old <i>Cladophora</i> with epiphytic diatoms, <i>Spirogyra</i> , <i>Zygnema</i> , <i>Oedogonium</i> , others, also Cyanobacteria), aquatic vegetation; aquatic vegetation with algae.
38	8/1/19	8/20/19	Suspected (poor clarity)	YES	YES	Upper Truckee River Mouth	Areas of bright green at surface, tan or orange color in water	Mix of emergent aquatic plants, associated filamentous algae, and very heavy filamentous algae growth <i>Tribonema</i>

Appendix 2. Additional Aerial and ground-truthing images



Figure A2-1. Woody debris (black patches indicated with arrows) D.L. Bliss State Park, 9/4/19.



Figure A2-2. Tahoe City near Truckee River outlet 9/4/19, (zoom-in) section of image taken from helicopter, showing aquatic plants, associated green filamentous algae (*Zygnema*) and metaphyton (*Zygnema*).



Figure A2-3. Aquatic plants and associated filamentous algae at mouth of Upper Truckee River, 9/4/19, (zoom-in) section of image taken from helicopter.



Figure A2-4. Filamentous Xanthophyte algae (*Tribonema*), on surface, observed at mouth of Upper Truckee River observed in follow-up ground-truthing 8/20/19.



Figure A2-5. Regan 8/1/19 from helicopter DJI camera image, (zoom in view) area of heavy periphyton (*Cladophora*) (red arrow) growth on boulders all along wall bordering park

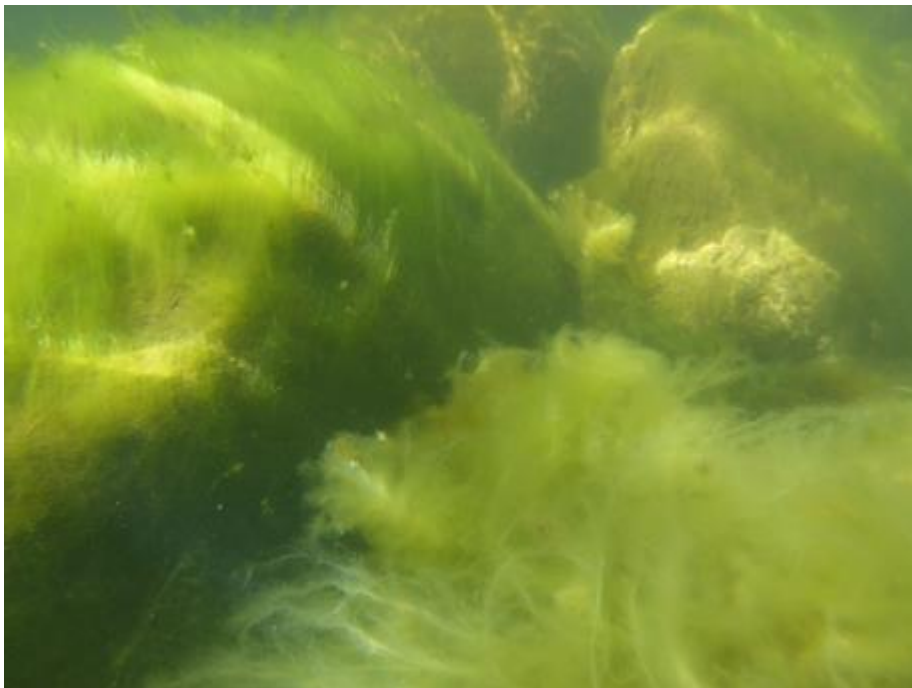


Figure A2-6. Heavy summer growth of periphyton, composed of attached green filamentous algae (*Cladophora*) on boulders along wall bordering park at Regan Beach 8/13/19.

Appendix 3 – UAV Flight Parameters

Table A3-1. Lakeside UAV Flight Parameters

Metaphyton - UAV Flight Data				
UAV	Phantom 4 Pro			
Site	Lakeside Marina			
Location	38.960910, -119.952162			
Flight Grid				
Type	Polygon			
Dimensions	Feet		Meters	
	1299	1338	395.9	407.8
Area	1738062 ft ²		161471.2 m ²	
Flight Path				
Speed*	mph		m/s	
	28		12.5	
Altitude	Feet		Meters	
	350		106.7	
Path	8613		2625.2	
Time	7 min : 18 s			
Images	120			
Overlap	Front		Side	
	80%		70%	
Camera Specs				
Sensor	1" CMOS			
Megapixels	20			
Angle of camera	90°			
Trigger mode	Fast			
Reference markers deployed:	Yes			
Processing				
Image Produced	Orthomosaic			
Format	GeoTiff			
GSD	3 in/px			
Bands	Red, Green, Blue, Alpha			

*UAV speed calculated based off 90% of maximum flight speed (31 mph). Speed may vary during flight path.

Table A3-2. Regan Beach UAV Flight Parameters

Metaphyton - UAV Flight Data			
UAV	Phantom 4 Pro		
Site	Regan Beach		
Location	38.944789, -119.983584		
Flight Grid			
Type	Polygon		
Dimensions	Feet		Meters
	889	332	271.0 101.2
Area	295148 ft ²		27420.1 m ²
Flight Path			
Speed*	mph		m/s
	28		12.5
Altitude	Feet		Meters
	100		30.5
Path	5138		1566.1
Time	10 min : 51 s		
Images	256		
Overlap	Front	Side	
	80%	70%	
Camera Specs			
Sensor	1" CMOS		
Megapixels	20		
Angle of camera	90°		
Trigger mode	Fast		
Reference markers deployed:	Yes		
Processing			
Image Produced	Orthomosaic		
Format	GeoTiff		
GSD	1 in/px		
Bands	Red, Green, Blue, Alpha		

*UAV speed calculated based off 90% of maximum flight speed (31 mph). Speed may vary during flight path.

Table A3-3. Skyland UAV Flight Parameters

Metaphyton - UAV Flight Data				
UAV	Phantom 4 Pro			
Site	Skyland			
Location	39.015926, -119.953363			
Flight Grid				
Type	Polygon			
Dimensions	Feet		Meters	
	1525	2094	464.8	638.3
Area	3193350 ft ²		296671.9 m ²	
Flight Path				
Speed*	mph		m/s	
	28		12.5	
Altitude	Feet		Meters	
	350		106.7	
Path	13457		4101.7	
Time	10 min : 3 s			
Images	184			
Overlap	Front		Side	
	80%		70%	
Camera Specs				
Sensor	1" CMOS			
Megapixels	20			
Angle of camera	90°			
Trigger mode	Fast			
Reference markers deployed:	Yes			
Processing				
Image Produced	Orthomosaic			
Format	GeoTiff			
GSD	4 in/px			
Bands	Red, Green, Blue, Alpha			

*UAV speed calculated based off 90% of maximum flight speed (31 mph). Speed may vary during flight path.

Table A3-4. Hidden Beach UAV Flight Parameters

Metaphyton - UAV Flight Data			
UAV	Phantom 4 Pro		
Site	Hidden Beach		
Location	39.220931, -119.929345		
Flight Grid			
Type	Polygon		
Dimensions	Feet		Meters
	952	901	290.2 274.6
Area	857752 ft ²		79687.8 m ²
Flight Path			
Speed*	mph		m/s
	28		12.5
Altitude	Feet		Meters
	350		106.7
Path	3971		1210.4
Time	4 min : 13 s		
Images	59		
Overlap	Front	Side	
	80%	70%	
Camera Specs			
Sensor	1" CMOS		
Megapixels	20		
Angle of camera	90°		
Trigger mode	Fast		
Reference markers deployed:	No		
Processing			
Image Produced	Orthomosaic		
Format	GeoTiff		
GSD	2 in/px		
Bands	Red, Green, Blue, Alpha		

*UAV speed calculated based off 90% of maximum flight speed (31 mph). Speed may vary during flight path.

Table A3-5. Sugar Pine Pt. UAV Flight Parameters

Metaphyton - UAV Flight Data			
UAV	Phantom 4 Pro		
Site	Sugar Pine		
Location	39.056360, -120.113329		
Flight Grid			
Type	Polygon		
Dimensions	Feet		Meters
	664	1190	202.4 362.7
Area	790160 ft ²		73408.3 m ²
Flight Path			
Speed*	mph		m/s
	28		12.5
Altitude	Feet		Meters
	350		106.7
Path	4767		1453.0
Time	4 min : 39 s		
Images	68		
Overlap	Front	Side	
	80%	70%	
Camera Specs			
Sensor	1" CMOS		
Megapixels	20		
Angle of camera	90°		
Trigger mode	Fast		
Reference markers deployed:	No		
Processing			
Image Produced	Orthomosaic		
Format	GeoTiff		
GSD	2 in/px		
Bands	Red, Green, Blue, Alpha		

*UAV speed calculated based off 90% of maximum flight speed (31 mph). Speed may vary during flight path.

Appendix 4. Accuracy tables, original UAV images and images after classification of pixels.

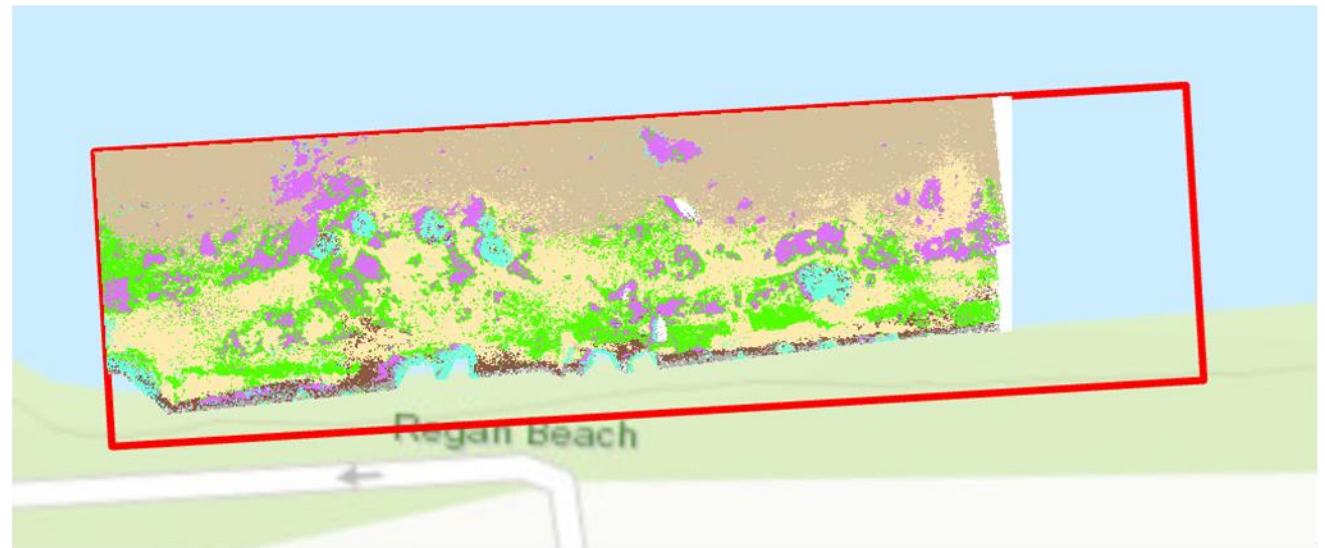
A4-1. Regan Beach – August 1, 2018 accuracy table, original UAV images and images after classification of pixels.

ClassValue	Sand - Shallow	Sand - Deep	Rock – Above Water	Rock - Shallow	Grid	Metaphyton	Vegetation - Above	Vegetation - Submerged	Total	U_Accuracy	Kappa
Sand - Shallow	26	0	0	1	0	0	1	0	28	92.9%	0
Sand - Deep	0	33	0	0	0	0	0	1	34	97.1%	0
Rock – Above Water	0	0	9	0	0	0	0	0	9	100.0%	0
Rock - Shallow	1	0	0	7	0	1	1	0	10	70.0%	0
Grid	0	0	0	0	10	0	0	0	10	100.0%	0
Metaphyton	0	2	0	0	0	6	0	9	17	35.3%	0
Vegetation - Above	0	1	0	0	0	0	8	1	10	80.0%	0
Vegetation - Submerged	0	0	0	0	0	0	0	10	10	100.0%	0
Total	27	36	9	8	10	7	10	21	128	0.0%	0
P_Accuracy	96.3%	91.7%	100.0%	87.5%	100.0%	85.7%	80.0%	47.6%	0.0%	85.2%	0
Kappa	0	0	0	0	0	0	0	0	0	0	82.3%

Regan Beach – August 1, 2018

Key for classified images at Reagan Beach

Class_name	Class_name
 Sand_Shallow	 Grid
 Sand_Deep	 Metaphyton_Shallow
 Rock_AboveWater	 Above vegetation
 Rock_Shallow	 Underwater vegetation



A4-2. Regan Beach – September 6, 2018 accuracy table, original UAV images and images after classification of pixels.

ClassValue	Sand - Shallow	Sand - Deep	Rock – Above Water	Rock - Shallow	Shadow	Grid	Metaphyton	Vegetation - Above	Vegetation-Submerged	Total	U_Accuracy	Kappa
Sand - Shallow	23	0	0	0	0	0	1	0	0	24	95.8%	0
Sand - Deep	0	40	0	0	0	0	0	0	0	40	100.0%	0
Rock - AboveWater	0	0	9	0	0	0	0	1	0	10	90.0%	0
Rock - Shallow	1	0	0	7	0	0	1	1	0	10	70.0%	0
Shadow	0	0	0	0	10	0	0	0	0	10	100.0%	0
Grid	1	0	0	0	0	7	0	2	0	10	70.0%	0
Metaphyton	0	1	0	0	0	0	6	0	5	12	50.0%	0
Vegetation - Above	2	1	0	0	0	0	3	3	1	10	30.0%	0
Vegetation - Submerged	0	0	0	0	0	0	0	0	12	12	100.0%	0
Total	27	42	9	7	10	7	11	7	18	138	0.0%	0
P_Accuracy	85.2%	95.2%	100.0%	100.0%	100.0%	100.0%	54.5%	42.9%	66.7%	0.0%	84.8%	0
Kappa	0	0	0	0	0	0	0	0	0	0	0	81.9%

Regan Beach – Sept 6, 2018



Key for classified images at Regan Beach

Class_name	Class_name
 Sand_Shallow	 Grid
 Sand_Deep	 Metaphyton_Shallow
 Rock_AboveWater	 Above vegetation
 Rock_Shallow	 Underwater vegetation



A4-3. Regan Beach – May 2, 2019 accuracy table, original UAV images and images after classification of pixels.

ClassValue	Sand - Shallow	Sand - Deep	Rock – Above Water	Rock - Shallow	Shadow	Grid	Metaphyton	Vegetation - Above	Vegetation-Submerged	Total	U_Accuracy	Kappa
Sand - Shallow	26	0	0	0	0	0	0	0	0	26	100.0%	0
Sand - Deep	0	40	0	0	0	0	0	0	0	40	100.0%	0
Rock – Above Water	0	0	10	0	0	0	0	0	0	10	100.0%	0
Rock - Shallow	0	0	0	8	0	0	0	2	0	10	80.0%	0
Shadow	0	0	0	0	9	0	0	0	0	9	100.0%	0
Grid	4	0	0	0	0	6	0	0	0	10	60.0%	0
Metaphyton	0	0	0	0	0	0	6	0	5	11	54.5%	0
Vegetation - Above	0	0	0	0	0	0	1	9	0	10	90.0%	0
Vegetation - Submerged	2	0	0	0	0	0	0	0	8	10	80.0%	0
Total	32	40	10	8	9	6	7	11	13	136	0.0%	0
P_Accuracy	81.3%	100.0%	100.0%	100.0%	100.0%	100.0%	85.7%	81.8%	61.5%	0.0%	89.7%	0
Kappa	0	0	0	0	0	0	0	0	0	0	0	87.7%

Regan Beach – May 2, 2019

Key for classified images at Reagan Beach

Class_name	Class_name
 Sand_Shallow	 Grid
 Sand_Deep	 Metaphyton_Shallow
 Rock_AboveWater	 Above vegetation
 Rock_Shallow	 Underwater vegetation



A4-4. Regan Beach – August 1, 2019 accuracy table, original UAV images and images after classification of pixels.

ClassValue	Sand - Shallow	Sand - Deep	Rock – Above Water	Rock - Shallow	Shadow	Grid	Metaphyton	Vegetation - Above	Vegetation-Submerged	Total	U_Accuracy	Kappa
Sand - Shallow	30	0	0	0	0	0	1	0	0	31	96.8%	0
Sand - Deep	0	26	0	0	0	0	0	0	0	26	100.0%	0
Rock – Above Water	0	0	10	0	0	0	0	0	0	10	100.0%	0
Rock - Shallow	0	0	0	8	1	0	0	0	1	10	80.0%	0
Shadow	0	0	0	0	10	0	0	0	0	10	100.0%	0
Grid	0	0	0	0	0	8	0	2	0	10	80.0%	0
Metaphyton	0	0	0	0	0	0	5	0	5	10	50.0%	0
Vegetation - Above	0	0	0	0	0	0	0	9	1	10	90.0%	0
Vegetation - Submerged	0	0	0	1	0	0	2	0	22	25	88.0%	0
Total	30	26	10	9	11	8	8	11	29	142	0.0%	0
P_Accuracy	100.0%	100.0%	100.0%	88.9%	90.9%	100.0%	62.5%	81.8%	75.9%	0.0%	90.1%	0
Kappa	0	0	0	0	0	0	0	0	0	0	0	88.5%

Regan Beach – August 1, 2019

Key for classified images at Reagan Beach

Class_name	Class_name
 Sand_Shallow	 Grid
 Sand_Deep	 Metaphyton_Shallow
 Rock_AboveWater	 Above vegetation
 Rock_Shallow	 Underwater vegetation



A4-5. Regan Beach – September 4, 2019 accuracy table, original UAV images and images after classification of pixels.

ClassValue	Sand - Shallow	Sand - Deep	Rock – Above Water	Rock - Shallow	Shadow	Grid	Metaphyton	Vegetation - Above	Vegetation-Submerged	Total	U_Accuracy	Kappa
Sand - Shallow	28	0	0	0	0	0	0	0	0	28	100.0%	0
Sand - Deep	0	36	0	0	0	0	0	0	0	36	100.0%	0
Rock – Above Water	0	0	9	0	0	0	0	0	0	9	100.0%	0
Rock - Shallow	0	2	0	8	0	0	0	0	0	10	80.0%	0
Shadow	0	0	0	0	10	0	0	0	0	10	100.0%	0
Grid	0	0	0	0	0	10	0	0	0	10	100.0%	0
Metaphyton	1	2	0	0	0	0	3	0	6	12	25.0%	0
Vegetation - Above	2	3	0	0	1	0	0	1	3	10	10.0%	0
Vegetation - Submerged	0	0	0	0	0	0	0	0	10	10	100.0%	0
Total	31	43	9	8	11	10	3	1	19	135	0.0%	0
P_Accuracy	90.3%	83.7%	100.0%	100.0%	90.9%	100.0%	100.0%	100.0%	52.6%	0.0%	85.2%	0
Kappa	0	0	0	0	0	0	0	0	0	0	0	82.2%

Regan Beach – Sept 4, 2019



Key for classified images at Regan Beach

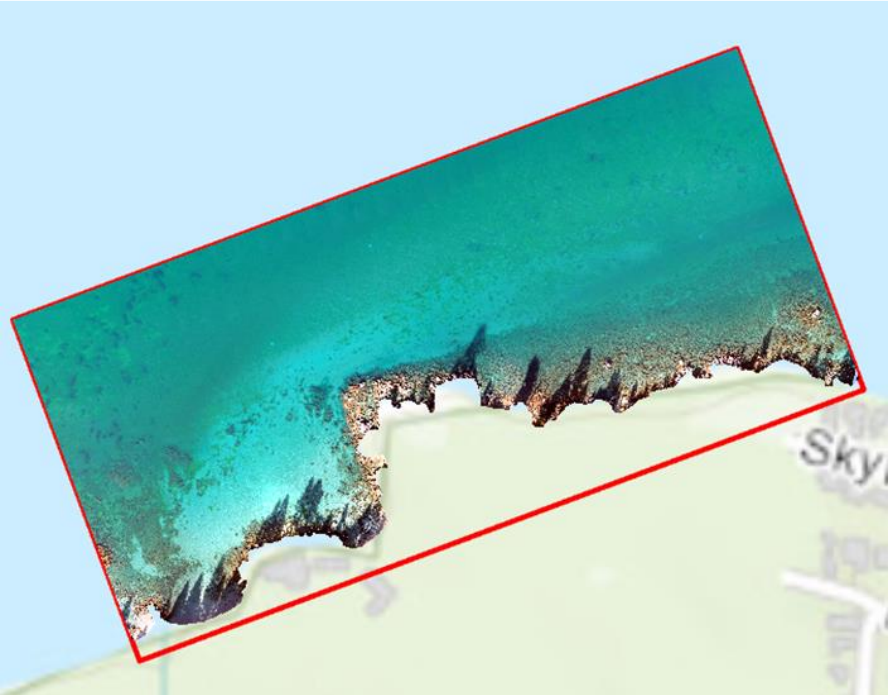
Class_name	Class_name
Sand_Shallow	Grid
Sand_Deep	Metaphyton_Shallow
Rock_AboveWater	Above vegetation
Rock_Shallow	Underwater vegetation



A4-6. Skyland – September 6, 2018 accuracy table, original UAV images and images after classification of pixels.

ClassValue	Sand - Above	Sand - Shallow	Sand - Deep	Rock – Above Water	Rock - Shallow	Rock - Mid Depth	Rock - Deep	Shadow	Grid	Meta - Shallow	Meta - Deep	Meta - Dead	Total	U_Acc	Kappa
Sand - Above	7	2	0	1	0	0	0	0	0	0	0	0	10	70.0%	0
Sand - Shallow	0	15	0	0	0	0	0	0	0	0	0	0	15	100.0%	0
Sand - Deep	0	0	10	0	0	0	0	0	0	1	2	0	13	76.9%	0
Rock – Above Water	1	1	0	7	1	0	0	0	0	0	0	0	10	70.0%	0
Rock - Shallow	0	0	0	0	10	0	0	0	0	0	0	0	10	100.0%	0
Rock - Mid Depth	0	0	0	0	0	8	0	2	0	0	0	0	10	80.0%	0
Rock - Deep	0	0	0	0	0	0	9	1	0	0	5	1	16	56.3%	0
Shadow	0	0	0	0	0	0	0	10	0	0	0	0	10	100.0%	0
Grid	0	0	0	0	0	0	0	0	10	0	0	0	10	100.0%	0
Metaphyton - Shallow	0	1	0	0	0	0	0	0	0	9	0	0	10	90.0%	0
Metaphyton - Deep	0	0	2	0	0	0	0	0	0	0	28	0	30	93.3%	0
Metaphyton - Dead	0	1	0	0	0	0	1	0	0	0	0	8	10	80.0%	0
Total	8	20	12	8	11	8	10	13	10	10	35	9	154	0.0%	0
P_Accuracy	87.5%	75.0%	83.3%	87.5%	90.9%	100.0%	90.0%	76.9%	100.0%	90.0%	80.0%	88.9%	0.0%	85.1%	0
Kappa	0	0	0	0	0	0	0	0	0	0	0	0	0	0	83.4%

Skyland – Sept 6, 2018



Key for classified images at Skyland

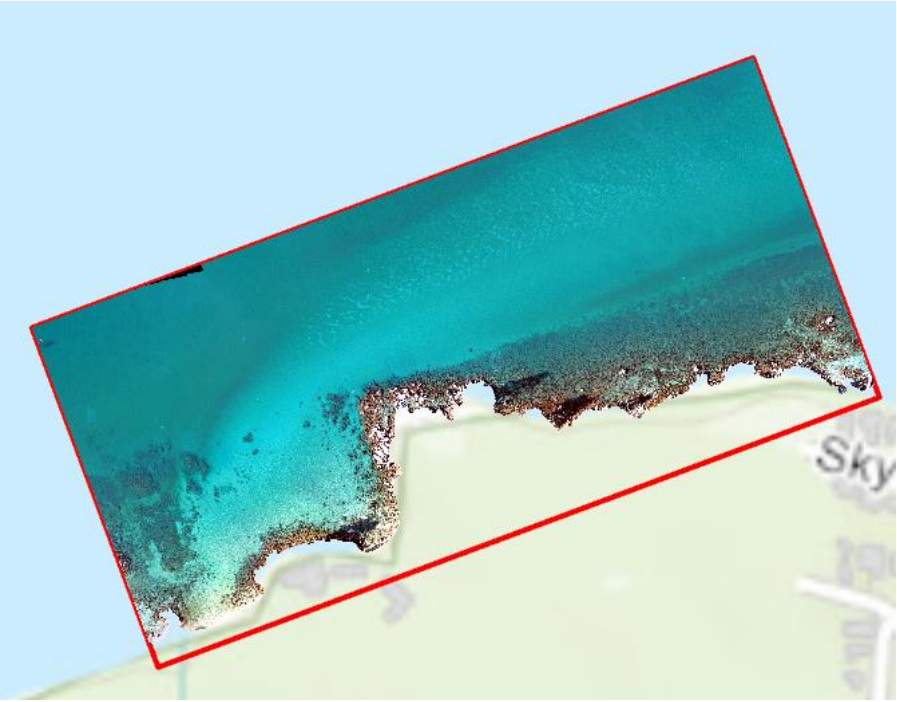
Class_name	Class_name
Grid	Rock_Mid
Metaphyton_Deep	Rock_Shallow
Metaphyton_Deep	Sand_Above
Metaphyton_Shallow	Sand_Deep
Rock_AboveWater	Sand_Shallow
Rock_Deep	Shadow



A4-7. Skyland – January 25, 2019 accuracy table, original UAV images and images after classification of pixels.

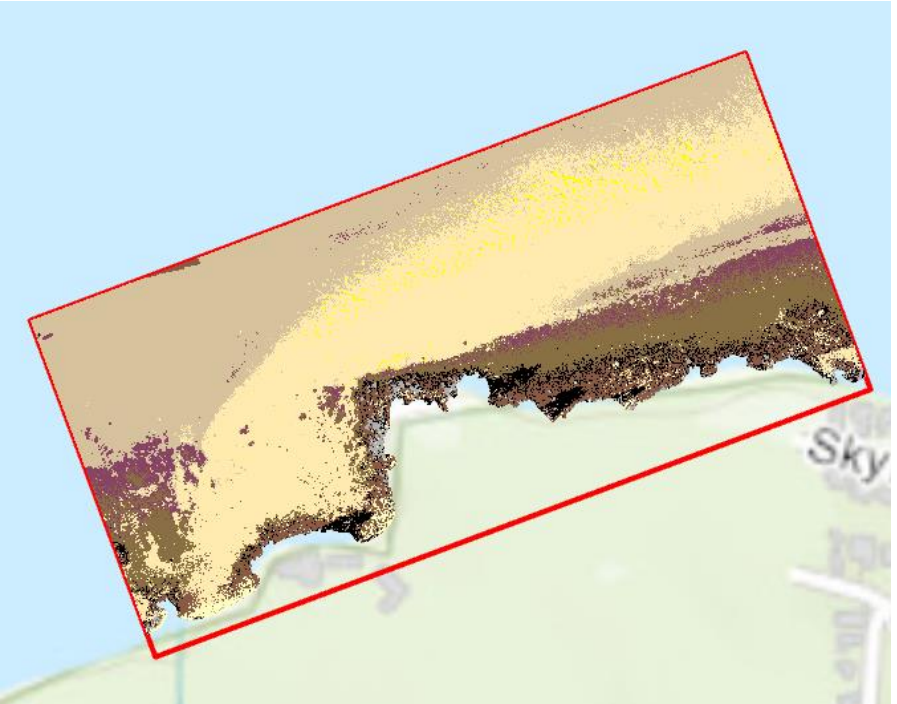
ClassValue	Sand - Above	Sand - Shallow	Sand - Deep	Rock - AboveWater	Rock - Shallow	Rock - Mid Depth	Rock - Deep	Shadow	Grid	Clams	Total	U_Accuracy	Kappa
Sand - Above	10	0	0	0	0	0	0	0	0	0	10	100.0%	0
Sand - Shallow	0	36	0	0	0	0	0	0	0	2	38	94.7%	0
Sand - Deep	0	0	32	0	0	0	0	0	0	0	32	100.0%	0
Rock - Above Water	0	0	0	10	0	0	0	0	0	0	10	100.0%	0
Rock - Shallow	0	0	0	0	10	0	0	0	0	0	10	100.0%	0
Rock - Mid Depth	0	0	1	0	0	11	0	0	0	0	12	91.7%	0
Rock - Deep	0	0	2	0	0	0	8	0	0	0	10	80.0%	0
Shadow	0	0	0	0	0	0	0	10	0	0	10	100.0%	0
Grid	0	0	0	0	0	0	0	0	10	0	10	100.0%	0
Clams	0	1	0	0	0	0	0	0	0	9	10	90.0%	0
Total	10	37	35	10	10	11	8	10	10	11	152	0.0%	0
P_Accuracy	100.0%	97.3%	91.4%	100.0%	100.0%	100.0%	100.0%	100.0%	100.0%	81.8%	0.0%	96.1%	0
Kappa	0	0	0	0	0	0	0	0	0	0	0	0	95.4%

Skyland – January 25, 2019



Key for classified images at Skyland

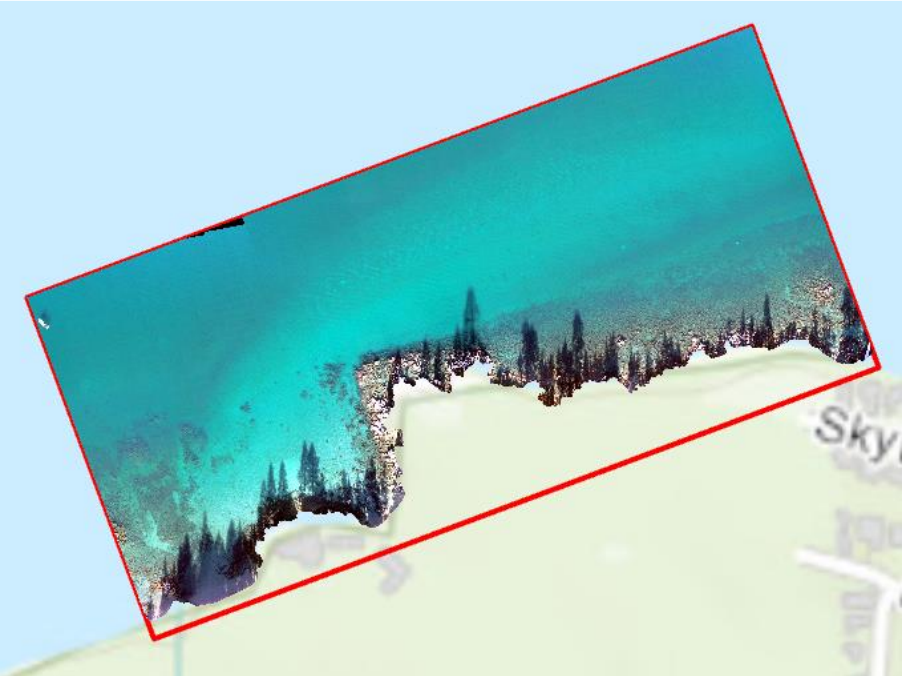
Class_name	Class_name
Grid	Rock_Mid
Metaphyton_Deep	Rock_Shallow
Metaphyton_Deep	Sand_Above
Metaphyton_Shallow	Sand_Deep
Rock_AboveWater	Sand_Shallow
Rock_Deep	Shadow



A4-8. Skyland – July 31, 2019 accuracy table, original UAV images and images after classification of pixels.

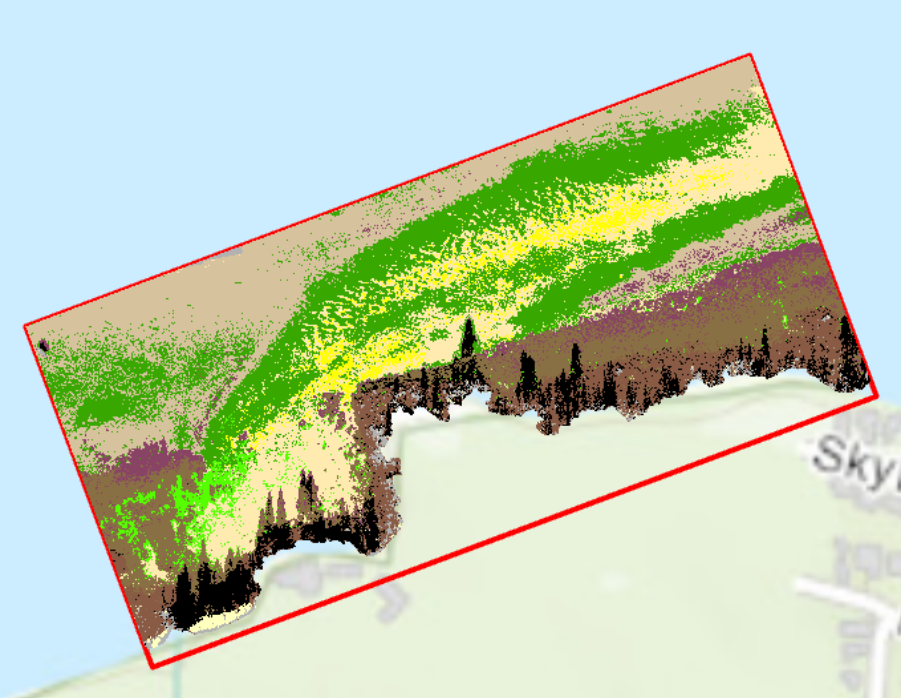
ClassValue	Sand - Above	Sand - Shallow	Sand - Deep	Rock - AboveWater	Rock - Shallow	Rock - Mid Depth	Rock - Deep	Shadow	Grid	Metaphyton - Shallow	Metaphyton - Deep	Clams	Total	U_Accuracy
Sand - Above	9	0	0	1	0	0	0	0	0	0	0	0	10	90.0%
Sand - Shallow	0	13	0	0	0	0	0	0	0	0	2	0	15	86.7%
Sand - Deep	0	0	18	0	0	0	1	0	0	0	3	0	22	81.8%
Rock - Above Water	0	0	0	10	0	0	0	0	0	0	0	0	10	100.0%
Rock - Shallow	0	0	0	0	10	0	0	0	0	0	0	0	10	100.0%
Rock - Mid Depth	0	0	0	0	0	12	0	0	0	0	0	0	12	100.0%
Rock - Deep	0	0	0	0	0	0	10	0	0	0	0	0	10	100.0%
Shadow	0	0	0	0	0	0	0	9	0	0	0	0	9	100.0%
Grid	0	0	0	0	0	0	0	0	10	0	0	0	10	100.0%
Metaphyton - Shallow	0	1	0	0	1	0	1	0	0	7	0	0	10	70.0%
Metaphyton - Deep	0	3	1	0	0	0	0	0	0	0	21	0	25	84.0%
Clams	0	6	0	1	0	0	0	0	0	0	0	3	10	30.0%
Total	9	23	19	12	11	12	12	9	10	7	26	3	153	0.0%
P_Accuracy	100.0%	56.5%	94.7%	83.3%	90.9%	100.0%	83.3%	100.0%	100.0%	100.0%	80.8%	100.0%	0	86.3%
Kappa	0	0	0	0	0	0	0	0	0	0	0	0	0	0

Skyland – July 31, 2019



Key for classified images at Skyland

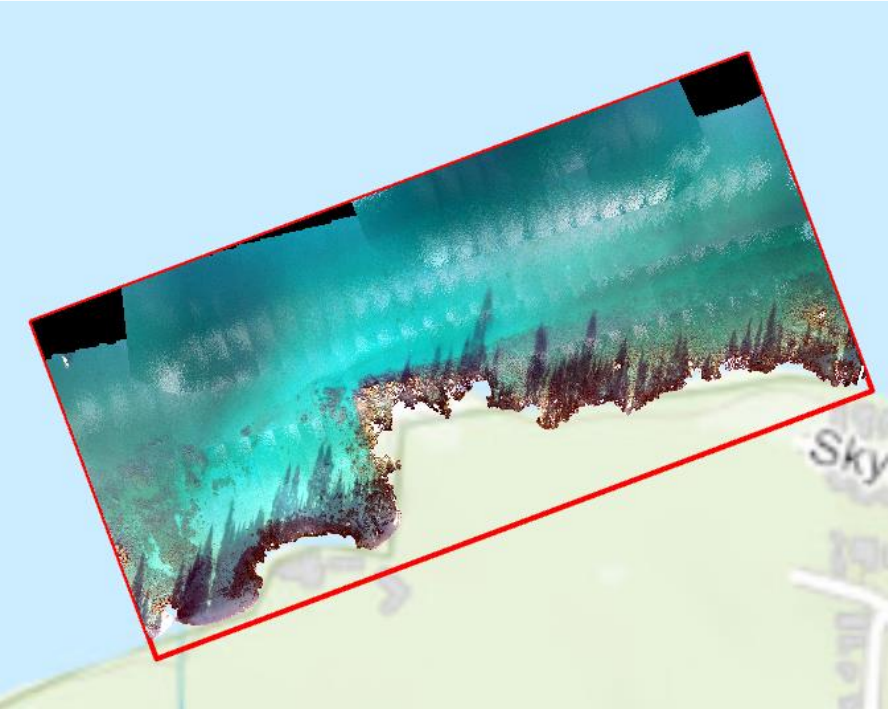
Class_name	Class_name
Grid	Rock_Mid
Metaphyton_Dead	Rock_Shallow
Metaphyton_Deep	Sand_Above
Metaphyton_Shallow	Sand_Deep
Rock_AboveWater	Sand_Shallow
Rock_Deep	Shadow



A4-9. Skyland – September 4, 2019 accuracy table, original UAV images and images after classification of pixels.

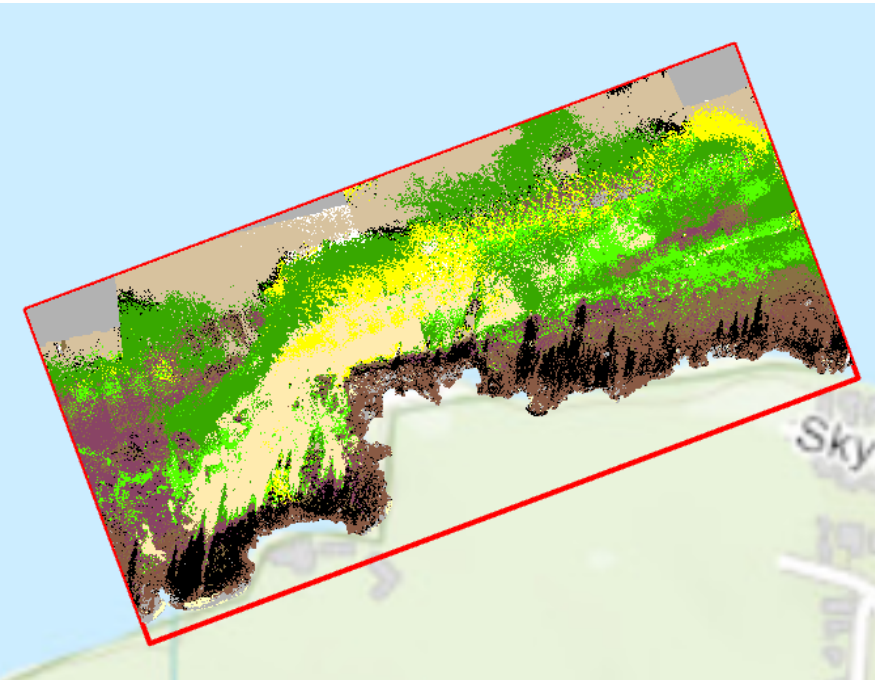
ClassValue	Sand - Above	Sand - Shallow	Sand - Deep	Rock - AboveWater	Rock - Shallow	Rock - Mid Depth	Rock - Deep	Shadow	Grid	Metaphyton - Shallow	Metaphyton - Deep	Clams	Total	U_Accuracy	Kappa
Sand - Above	10	0	0	0	0	0	0	0	0	0	0	0	10	100.0%	0
Sand - Shallow	0	10	0	0	0	0	0	0	0	0	1	0	11	90.9%	0
Sand - Deep	0	0	12	0	0	0	0	1	0	0	0	0	13	92.3%	0
Rock - Above Water	1	0	0	9	0	0	0	0	0	0	0	0	10	90.0%	0
Rock - Shallow	0	0	0	0	9	0	0	0	0	0	1	0	10	90.0%	0
Rock - Mid Depth	0	0	3	0	0	7	0	0	0	0	0	0	10	70.0%	0
Rock - Deep	0	0	2	0	0	0	6	0	0	1	1	0	10	60.0%	0
Shadow	0	0	3	0	0	0	0	7	0	0	0	0	10	70.0%	0
Grid	0	0	8	0	0	0	0	0	1	0	1	0	10	10.0%	0
Metaphyton - Shallow	0	1	1	0	0	1	0	0	0	7	0	0	10	70.0%	0
Metaphyton - Deep	0	2	0	0	0	0	2	1	0	0	17	0	22	77.3%	0
Clams	0	5	1	0	0	0	0	0	0	0	0	4	10	40.0%	0
Total	11	18	30	9	9	8	8	9	1	8	21	4	136	0.0%	0
P_Accuracy	90.9%	55.6%	40.0%	100.0%	100.0%	87.5%	75.0%	77.8%	100.0%	87.5%	81.0%	100.0%	0.0%	72.8%	0
Kappa	0	0	0	0	0	0	0	0	0	0	0	0	0	0	70.0%

Skyland – September 4, 2019



Key for classified images at Skyland

Class_name	Class_name
Grid	Rock_Mid
Metaphyton_Deep	Rock_Shallow
Metaphyton_Deep	Sand_Above
Metaphyton_Shallow	Sand_Deep
Rock_AboveWater	Sand_Shallow
Rock_Deep	Shadow



A4-10. Lakeside – July 23, 2018 accuracy table, original UAV images and images after classification of pixels.

ClassValue	Sand	Beach Sand	Metaphyton	Metaphyton Shadow	Infrastructure	Shadow	Total	U_Accuracy	Kappa
Sand	71	0	3	0	0	0	74	95.9%	0
Beach Sand	0	10	0	0	0	0	10	100.0%	0
Metaphyton	5	0	11	0	0	0	16	68.8%	0
Metaphyton Shadow	0	0	0	10	0	0	10	100.0%	0
Infrastructure	1	0	0	0	6	3	10	60.0%	0
Shadow	0	0	0	0	0	10	10	100.0%	0
Total	77	10	14	10	6	13	130	0.0%	0
P_Accuracy	92.2%	100.0%	78.6%	100.0%	100.0%	76.9%	0.0%	90.8%	0
Kappa	0	0	0	0	0	0	0	0	85.3%

Lakeside – July 23, 2018

Key for classified images at Lakeside

Class_name	
	Metaphyton
	Sand
	Floating Objects
	Beach Sand
	Shadows
	Metaphyton_Shadow



A4-11. Lakeside – August 1, 2018 accuracy table, original UAV images and images after classification of pixels.

ClassValue	Sand	Metaphyton	Infrastructure	Shadows	Total	U_Accuracy	Kappa
Sand	63	1	0	0	64	98.4%	0
Metaphyton	1	32	0	0	33	97.0%	0
Infrastructure	4	0	6	0	10	60.0%	0
Shadows	0	6	0	4	10	40.0%	0
Total	68	39	6	4	117	0.0%	0
P_Accuracy	92.6%	82.1%	100.0%	100.0%	0.0%	89.7%	0
Kappa	0	0	0	0	0	0	82.3%

Lakeside – August 1, 2018

Key for classified images at Lakeside

Class_name	
	Metaphyton
	Sand
	Floating Objects
	Shadows



A4-12. Lakeside – September 4, 2018 accuracy table, original UAV images and images after classification of pixels.

ClassValue	Metaphyton	Sand	Infrastructure	Shadows	Total	U_Accuracy	Kappa
Metaphyton	33	0	0	0	33	100.0%	0
Sand	3	63	0	0	66	95.5%	0
Infrastructure	1	6	3	0	10	30.0%	0
Shadows	3	0	0	7	10	70.0%	0
Total	40	69	3	7	119	0.0%	0
P_Accuracy	82.5%	91.3%	100.0%	100.0%	0.0%	89.1%	0
Kappa	0	0	0	0	0	0	81.1%

Lakeside – September 4, 2018



Key for classified images at Lakeside

Class_name	
Metaphyton	Sand
Infrastructure	Shadows



A4-13. Lakeside – January 25, 2019 accuracy table, original UAV images and images after classification of pixels.

ClassValue	Sand	Beach Sand	Infrastructure	Woody Debris	Total	U_Accuracy	Kappa
Sand	96	0	0	0	96	100.0%	0
Beach Sand	0	10	0	0	10	100.0%	0
Infrastructure	4	0	6	0	10	60.0%	0
Woody Debris	0	0	0	10	10	100.0%	0
Total	100	10	6	10	126	0.0%	0
P_Accuracy	96.0%	100.0%	100.0%	100.0%	0.0%	96.8%	0%
Kappa	0	0	0	0	0	0%	91.6%

Lakeside - January 25, 2019

Key for classified images at Lakeside

Class_name	
	Sand
	Floating Objects
	Beach Sand
	Woody Debris



A4-14. Lakeside – August 1, 2019 accuracy table, original UAV images and images after classification of pixels.

ClassValue	Sand	Beach Sand	Metaphyton	Infrastructure	Shadows	Total	U_Accuracy	Kappa
Sand	46	0	3	0	0	49	93.9%	0
Beach Sand	0	10	0	0	0	10	100.0%	0
Metaphyton	1	0	40	0	0	41	97.6%	0
Infrastructure	2	2	4	0	2	10	0.0%	0
Shadows	0	0	0	0	10	10	100.0%	0
Total	49	12	47	0	12	120	0.0%	0
P_Accuracy	93.9%	83.3%	85.1%	0.0%	83.3%	0.0%	88.3%	0
Kappa	0	0	0	0	0	0	0%	82.9%

Lakeside – August 1, 2019

Key for classified images at Lakeside

Class_name	
	Metaphyton
	Sand
	Infrastructure
	Shadows
	Beach Sand



A4-15. Lakeside – September 4, 2019 accuracy table, original UAV images and images after classification of pixels.

ClassValue	Sand	Beach Sand	Metaphyton	Infrastructure	Shadows	Total	U_Accuracy	Kappa
Sand	50	0	7	0	0	57	87.7%	0
Beach Sand	0	10	0	0	0	10	100.0%	0
Metaphyton	2	0	33	0	0	35	94.3%	0
Infrastructure	5	1	0	3	1	10	30.0%	0
Shadows	0	0	4	0	6	10	60.0%	0
Total	57	11	44	3	7	122	0.0%	0
P_Accuracy	87.7%	90.9%	75.0%	100.0%	85.7%	0.0%	83.6%	0
Kappa	0	0	0	0	0	0	0	75.3%

Lakeside – September 4, 2019

Key for classified images at Lakeside

Class_name	
	Metaphyton
	Sand
	Infrastructure
	Shadows
	Beach Sand



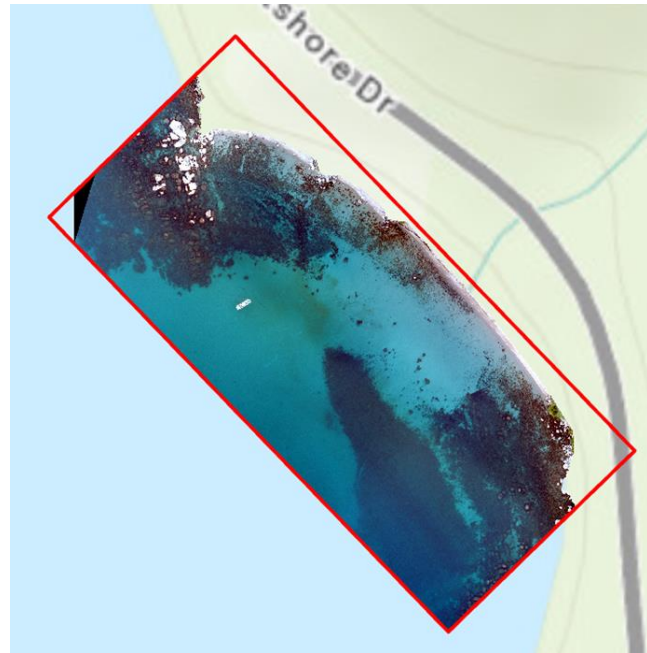
A4-16, A4-17. Hidden Beach original UAV images Aug. 1, 2018 and Sept. 10, 2018.

**** Hidden Beach was not processed with image classification as no metaphyton was present at site.**

Hidden Beach – August 1, 2018

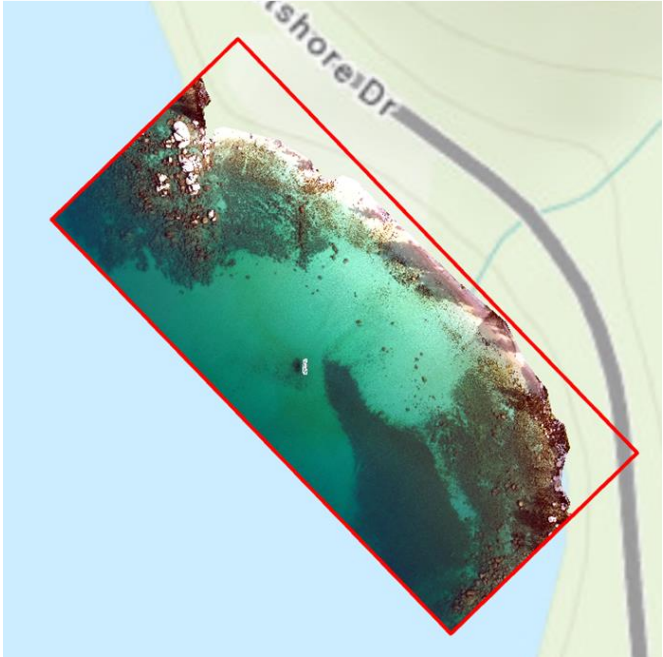


Hidden Beach – September 10, 2018



A4-18, A4-19. Hidden Beach original UAV images May 3, 2019 and July 22, 2019.

Hidden Beach – May 3, 2019

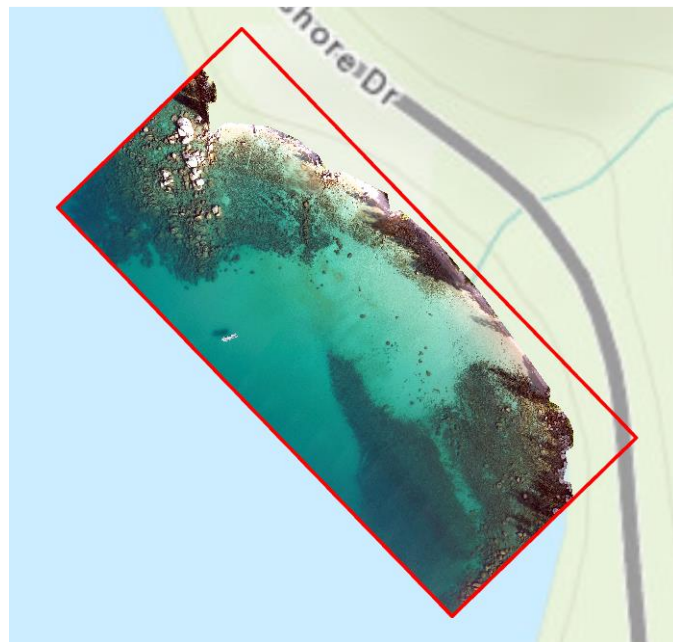


Hidden Beach – July 22, 2019



A4-20. Hidden Beach original UAV image Sept. 5, 2019.

**Hidden Beach - September 5,
2019**



Appendix 5. Predominant algal types and predominant genera present in samples.

Sample	Date	Types	Predominant Algae Present
Lakeside			
Main Patch Rep 1	8/1/18	Mixed Fil. Green Algae	Mixed filamentous greens (including <i>Zygnema</i> , <i>Bulbochaete</i>); Cyanobacteria; Charophytes
Main Patch Rep 2	8/1/18	Mixed Fil. Green Algae	Mixed filamentous greens (including <i>Zygnema</i> , <i>Bulbochaete</i> , <i>others</i>); Charophytes
Main Patch Rep 3	8/1/18	Mixed Fil. Green Algae	Mixed filamentous greens (including <i>Zygnema</i> , <i>Bulbochaete</i> , <i>Spirogyra</i>); Charophytes
Main Patch Rep 1	9/4/18	Mixed Fil. Green Algae	Mixed filamentous greens (primarily <i>Zygnema</i> , also <i>Bulbochaete</i> , <i>others</i>); Cyanobacteria; large amount Charophytes
Main Patch Rep 2	9/4/18	Mixed Fil. Green Algae	Mixed filamentous greens (primarily <i>Zygnema</i> , also <i>Spirogyra</i> , <i>others</i>); large amount Charophytes; detritus
Main Patch (Rep 1)	7/24/19	Mixed Fil. Green Algae	Mixed filamentous greens (<i>Spirogyra</i> , <i>Zygnema</i> , <i>Oedogonium</i>); Diatoms; detritus
Outside Patch near Pore Water samples (Rep.2)	7/24/19	Mixed Fil. Green Algae	Mixed filamentous greens (<i>Spirogyra</i> , <i>Zygnema</i>); some detritus
Outside Patch near Pore Water samples (Rep.3)	7/24/19	Mixed Fil. Green Algae	Mixed filamentous greens (<i>Spirogyra</i> , <i>Zygnema</i> , <i>Mougeotia</i>); Cyanobacteria (<i>Rivularia</i>)
Inside Main Patch Rep.1	8/1/19	Mixed Fil. Green Algae	Mixed filamentous greens (primary: <i>Zygnema</i> , also <i>Spirogyra</i> , <i>Mougeotia</i> , some <i>Bulbochaete</i> and <i>Cladophora</i>); some Cyanobacteria
Inside Main Patch Rep.2	8/1/19	Mixed Fil. Green Algae	Mixed filamentous greens (primary: <i>Zygnema</i> , also <i>Spirogyra</i>); some Charophytes
Inside Main Patch Rep.3	8/1/19	Mixed Fil. Green Algae	Mixed filamentous greens (primary: <i>Zygnema</i>); detritus
Outside Main Patch	8/1/19	Mixed Fil. Green Algae	Mixed filamentous greens (<i>Zygnema</i> , <i>Spirogyra</i> , <i>Oedogonium</i>); detritus
Inside Main Patch Rep.1	9/4/19	Mixed Fil. Green Algae	Mixed filamentous greens (<i>Oedogonium</i> , <i>Zygnema</i>), some Charophytes; some Cyanobacteria
Inside Main Patch Rep.2	9/4/19	Mixed Fil. Green Algae	Mixed filamentous greens (<i>Zygnema</i> , <i>Spirogyra</i> , <i>Bulbochaete</i>), some Charophytes; some Eurasian milfoil fragments
Inside Main Patch Rep.3	9/4/19	Mixed Fil. Green Algae	Mixed filamentous greens (<i>Zygnema</i> , <i>Oedogonium</i>), some Cyanobacteria some aquatic plant fragments
Skyland			
Ground-truthing nearshore	8/24/18	<i>Mougeotia</i> (genuflexing)	<i>Mougeotia</i> (genuflexing); also some <i>Zygnema</i> and <i>Spirogyra</i>
0.25m2 Quad. A1	7/31/19	Mixed Fil. Green Algae	Mixed filamentous greens (<i>Mougeotia</i> - genuflexing), <i>Spirogyra</i> , <i>Zygnema</i> , <i>others</i>)

Sample	Date	Types	Predominant Algae Present
Skyland cont'd.			
0.25m2 Quad. B3	7/31/19	Mixed Fil. Green Algae	Primary: <i>Spirogyra</i> ; secondary: <i>Zygnema</i>
0.25m2 Quad. C2	7/31/19	Mixed Fil. Green Algae	Primary: <i>Spirogyra</i> ; secondary: <i>Zygnema</i>
Large Patch #1	9/3/19	<i>Mougeotia</i> (genuflexing)	Majority: <i>Mougeotia</i> (genuflexing); some <i>Zygnema</i>
Large Patch #2	9/3/19	<i>Mougeotia</i> (genuflexing)	Majority: <i>Mougeotia</i> (genuflexing); some <i>Zygnema</i> ; hairs
Large Patch #3	9/3/19	<i>Mougeotia</i> (genuflexing)	Majority: <i>Mougeotia</i> (genuflexing); some <i>Zygnema</i> , <i>Oedogonium</i>
0.25m2 Quad. A1	9/3/19	Mixed Fil. Green Algae	Primary: <i>Zygnema</i> ; secondary: <i>Mougeotia</i> (genuflexing); also some <i>Oedogonium</i> , others
0.25m2 Quad. B1	9/3/19	Mixed Fil. Green Algae	Primary: <i>Mougeotia</i> (genuflexing); also some <i>Zygnema</i> and <i>Spirogyra</i>
Regan (nearshore)			
Nearshore Patch Rep. 1	8/1/18	Mixed Fil. Green Algae	<i>Zygnema</i> , <i>Spirogyra</i> , <i>Oedogonium</i> , others; detritus
Nearshore Patch Rep. 2	8/1/18	Mixed Fil. Green Algae	<i>Spirogyra</i> , <i>Oedogonium</i> , <i>Mougeotia</i> , others.
Nearshore Patch Rep. 3	8/1/18	Mixed Fil. Green Algae	Mixed filamentous greens (including <i>Spirogyra</i> , <i>Bulbochaete</i> , others).
0.25m2 Quad. 1	9/6/18	Mixed Fil. Green Algae	Mixed filamentous greens (including <i>Spirogyra</i> , <i>Oedogonium</i> , <i>Bulbochaete</i> , others); Cyanobacteria; detritus
0.25m2 Quad. 2	9/6/18	Mixed Fil. Green Algae	Mixed filamentous greens (including <i>Spirogyra</i> , <i>Oedogonium</i> , <i>Bulbochaete</i> , others); detritus
0.25m2 Quad. 3	9/6/18	Mixed Fil. Green Algae	Mixed filamentous greens (including <i>Spirogyra</i> , others)
0.25m2 Quad. 4	9/6/18	Mixed Fil. Green Algae	Mixed filamentous greens (including <i>Spirogyra</i> , <i>Oedogonium</i> , others); detritus
0.25m2 Quad. A0	8/1/19	Aquatic plants	Aquatic plant portion of A1 primarily Eurasian milfoil, also other aquatic plants; degrading algae
0.25m2 Quad. A1	8/1/19	Mixed Fil. Green Algae	Detritus; mixed filamentous green algae (<i>Spirogyra</i> , <i>Oedogonium</i> , <i>Zygnema</i>)
0.25m2 Quad. B2	8/1/19	Mixed Fil. Green Algae	Detritus; mixed filamentous green algae (<i>Spirogyra</i> , <i>Zygnema</i> , <i>Oedogonium</i>); some Cyanobacteria
Nearshore Patch 100% Cover-1	9/4/19	Detritus, Mixed algal	Heterogeneous mix: detritus, cyanobacteria; <i>Oedogonium</i> <i>Zygnema</i> , <i>Cladophora</i> and diatoms
Nearshore Patch 100% Cover-2	9/4/19	Detritus, Mixed algal	Heterogeneous mix: detritus, plant fragments, cyanobacteria; <i>Oedogonium</i> filamentous greens and diatoms
0.25m2 Quad. A1	9/4/19	Mixed Fil. Green Algae	Much detritus; mixed filamentous green algae (old <i>Cladophora</i> with diatoms, some <i>Bulbochaete</i> , <i>Oedogonium</i>); some Cyanobacteria

Sample	Date	Types	Predominant Algae Present
0.25m2 Quad. B2	9/4/19	Mixed Fil. Green Algae	Mixed filamentous green algae (<i>Spirogyra</i> , <i>Zygnema</i> , old <i>Cladophora</i> with diatoms, <i>Oedogonium</i>); some Cyanobacteria
<u>Regan (offshore)</u>			
0.25m2 Quad. C2	8/1/19	Mixed Fil. Green Algae	Primary: <i>Zygnema</i> ; also some <i>Spirogyra</i> ; detritus
<u>Hidden Beach</u>			
Hidden Rep. 1	7/22/19	Detritus	Much detritus (plant debris, hairs); mixed Cyanobacteria; Diatoms
Hidden Rep. 2	7/22/19	Detritus	Much detritus
Hidden Rep. 3	7/22/19	Detritus	Much detritus; Cyanobacteria
Hidden (nearshore)	7/22/19	Stalked Diatoms	Small stalked diatoms in mat material; detritus
Hidden (offshore)			
Hidden Rep. 1	9/3/19	Detritus	Detritus (hairs); Cyanobacteria (<i>Scytonema</i> , <i>others</i>)
Hidden Rep. 2	9/3/19	Detritus	Detritus (hairs); Cyanobacteria (<i>Scytonema</i> , <i>others</i>)
Hidden Rep. 31	9/3/19	Detritus	Detritus (hairs); Cyanobacteria; some green filamentous (<i>Zygnema</i>)
<u>Elk Point</u>			
Elk Point Rep. 1	7/23/19	<i>Spirogyra</i>	95% <i>Spirogyra</i> ; some other filamentous greens: <i>Zygnema</i> , <i>Mougeotia</i>
Elk Point Rep. 2	7/23/19	<i>Spirogyra</i>	95% <i>Spirogyra</i> ; some <i>Zygnema</i>
Elk Point Rep. 3	7/23/19	<i>Spirogyra</i>	95% <i>Spirogyra</i> ; some <i>Zygnema</i> and detritus
Elk Point Rep. 4	7/23/19	<i>Spirogyra</i>	95% <i>Spirogyra</i> ; some <i>Zygnema</i> and detritus

